Department of Natural Resources
MARYLAND GEOLOGICAL SURVEY
Kenneth N. Weaver, Director

REPORT OF INVESTIGATIONS NO. 50

QUATERNARY STRATIGRAPHY OF THE INNER CONTINENTAL SHELF OF MARYLAND

by

Marguerite A. Toscano, Randall T. Kerhin,
Linda L. York*, Thomas M. Cronin**, and S. Jeffress Williams**

Prepared in cooperation with
Minerals Management Service
Geological Survey
United States Department of the Interior
and
Association of American State Geologists

1989

Department of Natural Resources
MARYLAND GEOLOGICAL SURVEY
Kenneth N. Weaver, Director

REPORT OF INVESTIGATIONS NO. 50

QUATERNARY STRATIGRAPHY OF THE INNER CONTINENTAL SHELF OF MARYLAND

by

Marguerite A. Toscano, Randall T. Kerhin,
Linda L. York*, Thomas M. Cronin, and S. Jeffress Williams****

Maryland Geological Survey
2300 St. Paul Street
Baltimore, Maryland 21218

***University of Delaware**
Department of Geology
Newark, Delaware 19716

****U.S. Geological Survey**
926 National Center
Reston, Virginia 22092

1989

COMMISSION
OF THE
MARYLAND GEOLOGICAL SURVEY

M. Gordon Wolman, *Chairman* ..... Baltimore

S. James Campbell ..... Towson

Robert W. Ridky ..... College Park

Richard W. Cooper ..... Salisbury

Philip J. Jenkins ..... Frostburg

CONTENTS

	Page
Abstract	1
Introduction	2
Study Area	2
Shelf Morphology	2
Paleodrainage	2
Acknowledgements	4
Eustatic Sea Level History	5
Pre-Holocene Sea Level	5
Holocene Sea Level	6
Coastal Plain Stratigraphy	7
Tertiary Deposits	7
Quaternary (Pleistocene and Holocene) Deposits	7
Methods	11
Surficial Sediment Sampling	11
Seismic Profiling	11
Vibracoring	11
Amino Acid Racemization Analyses	11
Ostracode Analysis	13
Surficial Shelf Sediments	13
Sand	13
Mud	14
Gravel	14
Seismic-Reflection Profiles	14
Subsurface Units in Maryland	14
Subsurface Units in Virginia	14
Maryland Subsurface Units — This Study	21
Depositional Sequence 1	21
Unit T1 (Tertiary)	21
Depositional Sequence 2	21
Units Q1 and Q2 (Quaternary)	21
Unit Q3 (Quaternary)	21
Units Q4 and Q5 (Quaternary)	22
Lithology and Stratigraphy of the Shelf	22
Tertiary Units	22
Quaternary Units	22
Late Pleistocene (Unit Q1)	22
Last Interglacial (Unit Q2)	24
Ostracode Paleoclimatic Zones — Q2	29
Previous Age Estimates — Q2	29
Amino Acid Age Estimates — Q2	33
Unit Q2 — Age and Correlation	38
Last Glacial (Unit Q3)	38
Early Holocene (Unit Q4)	44
Modern Shelf Sands (Unit Q5)	47
Conclusions	49
References Cited	50
Appendices	55

PLATES

Page

Plate 1. High-Resolution seismic reflection profiles ..... in pocket
2. Vibracore Locations ..... in pocket
3. Structure contour on M1 reflector ..... in pocket
4. Interpretative geophysical records, Unit Q2 ..... in pocket
5. Stratigraphic cross-section from south to north, offshore along Assateague Island ..... in pocket

FIGURES

Page

Figure 1. Location map 3
2. Generalized late Pleistocene glacioeustatic sea level curve 5
3. Local-relative Holocene sea level curve from coastal areas surrounding Maryland. After Belknap and Kraft (1977)..... 6
4. Depth to erosional surface at top of Tertiary, after Mixon (1985), Colman and Mixon (1988), and Shideler *et al* 8
5. Late Pleistocene shoreline trend with dated, stratigraphically documented reference localities 9
6. Generalized Delmarva Peninsula — Chesapeake Bay stratigraphic correlation chart. After Mixon (1985) 12
7. Surficial shelf sediment distribution 15
8. Percent sand distribution, Maryland inner continental margin .. 16
9. Percent sand distribution and bathymetry, Maryland inner continental margin 17
10. Percent mud distribution, Maryland inner continental margin .. 18
11. Percent gravel distribution, Maryland inner continental margin. 19
12. Maryland inner continental margin a) subbottom structure; b, c) stratigraphic sequence. After Field (1976; 1980) 20
13. Interpreted ORE Geopulse 280 joules shore-normal seismic profiles 23
14. Maryland inner continental margin stratigraphy, this study 24
15. Evidence of shoal-like sand body remnant in Unit Q2 25
16. Buried paleochannel locations from 1985-1987 seismic-reflection data 26
17. Depth to top of Pliocene Beaverdam Sand from onshore well data (Maryland), to top of Yorktown Formation (Virginia; Mixon, 1985), and to the M1 reflector offshore 27
18. Xeroradiographs illustrating the characteristic bedding and shell lenses *(Mulinia lateralis)* of the Q2 muds 28
19. Percentages of climatically significant ostracodes, core 16–905 .. 30
20. Percentages of climatically significant ostracode genera in core 18-1230 31
21. Percentages of climatically significant ostracode genera in core 27-1520 32
22. Generalized ostracode paleoclimatic zones in stratigraphic sequence for studied cores 33
23. Cross-shelf aminostratigraphy 34

FIGURES (continued)

Page

24. A/I *Mulinia* values versus latitude in Maryland shelf cores analyzed 35
25. Continental shelf A/I *Mulinia* data (Maryland Q1 and Maryland Q2) shown in the Region II aminozone framework of Wehmiller *et al* (1988) 37
26. Reconstruction of drainage system associated with channels (M3–M1) filled by unit Q3 41
27. Area of line 16 showing cross section of M3 channel feature and 2 vibracores (16-935 and 16-945) that penetrated fluvial sediments in the channel fill 42
28. Smaller channels, tributary to the main M3 channel 43
29. Selected xeroradiographs showing radiocarbon-dated woody materials in 3 Holocene estuarine sequences 45
30. Local-relative Holocene sea level curve derived from basal peats, Delaware 46
31. Core 20–1340 and seismic cross-section of near-shore channel feature 48
32. Assignment of Maryland shelf lithologic units and erosional surfaces to appropriate time frames 49
33. Plot of number of ostracodes vs. depth in core from vibracores 16-905 (A), 18-1230 (B), and 27-1520 (C) 80

TABLES

Page

Table I *Mulinia* amino acid summary 34
II Overlap of standard deviations of mean A/I ratios in three portions of unit Q2 in core 18-1248 36
III Comparison of D/L, leucine, radiometric, and A/I *Mulinia* data for Delmarva localities TI, BN, and BB and previous age estimates 39
IV Light mineral petrology, cores 16-935 and 16-945 40
V Summary of radiocarbon data, early Holocene continental shelf samples, Maryland 45
VI Textural parameters of the surficial sediments 56
VII List of samples analyzed for extent of amino acid racemization in selected vibracores 60
VIII Previous data and re-analyzed data for numerical age assignments from A/I ratios 69
IX Age calculations where first order constant (K) is 9.2×10^{-7} and the Effective Quaternary Temperature (T_{eff}) is -0.79°C 70
X Age calculations where first order constant (K) is 7.7×10^{-7} and the Effective Quaternary Temperature (T_{eff-}) is -1.79°C 71
XI Age calculation where first order constant (K) is 7.7×10^{-7}) for A/I ratios between 0.0875 to 0.0928 and 9.2×10^{-7} for A/I ratios between 0.1017 to 0.121. A/I ratio 0.1162 equals 125,000 years 71

TABLES (continued)

Page

XII List of samples studies for ostracode assemblages in centimeters from top of core for all cores studied 74
XIII Ostracode paleoclimatology data 76
XIV Number of individuals for each ostracode species per sample in core 77
XV Paleochannel dimensions, determined from geophysical records, used in construction of Figures 26, 27, and 28 114

APPENDICES

Page

Appendix I Surficial sediment samples 55
II List of samples analyzed for extent of amino acid racemization in selected vibracores 59
III Numerical age assignments calculated from amino acid racemization A/I ratios 67
IV Paleontology for vibracores 16-905, 18-1230, and 27-1520 . . . 73
V Lithologic logs for twenty-nine (29) vibracores collected offshore of Assateague Island, Maryland. See Plate 2 for location of vibracores 81
VI Paleochannel Dimensions 113

QUATERNARY STRATIGRAPHY OF THE INNER CONTINENTAL SHELF OF MARYLAND

by

Marguerite A. Toscano, Randall T. Kerhin,
Linda L. York, Thomas M. Cronin, and S. Jeffress Williams

ABSTRACT

Five distinct stratigraphic units are identified for the Maryland inner shelf from high-resolution seismic-reflection profiles, vibracores, amino acid racemization age determinations and paleontology. The lowermost unit, T1 (Tertiary), lies below -21 meters (MSL) at the shoreface and is characterized by steep internal reflectors and extensive channeling near its top. T1 is truncated by a persistent high amplitude, essentially horizontal reflector (horizon M1), which is coincident with the Tertiary/Quaternary unconformity immediately onshore. M1 likely represents the Illinoian glacial (stage 6) erosional surface. Overlying M1 are approximately 10 meters of units (Q2-Q1) of concordant strata with parallel to subparallel bedding. Horizon M2, a less prominent reflector, is associated with channeling and separates unit Q1 from Q2. Just above M2 are localized sands that range from thin (less than 1 meter) beds to remnant sand bodies on the same scale as modern shelf shoals. The 6-meter section above M2 consists of a dewatered, fossiliferous clayey silt (Q2), estimated from amino acid racemization data to be of last interglacial, oxygen-isotope stage 5 (128-75 ka) age. This mud sequence contains at least 4 distinct paleoclimatic zones as defined by ostracode assemblages, each representing particular paleocliminatic-oceanographic conditions. A warmer than present sandy zone (Zone 1) occurs below -22 meters MSL, a colder than present zone (Zone 2) occurs from -22 to -20 meters MSL, and a cool zone (Zone 3) occurs above -20 meters. A fourth zone (Zone 4), representing a warm interval, is tentatively identified above Zone 3; this zone appears to become more prominent southward in the study area. All ostracode assemblages from unit Q2 were representative of normal marine salinities, indicating an open shelf depositional environment. The Q2 mud is interpreted as a regressive, shallow shelf deposit of oxygen-isotope substages 5d-c, with the warmer climate sand below representing the transgressive portion of substage 5e.

Unit Q1, below horizon M2, consists of shelly sands at its top meter and is interpreted to represent remnants of transgressive shelf sands 1 of pre-Illinoian (possibly oxygen-isotope stages 7 and/or 9) age.

Incised into units Q2 and Q1 are numerous paleochannels. Unit Q3 fills an extensive ancestral channel and tributary system, marked by reflectors M3 and M1, traceable to the present St. Martin River estuary, that was incised into the shelf during the most recent Pleistocene (Wisconsin) glaciation (oxygen-isotope stages 4, 3 and 2). Iron-stained gravels and fluvial sandy silts barren of microfauna have been cored in this unit. The channels cut during the Wisconsin probably contain continuous fluvial-estuarine tidal channel fill sequences representing the oxygen-isotope stage 2-1 transition. The cored, upper portions of these channel fills contain radiocarbon-dated early Holocene (unit Q4) estuarine deposits. Transgressive, leading-edge coastal deposits (lowland swamp) of unit Q4 cut into and overlap portions of unit Q2, and have degrees of preservation below the shoreface ravinement unconformity that are demonstrably related to rates of sea level rise and pre-transgression topography. No Holocene back-barrier remnants were found within a distance of 40 km from shore or between depths of -12 to -22 meters MSL. Modern trailing-edge transgressive shelf shoals (unit Q5) discontinuously cap the sequence.

These data indicate that oxygen-isotope substages 5d-a represented a unique, relatively high, sea level stand of sufficient duration (40 ka) to deposit a thick regressive shelf mud. The Holocene transgression is represented only by remnants in truncated channels or by relict facies preserved far offshore due to initially high rates of sea level rise. From approximately 7000 yrs BP to the present the Holocene depositional record has been mostly obliterated by shoreface ravinement processes in connection with a slow rate of sea level rise.

Preservation of late Holocene transgressive deposits of barrier island systems seaward of barrier strandlines on the mid-Atlantic coastal plain should thus be rare and topographically confined. Remnants of trailing-edge shelf sands are most likely the only transgressive deposits preserved on the shelf during intervals of slow sea-level rise. Major preserved shelf sequences are more likely to be seaward thickening, finer grained sediments deposited during long, low energy, regressive phases of interglaciations. Consequently the mud sequence of unit Q2 is probably unique, at least in terms of the Pleistocene glacial/interglacial record on the mid-Atlantic continental shelf.

INTRODUCTION

The inner continental shelf of Maryland (Figure 1) has been extensively studied in terms of ongoing nearshore processes and resulting seafloor morphology. The majority of previous research has been devoted to linear sand ridge genesis and evolution whereas less attention has been paid to the underlying stratigraphic sequence and its relationship to late Quaternary sea level fluctuations. In theory, the regressive phase of the interglacial stratigraphic sequence becomes thicker and more complete with increasing distance from shore, making the shelf record an excellent, continuous source of information on Quaternary interglacial history, which may be linked to the onshore peak transgression stratigraphy.

Much of the present knowledge of the Maryland shelf, both morphologically and stratigraphically, has been advanced by Field (1976, 1980). Field's seismic-reflection and core data, however, were mostly restricted to the linear ridge system, which was the primary focus of his investigations, although he attempted to clarify stratigraphic elements within his study area. Significant areas of the inner continental shelf have not been mapped or stratigraphically documented. This shelf is an extension of Field's (1980) in terms of seismic-reflection surveys; however, this study is stratigraphically oriented, employing several independent lines of evidence to achieve the first spatial, temporal, climatic, and geomorphologic Quaternary history of an inner continental shelf in a nonglaciated area.

STUDY AREA

The Atlantic coast of Maryland and Northern Virginia (Figure 1) comprises the Barrier Island/Southern Spit unit of the Delmarva coastal compartment (Fisher, 1967). Pleistocene headlands at Bethany Beach, Delaware form the northern boundary of the Barrier/Spit unit, which is at present interrupted by only one (stabilized) tidal inlet at Ocean City, separating Fenwick and Assateague Islands. However, numerous short- and long-lived inlets have been documented along this barrier coast since 1649 (Truitt, 1968; McBride, 1986). The Barrier/Spit unit terminates southward of the Maryland-Virginia border in a complex recurved spit at Fishing Point, Virginia.

The portion of the continental shelf studied lies approximately between 38°27′N (MD–DE border) and 38°02′N (MD–VA border) and between 75°15′W – 74°43′W. Our 40 km-wide area crosses 3 zones of depth-related linear ridge morphologies: (1) shoreface-attached ridges (to the base of the shoreface, ≈ 10 m), (2) nearshore ridges (to the 16 m isobath), and (3) offshore ridges (Swift and Field, 1981). Stratigraphy and sedimentary structures were determined by high resolution seismic reflection profiling to a maximum depth of 93.7 meters below the seabed.

Shelf Morphology

The inner continental margin of the eastern U.S. has been the subject of numerous and varied investigations, particularly with respect to the origin and characteristics of the ridge and swale topography (linear shoals) (Rine *et al.,* 1986, Duane *et al.,* 1972; Field, 1976, 1979, 1980; Swift and Field, 1981; Swift, 1973; Stahl *et al.,* 1974; Stubblefield *et al.,* 1984; McBride, 1986). These investigations will not be summarized here; however, it is generally understood that the linear ridges, ubiquitous from Florida to New York, represent a depositional response to transgressive shoreface retreat processes. Morphologic evolution of ridges occurs as a function of increasing water depth, i.e. as sea level rises, and as a way to maintain equilibrium with the shelf hydraulic regime.

Paleodrainage

Sheridan *et al.* (1974) conducted 3.5 and 7.0 kHz seismic–reflection surveys off the Atlantic coast of Delaware and mapped the trellis paleodrainage system of the ancestral Delaware River and tributaries (Indian River, Herring and Love Creeks). This pre-Holocene erosion surface is incised into earlier Pleistocene sediments of the shelf, and the deeper channels reach Tertiary strata (Sheridan *et al.,* 1974). Holocene paralic sediments are preserved above the unconformity in nearshore paleochannels.

Although Field (1976, 1980) reported numerous small inlet or tidal channels in the upper Maryland shelf deposits, he did not report evidence of any major fluvial systems. However Field (1980) schematically depicted an ancestral stream valley trending southeast from Ocean City inlet as a possible ancestral Susquehanna River channel. That the Susquehanna River never crossed the Delmarva Peninsula to reach the Atlantic shelf is evidenced by the recent work of Colman and Mixon (1988).

Three major paleochannels of the ancestral Susquehanna River have been documented through the work of Colman and Mixon (1988), Colman and Hobbs (1987), and Mixon (1985). Each channel records the successive southward displacement of the Susquehanna river valley during three major glacial-interglacial cycles. The southward succession of the Exmore

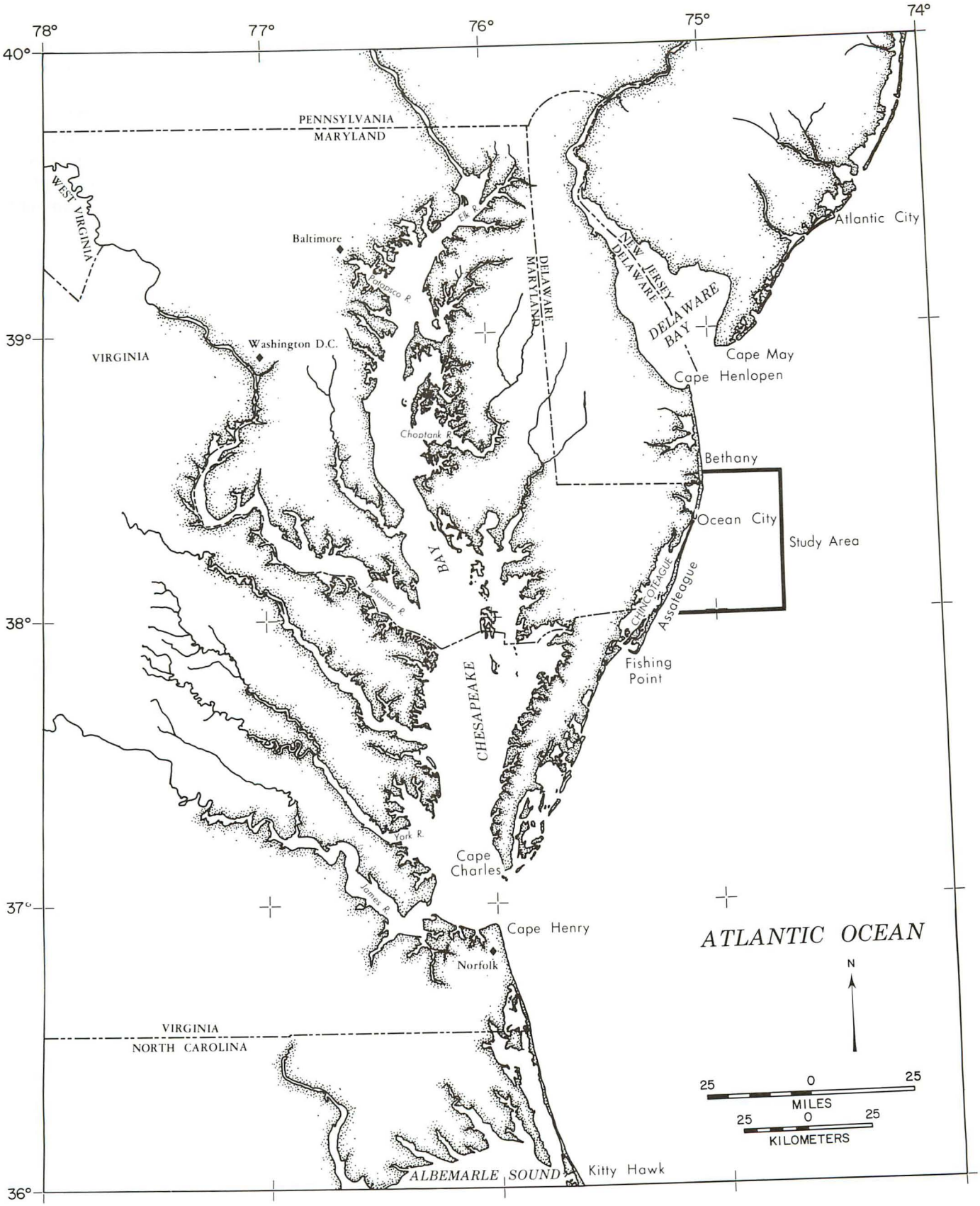

Figure 1.—Location map.

(oldest), Eastville, and Cape Charles (youngest) channels is explained by a climax model wherein the paleochannel is deeply incised into the older deposits of the Bay and adjacent shelf during glacial sea level minima, then immediately and continuously aggraded and filled during the ensuing interglacial sea level rise, until the climax of sea level in a barrier/strandline deposit. The complete infilling of the glacial channel during the transgressive phase has each time caused the active estuarine channel to be pushed south by the southward prograding barrier system (Colman and Mixon 1988).

The southernmost, Cape Charles (last glacial) paleochannel, the fill of which is ^{14}C dated between 8 and 15 ka, was probably initiated during marine oxygen-isotope stage 4, then deepened during stage 2 (the late Wisconsin glacial maximum) and is overlain by the stage 1 or Holocene barrier system as its climax feature.

The Stumptown Member of the Nassawadox Formation fills, and the Butler's Bluff Member forms the overlying barrier complex of the Eastville paleochannel. Dating of the Nassawadox by amino acid ratios, U-series methods, and stratigraphic correlations produced two age groups representing early and late oxygen-isotope stage 5 (Wehmiller *et al.,* 1988) and implying a stage 6 (150 ka, Illinoian glacial) age for the Eastville channel itself (Colman and Mixon, 1988).

The fill of the oldest, northernmost Exmore paleochannel (Mixon, 1985) culminates in the Accomack Member (barrier spit) of the Omar Formation and is problematical in terms of age determinations. Stratigraphic correlations across the Chesapeake Bay result in large radiometric age discrepancies; however amino acid ratios for the unit (and the Omar formation in general) of ≈ 500 ka, as well as a fossil assemblage representing > 300 ka, suggest a stage 11 age for the Accomack Member and a stage 12 age for the Exmore paleochannel.

One major point made by Colman and Mixon is that intermediate sea level deposits, such as that associated with oxygen-isotope stage 3, were confined to the channels and were not preserved. The succeeding low sea level fluvial system occupied the same channel, thereby eroding and destroying the record. Colman and Mixon (1988) report no record of oxygen-isotope stage 3 in the Chesapeake Bay area, which is significant in that no new paleochannel or continuous estuarine-barrier sequence can be attributed to a middle Wisconsin (oxygen-isotope stage 3) high sea level. The unsubstantiated concept of a middle Wisconsin high sea level is rampant in the coastal plain literature (Thom, 1973; Bloom, 1983; Colman *et al.,* 1989; Finkelstein and Kearney, 1988; Toscano, 1989).

ACKNOWLEDGEMENTS

This study was supported by the U.S. Minerals Management Service, Continental Margins Program, the Association of American State Geologists, and the State of Maryland, Department of Natural Resources. The U.S. Geological Survey's Coastal Geology program provided equipment (ORE Geopulse) and technicians for seismic reflection profiles. The USGS Climate Change program supported part of the micropaleontologic and paleoclimatic analyses. We especially thank D. Nichols and K. Parolski (USGS, Woods Hole, MA). Maryland Survey personnel who provided assistance in the field include Captain G. Cox and R. Younger (R/V Discovery), J.P. Halka, S.R. Jones, R. Conkwright, D. Wells, and R. Cuthbertson. The Johns Hopkins Hospital generously provided access to their radiology facilities, where Gabrielle Donovan expertly xeroradiographed 28 vibracores. Lauck W. Ward (USGS) helped us with bivalve identifications, R.P. Stumpf (NOAA) provided identifications of cored plant fragments, and P.J. Allen (University of Delaware) performed a variety of laboratory and computer-related functions. Special thanks are extended to J.F. Wehmiller, University of Delaware Geology Department, for making the amino acid lab available for our work, for providing data, materials, and for insight into many aspects of the interpretations. Steven M. Colman (USGS, Woods Hole, MA) gave an exhaustive review and editorial comments. Other editorial comments were given by Jack W. Pierce (Smithsonian Institution). Sally R. Jones typed the manuscript.

EUSTATIC SEA LEVEL HISTORY

PRE-HOLOCENE SEA LEVEL

Middle to latest Pleistocene sea level fluctuations have been documented from U-series-dated, tectonically rising reef tracts in New Guinea, Timor, Atauro, and Barbados, and from stable mid-oceanic carbonate platform settings in Bermuda, Hawaii, Bahamas, and Mallorca (Bloom *et al.,* 1974; Chappell, 1974; Chappell and Veeh, 1978; Mesolella, 1967; Bender *et al.,* 1979; Harmon *et al.,* 1978, 1983, Ku *et al.,* 1974; Newman and Moore, 1975). These glacioeustatic reconstructions are summarized in Cronin (1983) and in Figure 2 for the past 150,000 years. Glacioeustatic ice volume changes and the timing of the related climatic changes are supported by the $\delta^{18}O$ records in benthic foraminfera in cores from the equatorial Pacific (V-28-238; Shackleton and Opdyke, 1973) and the subpolar Indian Ocean (Imbrie *et al.,* 1984; Martinson *et al.,* 1987).

Stable carbonate areas such as those in Bermuda, Hawaii, and the Bahamas, consistently record a sea level of approximately +5 meters at 125 ka ± 4 ka, correlated to oxygen-isotope substage 5e as the last time that sea level was at or higher than present levels. Sea level records from these areas correlate well within the tectonically rising reef-tract records of New Guinea (reef crests V, VI, VIIb for substages 5e, c, a; Chappell, 1974) and Barbados (Rendezvous Hill — substage 5e, Worthing and Ventnor terraces — late stage 5; Bender *et al.,* 1979) among others.

It is generally accepted that sea level reached a peak during substage 5e of about +6 m, possibly dropped to approximately -20 m during substages 5d and 5b, with an uncertain amount of rise (to depths at or just below present sea level) during substages 5c and 5a. Bloom *et al.* (1974) indicated that -13 to -15 m MSL was a reasonable estimate for high sea levels during late oxygen-isotope stage 5. Bloom and Yonekura (1985) later revised the sea levels for substages 5c (0 meters) and 5a (-7 meters) based on a more rigorous model of actual uplift rates along the length of the Huon Peninsula (Figure 2).

Evidence for relatively low oxygen-isotope stage 3 sea levels is available from New Guinea reef crest II. Chappell's (1974) radiocarbon date of 28 ka for reef II

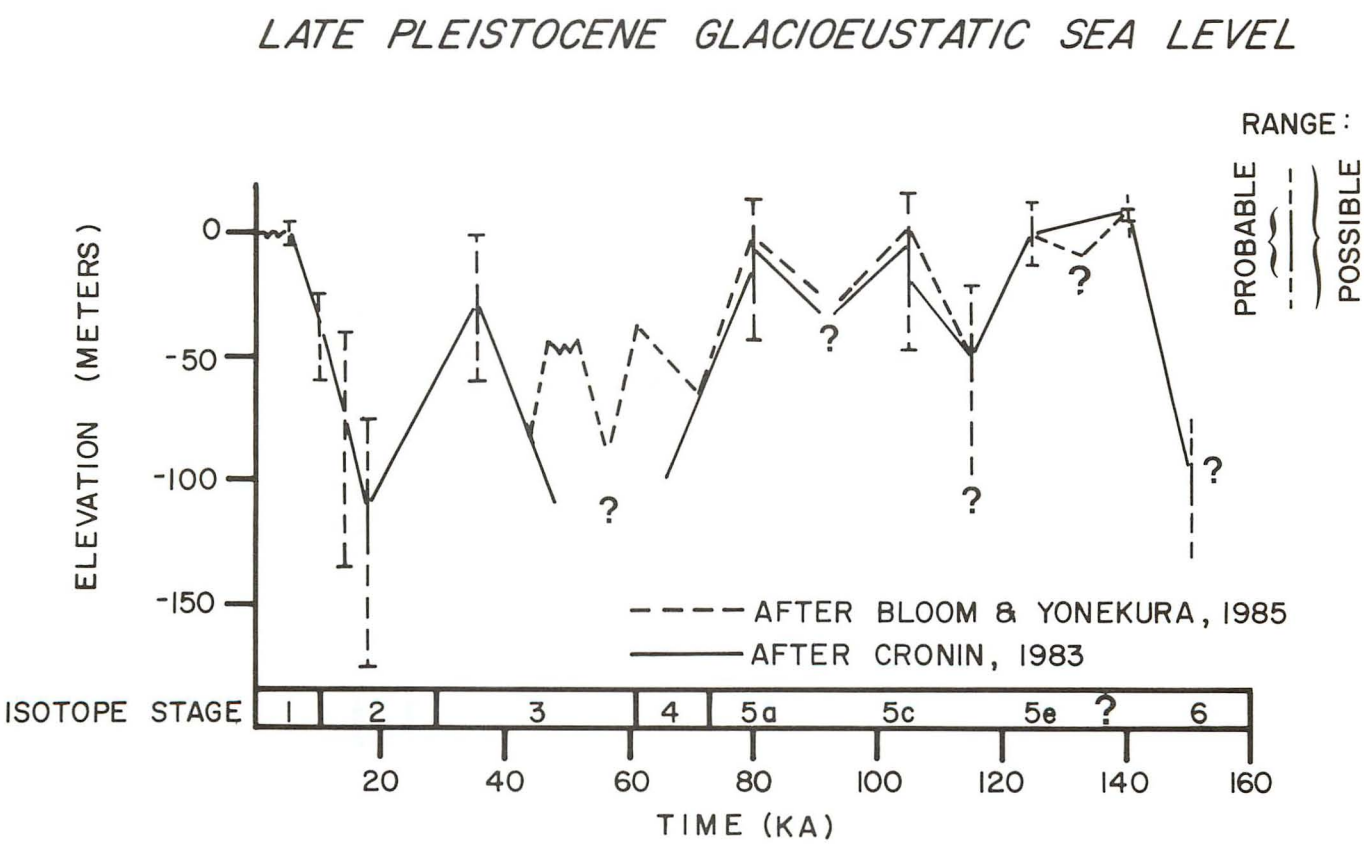

Figure 2.—Generalized late Pleistocene glacioeustatic sea level curve.

was supported by Th/U ages on corals (Chappell and Veeh, 1978) from reef II of 31 ka. Paleosealevels for this reef have been estimated at between -40 and -42 meters (Chappell, 1974; Bloom *et al.,* 1974) and -44 ± 2 meters (Chappell and Shackleton, 1986). The most recent work of Bloom and Yonekura (1985) contained sea level estimates for reef IV (stage 3/4, 60 ka) at -24.0 meters MSL, Reef IIIa (stage 3, 50-40 ka) at -45.8 meters MSL, Reef IIIb (stage 3, 40 ka) at -38.3 meters MSL, reef II (stage 3) of -35.1 meters MSL, and Reef II (28-31 ka, stage 2) at -35.1 m MSL.

The large uncertainty in Bloom's (1983) best estimate of sea level at 18 ka (oxygen-isotope stage 2) of -120 meters ± 60 meters is indicative of the difficulty in constraining full-glacial, low sea level. Currently the boundary between stages 2 and 1 is placed at approximately 11 ka (Imbrie *et al.,* 1984).

Whereas transgressive deposits and peak sea levels for the past 125 ka appear to be consistent in many areas worldwide, the intervening lowstands are not well documented in any emergent coastal section, and estimates of even relatively high lowstands (e.g. substages 5d - 5a) are presented with wide error ranges (Figure 2). The continental shelf, however, should contain areas with more complete vertical sequences of sea level fluctuations within interglacials, excluding barrier deposits of the peak transgressions. Most of the record of the 53 ka-long stage 5, the latest pre-Holocene interglacial highstand to have affected the Atlantic coast, should be preserved below present sea level because the majority of stage 5 was characterized by less-than-maximum sea levels. The shelf affords a unique opportunity to study the regressive phase of the last interglacial and the nature of deposits produced therein. This type of study cannot be accomplished in stable carbonate areas, nor in tectonically rising reef tracts, where only peak transgressive deposits are produced.

HOLOCENE SEA LEVEL

The late Holocene rise of sea level has been well documented for the New Jersey coast (Stuvier and Daddario, 1976), Delaware coast (Belknap and Kraft, 1977) and the Virginia coast (Newman and Rusnak, 1965). Previous Holocene sea level positions are indicated by basal peat elevations and ^{14}C dating (Figure 3). New radiocarbon ages on sea level from peats from the Maryland shelf gathered for this study are discussed in terms of these records in a later section.

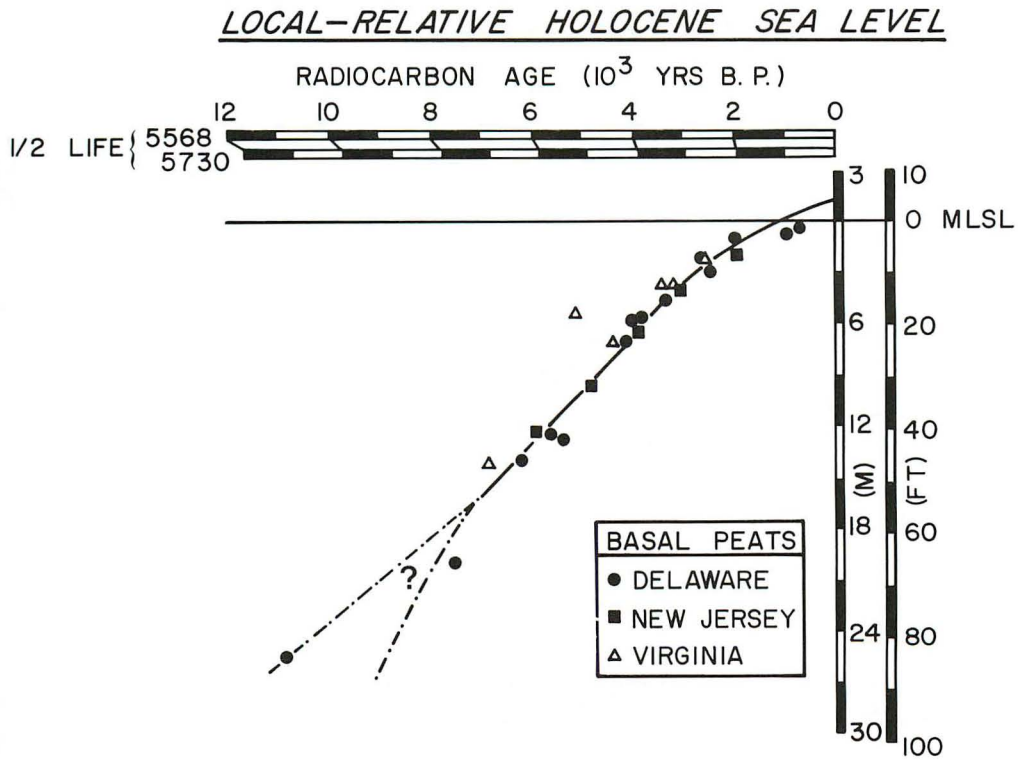

Figure 3.—Local-Relative Holocene sea level curve from coastal areas surrounding Maryland. After Belknap and Kraft (1977).

COASTAL PLAIN STRATIGRAPHY

TERTIARY DEPOSITS

The marine Yorktown Formation (Pliocene) underlies the Pleistocene deposits of coastal North Carolina, Virginia and at least the southern parts of Maryland along the Delmarva peninsula and the western shore of the Chesapeake Bay (Ward and Blackwelder, 1980). Mixon (1985) mapped the top of the Tertiary, i.e. the erosion surface above the Yorktown Formation, using extensive drillhole data on the Virginia part of the Delmarva Peninsula. Shideler *et al.* (1984) presented a more detailed map of the Yorktown surface from seismic data for the area between Fishermans Island and Cobb Island, Virginia (Figure 4). Shideler *et al.* 's (1984) map shows a furrowed surface at -20 meters MSL nearshore, deepening to -55 meters approximately 12 km offshore. The topography of the surface reflects a network of paleovalleys and interfluves interpreted as a composite erosional surface initiated in late Tertiary time and reoccupied during Pleistocene glacial episodes, possibly including the Illinoian (oxygen-isotope stage 6). Near the Maryland-Virginia border the surface slopes from approximately -6 meters inland at Hallwood (Virginia) to approximately -20 meters in the nearshore (Mixon, 1985). Unfortunately, no such surface is mapped for the Maryland coastal plain. Beneath the Maryland portion of the Delmarva Peninsula, the Pliocene Beaverdam Sand either interfingers with and/or overlies the Yorktown (or "Yorktown/Cohansey") in an undetermined relationship, possibly a facies change (Owens and Denny, 1979). Owens and Denny (1979) contoured only the "form of the base" of the Pliocene Beaverdam Sand from drillhole data.

QUATERNARY (PLEISTOCENE AND HOLOCENE) DEPOSITS

The surficial deposits of the emerged U.S. Atlantic coastal plain represent multiple relict shorelines in the form of paralic units and related marine sediments emplaced on consecutive terraces. A general model of terrace stratigraphy was developed by Peebles (1984), who described a complete transgressive sequence of basal fluvial channel-fill, paludal, estuarine, marsh, lagoonal, back-barrier, and barrier facies. Evidence for emplacement of paleoshorelines related to glacioeustatic sea level fluctuations is obtained from a combination of U-series dating of *in situ* corals and mollusks (Mixon *et al.,* 1982; Szabo *et al.,* 1985), amino acid ratios on mollusks and kinetic modeling of paleotemperatures (Wehmiller *et al.,* 1988), and ostracode paleoclimatic zonation (Cronin *et al.,* 1981). According to Cronin *et al.* (1981), both pollen and ostracode assemblages are indicative of warmer than present climates for most coastal plain deposits, directly linking their genesis to warm interglacial periods of low ice volume and high sea level. Ages of warm climate, high sea level coastal plain deposits cluster at ≈72 ka, ≈94 ka, ≈120 ka, ≈188 ka, and >400 ka, roughly corresponding to oxygen-isotope stages 5a, 5c, 5e, 7, and 11.

Superimposed on the primary glacioeustatic mechanism for emplacement of these paleoshorelines is a secondary tectonic uplift element that must be invoked in order to reconcile the present elevations of the deposits to the sea levels predicted by the glacioeustatic models previously presented. In attempting this reconciliation, Cronin *et al.* (1981) and Cronin (1981) reported that in many cases, the observed present strandline elevation exceeded the sea levels predicted by glacioeustacy, implying uplift rates of between 1-3 cm/1000 yrs and 4.2-9.3 cm/1000 yrs. Cronin *et al.* (1981) judged the latter rates to be unreasonably high; however they conclude that uplift rates of 1-3 cm/1000 yrs are reasonable. These rates do not preclude episodic rate increases to bring the terraces to their present level. Lithospheric flexure was postulated by Cronin (1981) as the most probable mechanism to account for much of the observed uplift in the South Carolina Coastal Plain/Carolina Trough. Hydroisostasy probably also has affected coastal plain elevations periodically (Cronin, 1981).

Adjacent to the study area and extending along the eastern shore of the Delmarva Peninsula is a major late Pleistocene shoreline complex, traceable from the well-preserved spits and barriers of the Wachapreague Formation on Mockhorn Island and Bell, Bradford, and Upshur Necks (Mixon, 1985) through Mills Island and Sinepuxent Neck (Sinepuxent Formation; Owens and Denny, 1979) in Maryland and veering northeast and offshore at Bethany Beach, Delaware (Omar Formation; Demarest, 1981) (Figure 5). This paleoshoreline complex was emplaced oblique to the present barrier system, leaving well-preserved shoreline features to the south, and progressive truncation of the features to the north where they are currently being eroded at the shoreface at Bethany Beach.

Stratigraphic and geochronologic analyses of the Bethany paralic unit were completed by McDonald (1982) who determined its age from radiocarbon and amino acid age determinations. All ^{14}C samples were isotopically dead (>40 ka). Amino acid leucine-isoleucine (D/L) ratios of 0.22-0.29 on *Mulinia* were determined, based on correlation to isotopically dated correlative coastal plain localities and kinetic models of

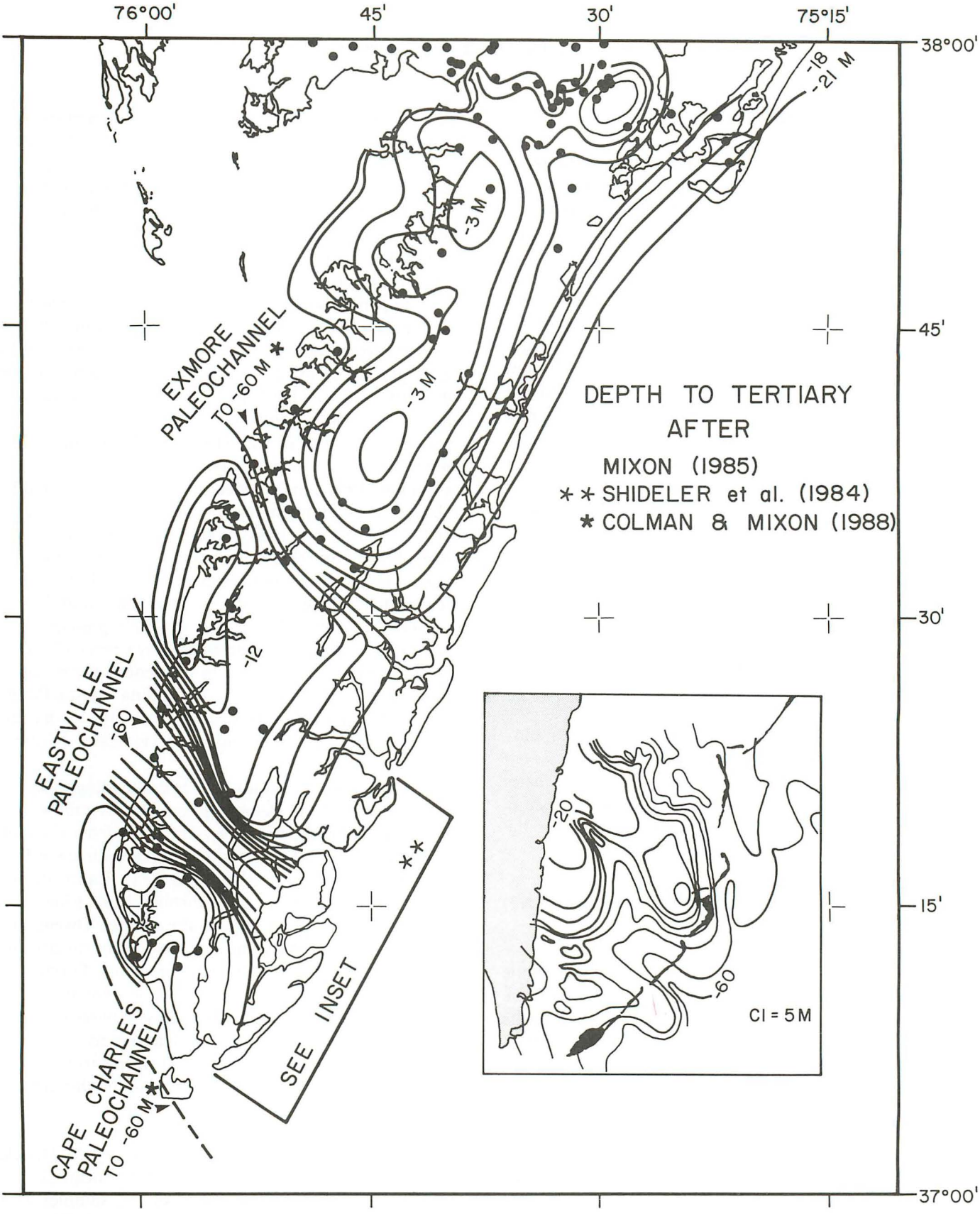

Figure 4.—Depth to erosional surface at top of Tertiary, after Mixon (1985), Colman and Mixon (1988), and Shideler et al. (1984). Depth of Exmore paleochannel revised to approximately −60 meters MSL, by Colman and Mixon (1988).

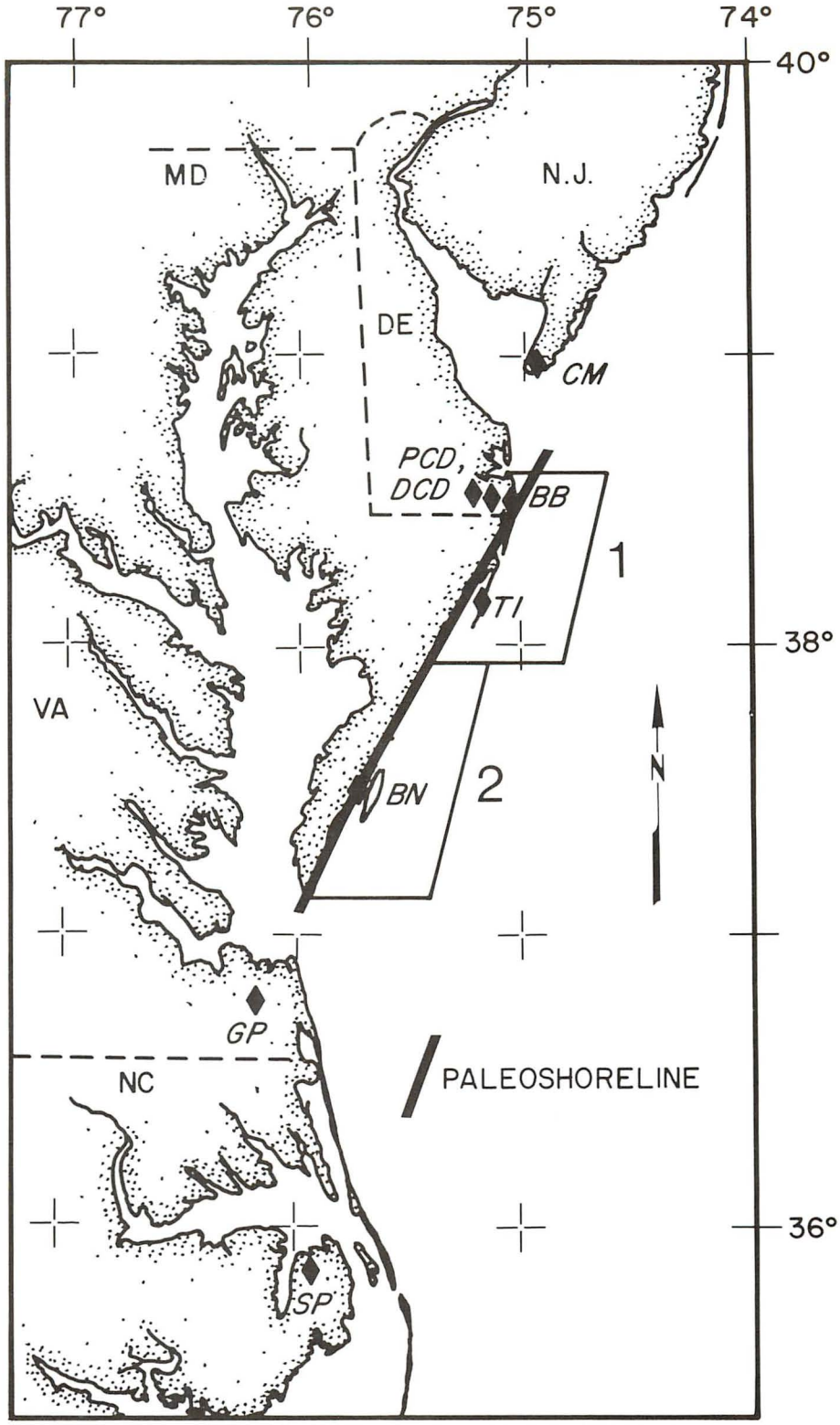

Figure 5.—Late Pleistocene shoreline trend with dated, stratigraphically documented reference localities. Area 1 includes the Omar Formation (BB — Bethany Beach, DE), the Ironshire/Sinepuxent Formations (TI) and Chincoteague Bay islands. Area 2 includes the Joynes Neck Sand and Wachapreague (Bell-Bradford-Upshur Neck spit complex — BN). BN (Bell Neck, VA) corresponds to the location of USGS core EX-24 (Mixon, 1985). Localities CM (Cape May, NJ), GP (Gomez Pit, VA), and SP (Stetson Pit, NC) are included as radiometrically and amino acid-dated reference points for the regional aminostratigraphy presented in Figure 25.

racemization (Belknap and Wehmiller, 1980), to represent an age of 100,000 ± 25,000 yrs BP, and a correlation with oxygen-isotope stage 5.

Any attempt to establish the continuity between the shoreline complex at Bethany Beach in Delaware and the Joynes Neck Sand/Wachapreague Formation in Virginia introduces a variety of problems for the Maryland portion of the paleoshoreline (Sinepuxent Neck and Chincoteague Bay Islands). The western side of Chincoteague and Sinepuxent Bays includes a prominent, east-facing scarp, the Berlin scarp of Owens and Denny (1979), which separates the sand and gravel of the Ironshire Formation from the seaward Sinepuxent Neck lowland underlain by the Sinepuxent Formation. Owens and Denny (1979) noted a peat layer in several USGS drillholes in Sinepuxent Neck, and apparently traced the peat eastward under Assateague Island. Weigle (1974) reported finding peat layers at -32 feet (-9.75 meters MSL) in core WOR-DG-13 on Assateague Island and at -27 feet (-8.23 meters MSL) in core WOR-BG-83 at Ocean City. Owens and Denny (1979) reported that radiocarbon analyses on some of the peat samples were near 31,000 ± 1000 yr BP whereas others were older than the upper limit for the method (34 ka in this case). However, in this age range, slight modern carbon contamination causes ^{14}C age determinations to become dramatically younger; therefore, it is reasonable to treat all such ages as minima. Although Owens and Denny (1979) acknowledged that shells typically give less reliable ages than woody materials, they obtained a ^{14}C age of 28 ka on unidentified shells from beneath the peaty unit under Assateague Island, and they viewed this 28 ka age as support for the 31 ka age of the peat under Sinepuxent neck, disregarding the other isotopically dead analyses of samples from the same unit. Their resulting interpretation of the Sinepuxent Formation as a marginal marine unit emplaced during a middle Wisconsin high stand of the sea, which they estimated at approximately +5 m MSL, contradicts those glacioeustatic and isotopic records previously discussed, none of which support high sea levels of +5 meters MSL, or even close to modern sea level, at 30 ka.

A problem arises from Owens and Denny's (1979) assumed lack of relationship between the Ironshire Formation, a sand and gravel, coast-parallel unit, and the marginal-marine Sinepuxent Formation. Owens and Denny (1979) stated that the Sinepuxent in no place overlies the Ironshire, that the Sinepuxent was emplaced in middle Wisconsin (oxygen-isotope stage 3) time after the bulk of the Ironshire had been "removed," and that they could identify no barrier facies associated with the Sinepuxent Formation. Owens and Denny (1979) interpreted the Ironshire as a late Sangamon (oxygen-isotope stage 5) deposit, distinct from the Omar Formation of Demarest *et al.* (1981), based on warm interglacial pollen assemblages.

Aligned with Sinepuxent Neck, just off the west shore of Chincoteague Bay, Robbins Marsh, Big Bay Point and Mills Island form the link between the Ironshire/Sinepuxent and Joynes Neck/Wachapreague portions of the paleoshoreline. Beneath surficial Holocene marsh sediments topping these islands are Pleistocene oxidized sands and some dewatered green-gray muds. No radiometric dating is available at these localities. The sands have been interpreted as Pleistocene beach ridge remnants (Biggs, 1970) as well as "mid Wisconsin" spits (Halsey, 1978).

The Virginia eastern shore contains the Wachapreague Formation of Mixon (1985) which consists of a series of well-preserved relict barrier spits lying seaward of the Mappsburg scarp at 3–4.5 meters MSL elevations. This Bell Neck sand ridge complex (Mixon, 1985) includes Bell, Bradford, and Upshur necks and Mockhorn Island at the southern end of the Delmarva Peninsula. The complex is interpreted as a regressive sequence of barriers and lagoons. North of Metomkin Bay the Joynes Neck Sand forms a somewhat older paleoshoreline and is separated from the Wachapreague by the Mappsburg scarp. Mixon (1985) attributes this break between the two units as a minor sea level fluctuation, so that the Joynes Neck and Wachapreague Formations may represent transgressive/regressive phases of a single sea level cycle. No radiometric dating is available for the Joynes Neck Sand.

At its type section (borehole EX-24; Mixon, 1985) at Upshur Neck, Virginia, on a relict barrier, the Wachapreague directly overlies the Yorktown Formation (Pliocene) and is defined by a lower, 6-meter thick clayey and silty, fine to very fine gray sand and clay-silt with pollen, ostracode, and molluscan assemblages indicative of a shallow shelf environment, and by an upper 5.2 meters of medium to very coarse gravelly sands with heavy mineral laminae and no macrofossils, which is characteristic of beach ridges.

From the lower unit, ostracode assemblages indicate generally mild-temperate climatic conditions, with a few cold-climate elements, suggesting oceanic conditions similar to those of today. Pollen assemblages, derived from adjacent land sources, document extremes of temperature more dramatically than do the marine data; specifically, the pollen assemblages indicate an upsection trend from warm temperature (in early Wachapreague time) to progressively cooler temperatures (in late Wachapreague time).

Age estimates for samples from the Bell Neck borehole (EX-24; Mixon, 1985) ranged from 128 ka (U-series on *Mercenaria* shells) to 82 ka (amino acid leucine-isoleucine ratios of 0.284 on *Mesodesma* shells) and are within oxygen-isotope stage 5 boundaries of 128-75 ka (Martinson *et al.,* 1987; Imbrie *et al.,* 1984). Radiocarbon dates of approximately 33 ka were viewed as representing only minimum ages (Mixon, 1985).

Biggs (1970) and Halsey (1978) investigated the late Quaternary stratigraphy of the Assateague Island-Chincoteague Bay area, with emphasis on the Holocene barrier system. Halsey (1978) combined much of Biggs' (1970) core and other data with numerous drillholes from several sources to derive her Pleistocene-Holocene history for the area. Beneath the undisputed Holocene barrier sequence is a ubiquitous "Tri-part lithosome" of dark greenish gray, dewatered ("stiff"), fossiliferous mud containing minor coarser sediments. Halsey (1978) applied a mid Wisconsin high sea level stand framework (based on radiocarbon ages) to interpret the muds; however, she acknowledged that there is no Holocene transgressive analog for such a thick and widespread mud lithosome. The Holocene depositional systems of Assateague Island and Chincoteague Bay are outlined by Bartberger (1976) and Leatherman (1979). General correlations for the Delmarva-Chesapeake area are given in Figure 6.

METHODS

SURFICIAL SEDIMENT SAMPLING

A one-kilometer grid system utilizing LORAN-C lanes was designed for sampling surficial sediments (Kerhin and Williams, 1987). Individual sample sites are plotted on Figures 7-11. Sediments were collected with Peterson and Van Veen samplers. The top 10 cm were reserved for laboratory analyses. Weight percents of clay and silt (from pipette analysis), and sand and gravel were determined in addition to statistical parameters (Mz, STD) determined on the washed sand fraction by RSA analysis. Grain size data is summarized in Appendix I.

SEISMIC PROFILING

High-resolution seismic-reflection surveys were conducted from the Maryland Geological Survey's research vessel *Discovery* in cooperation with the U.S. Geological Survey, who provided equipment, technicians, and scientists. In 1985, approximately 580 kilometers of tracklines were surveyed using both a Geopulse boomer system at a setting of 280 joules and a Datasonics 3.5 kHz acoustic profiler (Plate 1), with time fixes at 5 minute intervals. The EG&G seabed mapping system was used to collect sidescan sonar records for 200 kilometers of the 1985 tracklines. In 1987, approximately 407 kilometers of additional tracklines were surveyed using the same equipment. Tracklines followed LORAN-C lanes for ease of navigation.

VIBRACORING

Vibracores were collected in August of 1986. A total of 29 9 cm-diameter vibracores, most of which were 6 meters in length, were collected at sites selected after initial interpretation of the 1985 seismic reflection profiles (Plate 2). Cores were divided into 1.5 meter or smaller sections for ease of handling. The vibracores were xeroradiographed, photographed, and logged. Subsamples from the cores were collected for micropaleontology, grain-size analysis, heavy mineral identifications, and ^{14}C and amino acid racemization age determinations.

AMINO ACID RACEMIZATION ANALYSES

Between 5 and 26 molluscan bivalves were collected from nine cores and analyzed for the extent of amino acid racemization (Appendix II). These samples represent one of the most detailed collections of Pleistocene mollusks from marine deposits on a continental shelf ever made for amino acid analyses. The majority of shells that were analyzed from the cores are *Mulinia lateralis* (Say), which were present in all cores with the exception of cores 16-1002 and 16-935. Other bivalves analyzed (in order of decreasing frequency) are *Spisula solidissima, Ensis directus, Mercenaria* sp., *Anadara* sp. and *Astarte* sp.

The principles of amino acid racemization and the geochemical dating method based upon this reaction are summarized in Wehmiller (1984, 1986). Laboratory analysis of the samples followed a general ion-exchange chromatographic procedure employed by most amino-stratigraphic laboratories (Bowen *et al.,* 1985; Miller and Mangerud, 1985). Whole *Mulinia* valves and fragments of other genera were analyzed by High Pressure Liquid Chromatography (HPLC) with fluorescence detection and electronic peak integration. All samples were analyzed for the D-alloisoleucine to L-isoleucine ratio (A/I ratio), which is the only enantiomeric ratio determined by this HPLC analytical method. The A/I ratios shown in this report are peak area ratios determined for the total amino acid fraction (those amino acids released by acid hydrolysis) within the shell sample.

A/I ratios of mollusk samples analyzed from the nine cores are summarized in Appendix II. Mean A/I ratios were calculated for each genus within each lithologic unit in each core. Mean, standard deviation

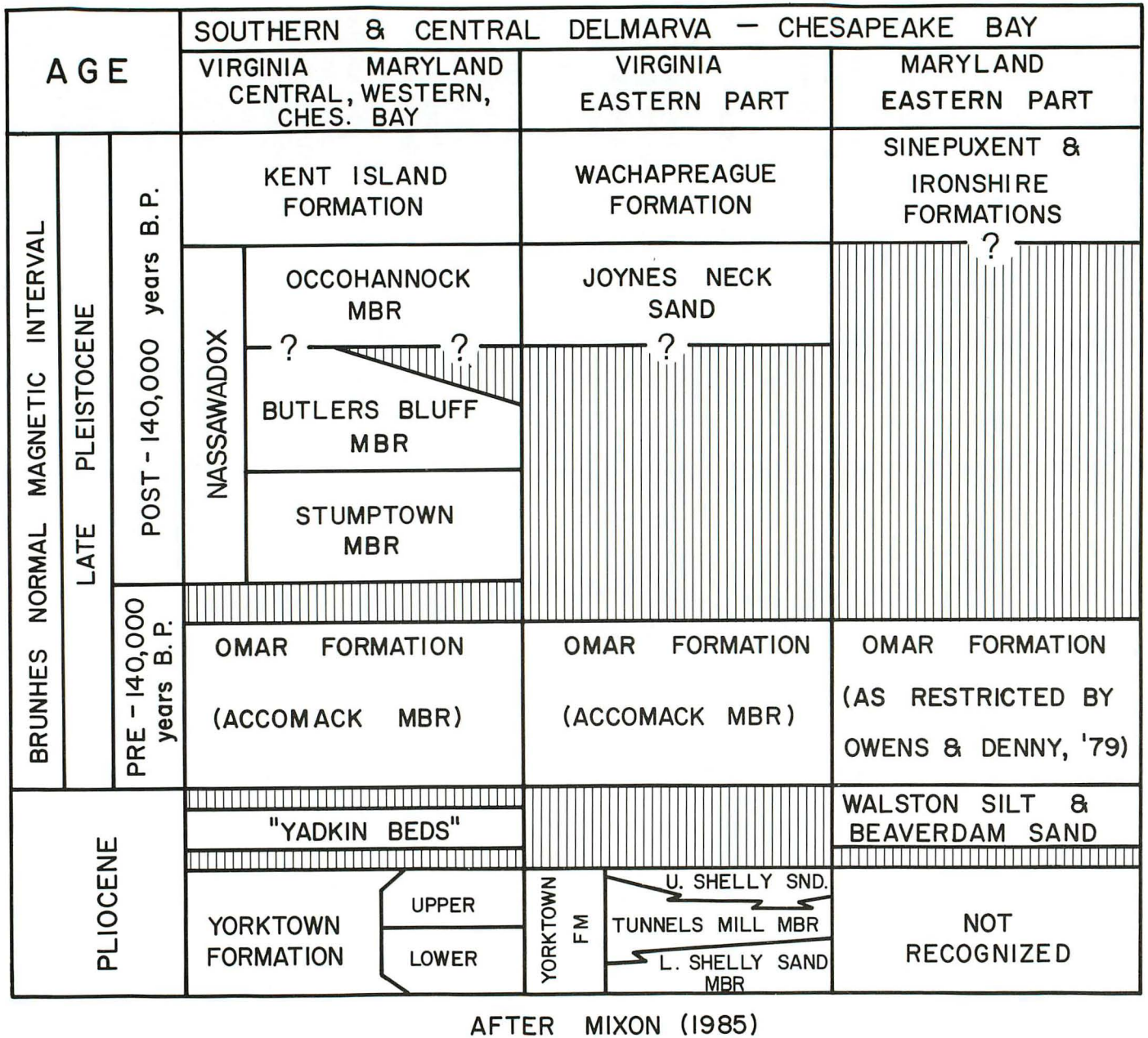

Figure 6.—Generalized Delmarva Peninsula — Chesapeake Bay stratigraphic correlation chart. After Mixon (1985).

and coefficient of variation (c.v.) values are shown in Appendix II. Coefficient of variation values (standard deviation/mean) are a measure of the variability of the data (Wehmiller *et al.,* 1988). A/I values and in-core depths of samples analyzed are shown for each genus in each lithologic unit.

OSTRACODE ANALYSIS

Marine Ostracoda (small bivalved Crustacea) occur in marine, back-barrier, and estuarine habitats and are common as fossils. Many modern ostracode species are climatically restricted and climatically-controlled assemblages have been documented in faunal provinces for the entire U.S. Atlantic coast (Hazel, 1968; 1970; Valentine, 1971; Cronin, 1988). In an attempt to reconstruct the paleoclimatic history of the Maryland shelf sediments, ostracode assemblages from twelve cores were examined (Appendix IV).

These data represent a detailed micropaleontological analysis of Pleistocene interglacial deposits for this region. A total of 9519 ostracode specimens from 105 samples taken from 12 cores were studied. In Appendix IV, Table XII lists the depths of the samples studied for each core and Figure 33 shows the numbers of ostracode specimens at different depths in the three most intensely studied cores (16-905, 18-1230, 27-1520). Ostracodes averaged about 89 specimens per sample, and frequently were abundant, reaching more than 100-200 specimens per sample (particularly in deposits representing Zone 3, discussed in a later section).

The cores contained many climatically significant species whose percentages varied with stratigraphic position in the cores. In Appendix IV, Table XIII lists the 38 species that occurred in the cores, listed according to the climatic zones they inhabit today. All species presently occur in euhaline conditions, i.e., no estuarine or backbarrier species were found in a ubiquitous shelf mud unit found in these cores, although *Cytheridea* sp. may inhabit slightly brackish water. The numbers of specimens of each of the 38 species in each sample of the most intensely studied cores (16-905, 18-1230, 27-1520) are given in Appendix IV, Table XIV. Changes in ostracode biofacies are interpreted as signifying climatically induced shifts in species zoogeography and from them a "climatostratigraphic" zonation can be developed for the area. This zonation allows correlation among the cores and with other Pleistocene units onshore. It also allows reconstruction of bottom water temperatures and inferences about paleoceanographic conditions. The application of ostracodes to paleoclimatology of the U.S. Atlantic is reviewed by Cronin (1988).

SURFICIAL SHELF SEDIMENTS

Sand is the dominant surficial sediment type found on the Maryland shelf (Kerhin and Williams, 1987). Field (1980) described the shelf sand body as a "thin (rarely exceeding 6 meters), locally discontinuous body having a nearly flat lower surface and an undulatory upper surface defined by the morphology of the seafloor." Sampling of surficial sediment and vibracoring in this study confirm this sand body geometry and its relationship to pre-Holocene units immediately underlying it.

One hundred and thirty one samples (Appendix I) were collected on the arbitrary 1 km grid and analyzed for grain size parameters and for percentages of clay and silt (mud), sand, and gravel (Folk, 1954). Kerhin and Williams (1987) gave a preliminary discussion of this data, herein expanded and re-illustrated. The wide spacing of these samples permits only general textural zones to be delineated. Other investigators (Swift and Field, 1981) have sampled within smaller grids (50 m); however, bedform complexities in ridge troughs and the great variability of grain size within shoals precluded resolution of possible trends or correlations between grain size and ridge morphology.

SAND

Figure 8 is a map of percent sand in each of the 131 surficial samples. Sand is consistently between 93 and 100% of each sample north of Ocean City inlet, with the exception of three small areas of less than 70% sand. South of Ocean City inlet the sand fraction does not predominate the sediment texture. Several zones occur where the sand fraction comprises less than 90% of the total sediment distribution. If bathymetry is superimposed over the percent sand map (Figure 9) it becomes apparent that zones of lower sand content trend oblique and perpendicular to the shoreline and to the orientation of the shelf shoal, indicating a little or no correlation between grain size and ridge morphology.

MUD

Two small areas of less than 70% sand occur near the shoreface north of Ocean City (Figure 8) and correspond exactly to two pockets of high mud content (Figure 10). Further south, a belt of relatively muddy

sediments occurs perpendicular to the shoreline, in less than 60 feet (18 meters) of water, corresponding to the elongate zone of relatively lower sand off Sinepuxent Neck (Figures 8 and 9). It is apparent that the muddy patches represent mixing of shelf sands with subcropping muds in troughs between shoals. Reworking of muds and intermixing with trough sands is probably a result of occasional long-period wave action on the shelf (Swift and Field, 1981).

GRAVEL

Gravel, which is not an important component of the sediments in the northern portion of the study area, becomes increasingly prominent both to the south and offshore (Figure 11). One vibracore (29-1640) taken on the flank of a shoal, contained at least two meters of sandy gravel underlain by relatively finer sands. However, most cores taken on shoal crests and flanks did not contain such high gravel contents.

SEISMIC-REFLECTION PROFILES

The spatial limitations of our study area may preclude the establishment of a regional character to our local seismic reflectors and therefore of seismic sequences in the strictest definition; however, studies by Field (1976, 1980) and Shideler *et al.* (1972) provide additional subbottom information appropriate for a regional synthesis.

SUBSURFACE UNITS IN MARYLAND

Field (1979, 1980) (Figure 12a) traced three major subsurface acoustic horizons (A1, B1, and C1). C1, between -67 and -76 meters MSL (0–6 km offshore) was inferred to be Tertiary in age, as was unit B between horizons B1 and C1. Horizon B1, at -27 to -38 meters MSL (2–10 km offshore) was inferred to represent the Quaternary-Tertiary unconformity, while horizon A1, directly underlying the linear shoals at -12 to -18 meters MSL (0–6 km offshore) was designated as the pre-Holocene erosion surface; the Pleistocene-Holocene boundary. Unit A was subdivided by reflectors A2, A3, and A4 according to Field (1976), who dropped A4 (see Field, 1980) and apparently equated A3 and A4, because they are confusingly plotted on his Figure 2a (Field, 1980) as the same reflector. According to Field (1976), the A4 is a persistent, mappable surface with no obvious relief, while A3 is discontinuous and difficult to distinguish as a discrete reflector. Henceforth they will be collectively referred to as horizon A3/A4. Field (1980) did not further describe his horizon A2, which appears to be at depths of -15 to -25 meters MSL, 0–10 km offshore.

In Field's (1976, 1980) study area, approximately 24 buried channels are incised into Unit A down to reflector A3/A4. Thalweg depths range from -16 to -30 meters below sea level (Field, 1980). Several of the buried paleochannels are positioned offshore of historic inlet sites along Assateague Island; however, the majority are more likely fluvial features.

SUBSURFACE UNITS IN VIRGINIA

According to Shideler *et al.* (1972), the base of the Quaternary sequence on the Virginia shelf is defined by a widespread, prominent, and relatively flat reflector (R1) overlying steeply-dipping Tertiary strata. Horizon R1 lies from approximately 30 to 75 meters below sea level, 1–25 km offshore, overlapping the depth range of Field's (1976, 1980) horizon B1 in nearshore areas. Above horizon R1 is a thick unit (B) composed of two facies, a lower one characterized by lenticular stratification cut by channels. Unit B is truncated at its top by another widespread horizon, R2, lying between 17 and 39 meters below sea level, overlapping inshore the depth range of Field's horizon A3/A4. Unit C above horizon R2 is described as an obscurely mottled to massive mud with thin fine sand lamina. The mud reportedly overlies a coarser-grained deposit in Unit C. The upper boundary of Unit C is horizon R3, which directly underlies the linear shoals of the inner shelf, equivalent to horizon A1 of Field (1980) for the Maryland shelf.

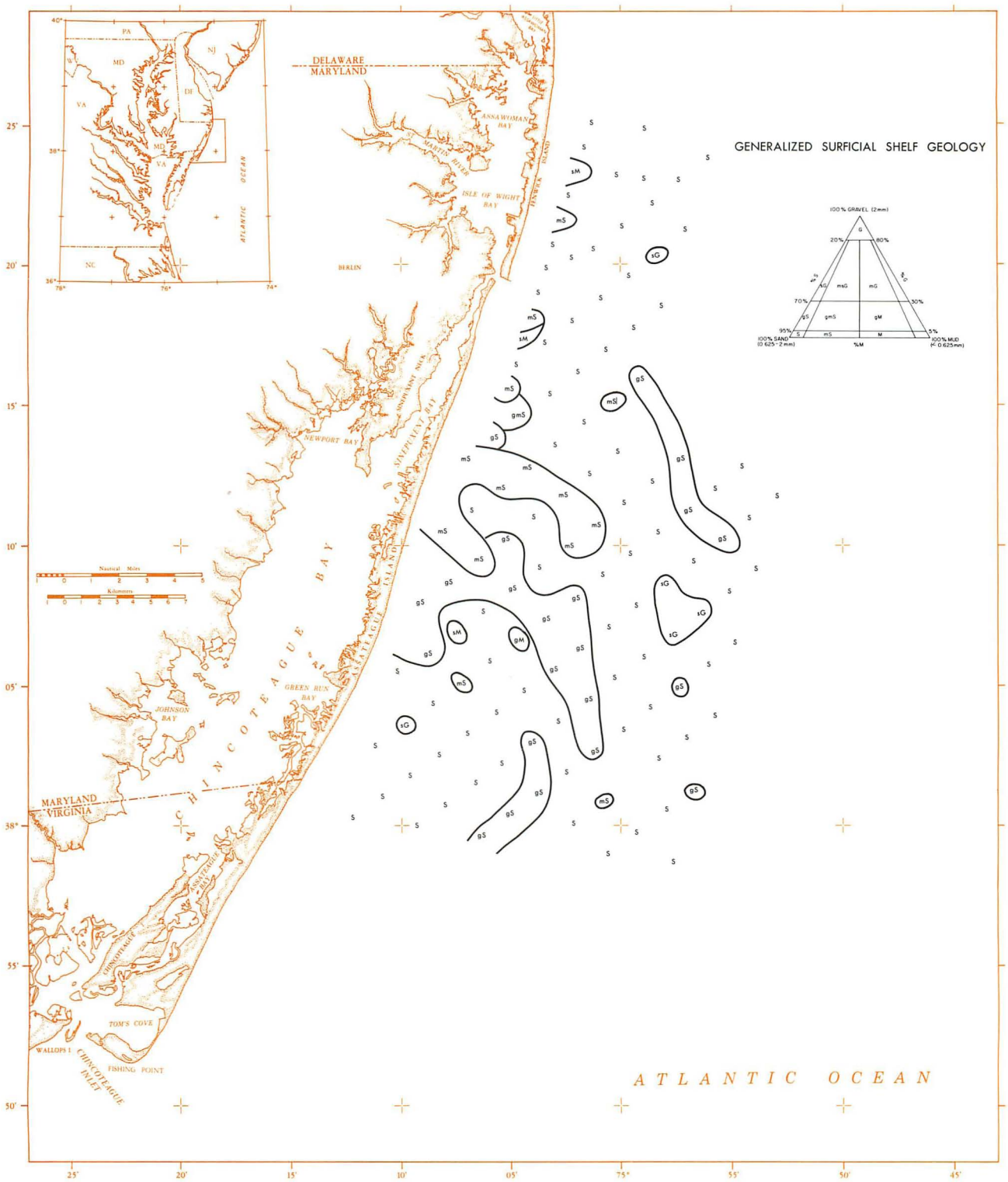

Figure 7.—Surficial shelf sediment distribution. Sample spacing 1 km.

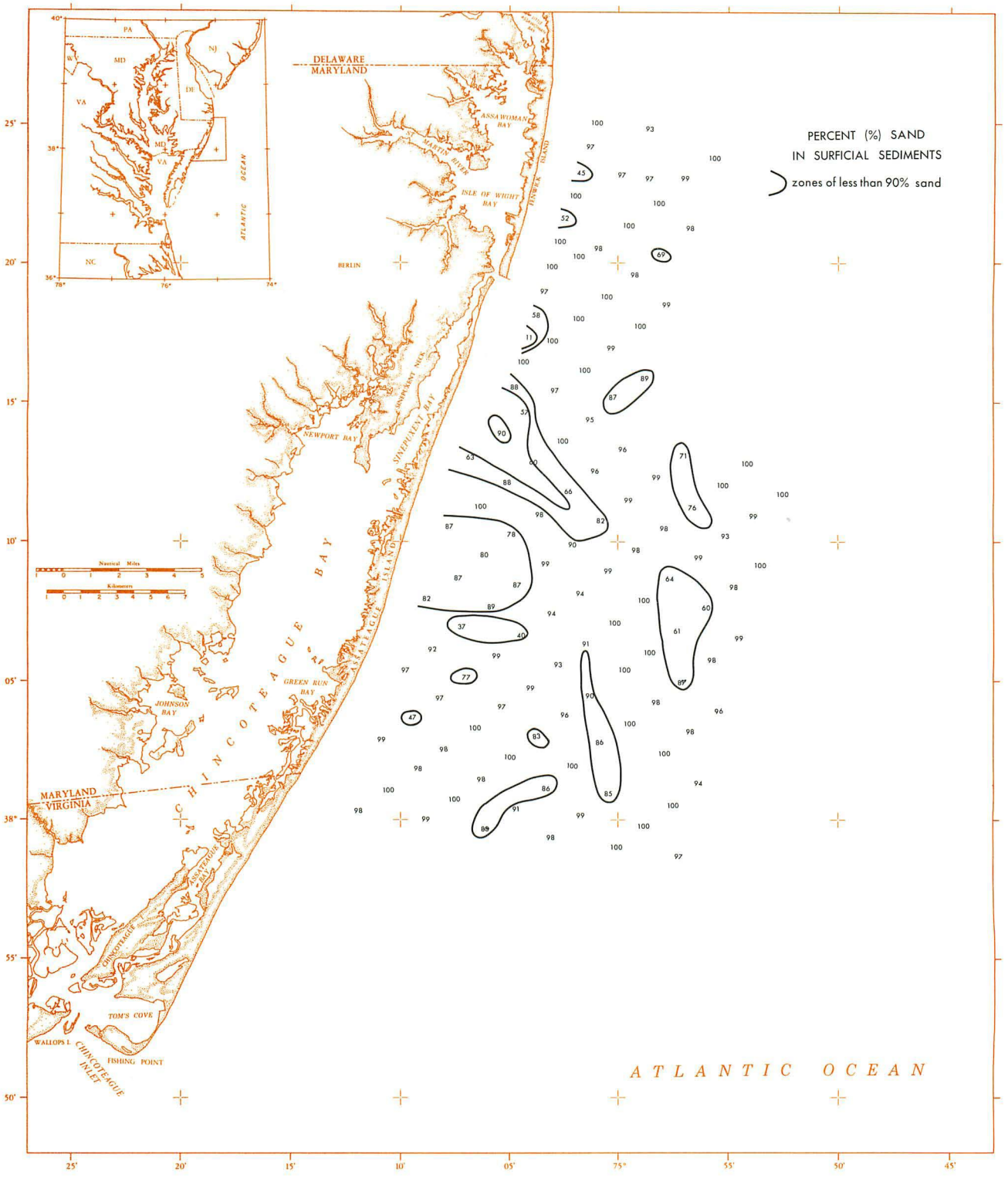

Figure 8.—Percent sand distribution, Maryland inner continental shelf. Zone lines do not represent contours.

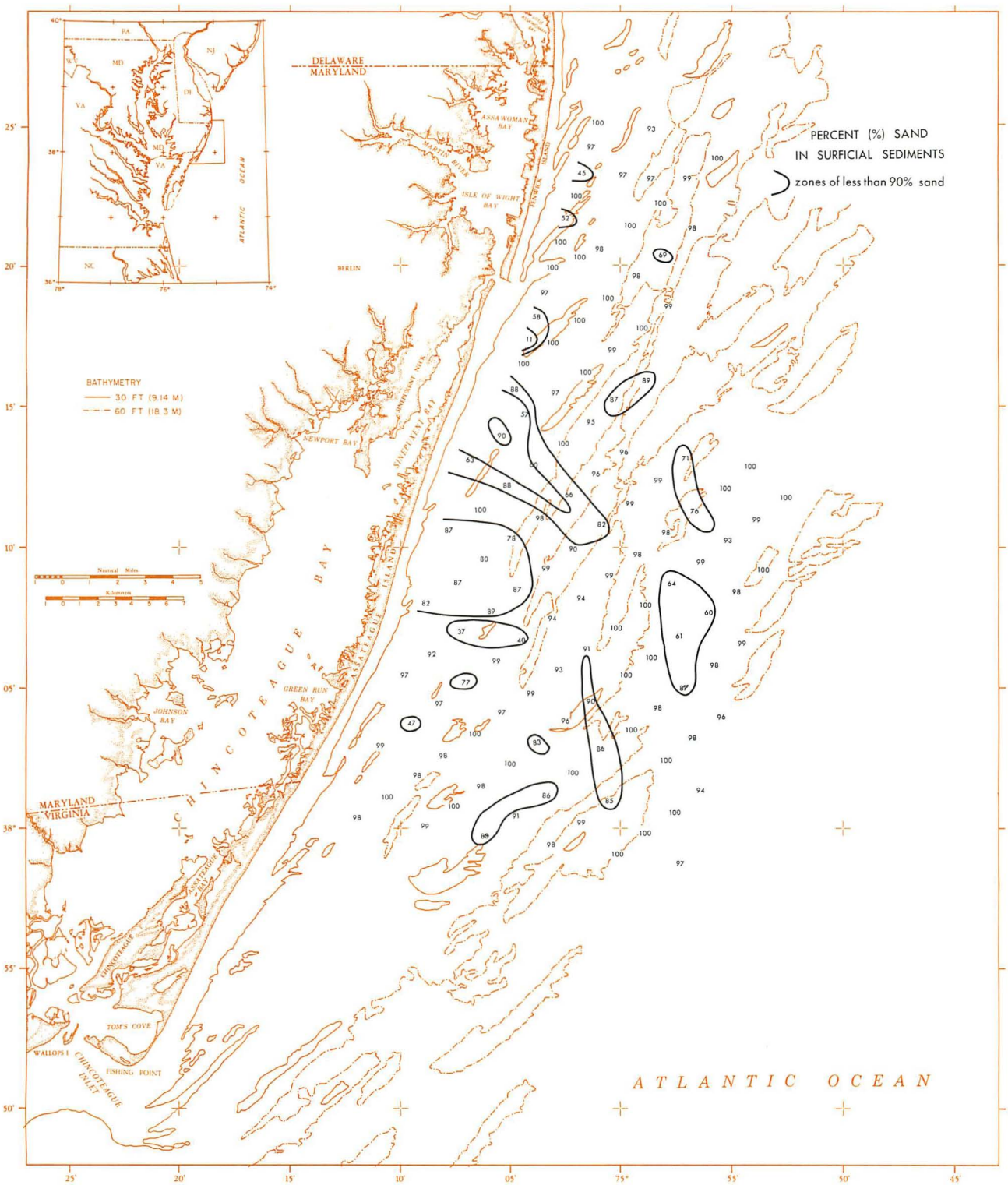

Figure 9.—Percent sand distribution and bathymetry, Maryland inner continental shelf. Zone lines do not represent contours.

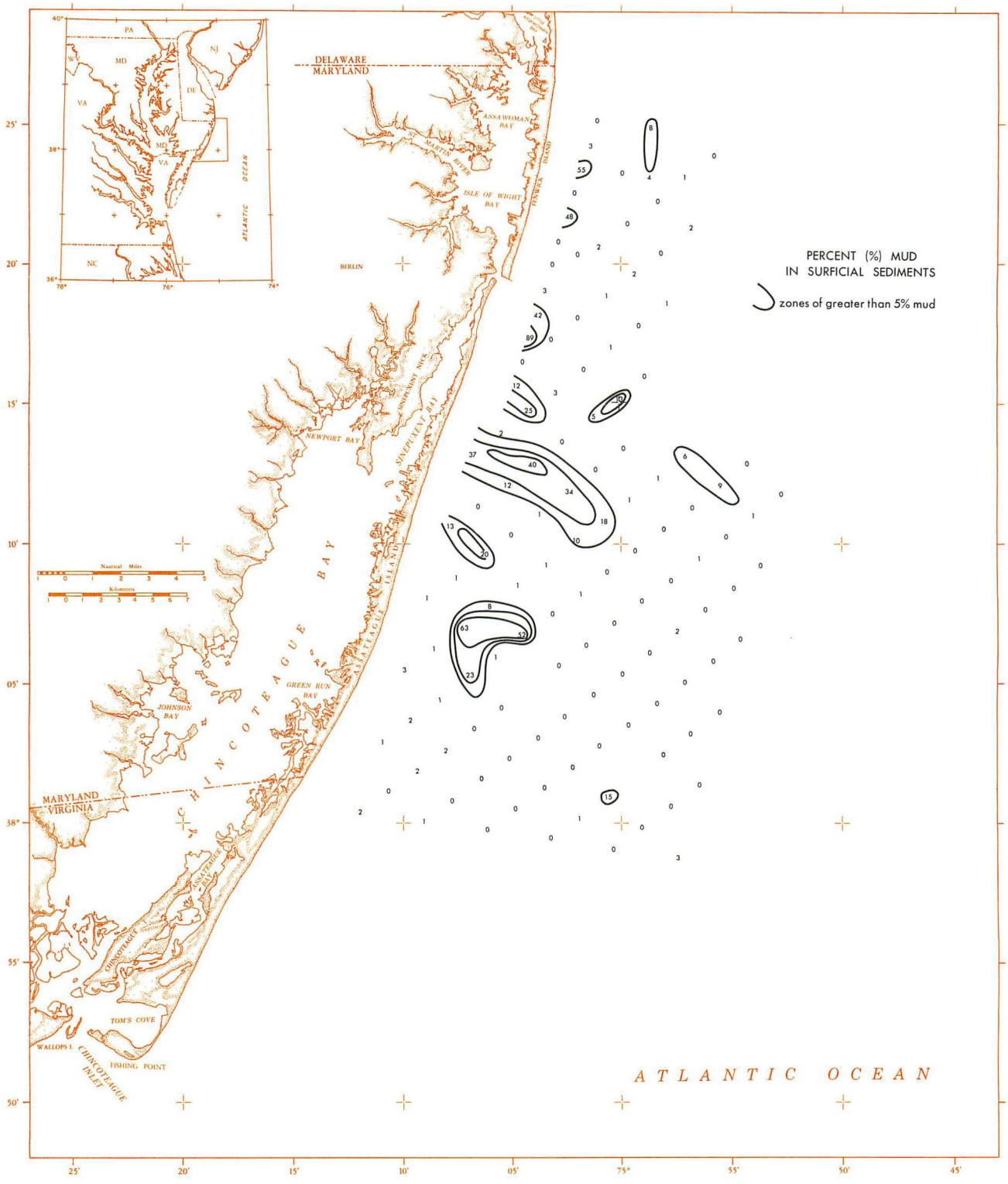

Figure 10.—Percent mud distribution, Maryland inner continental shelf. Zone lines do not represent contours.

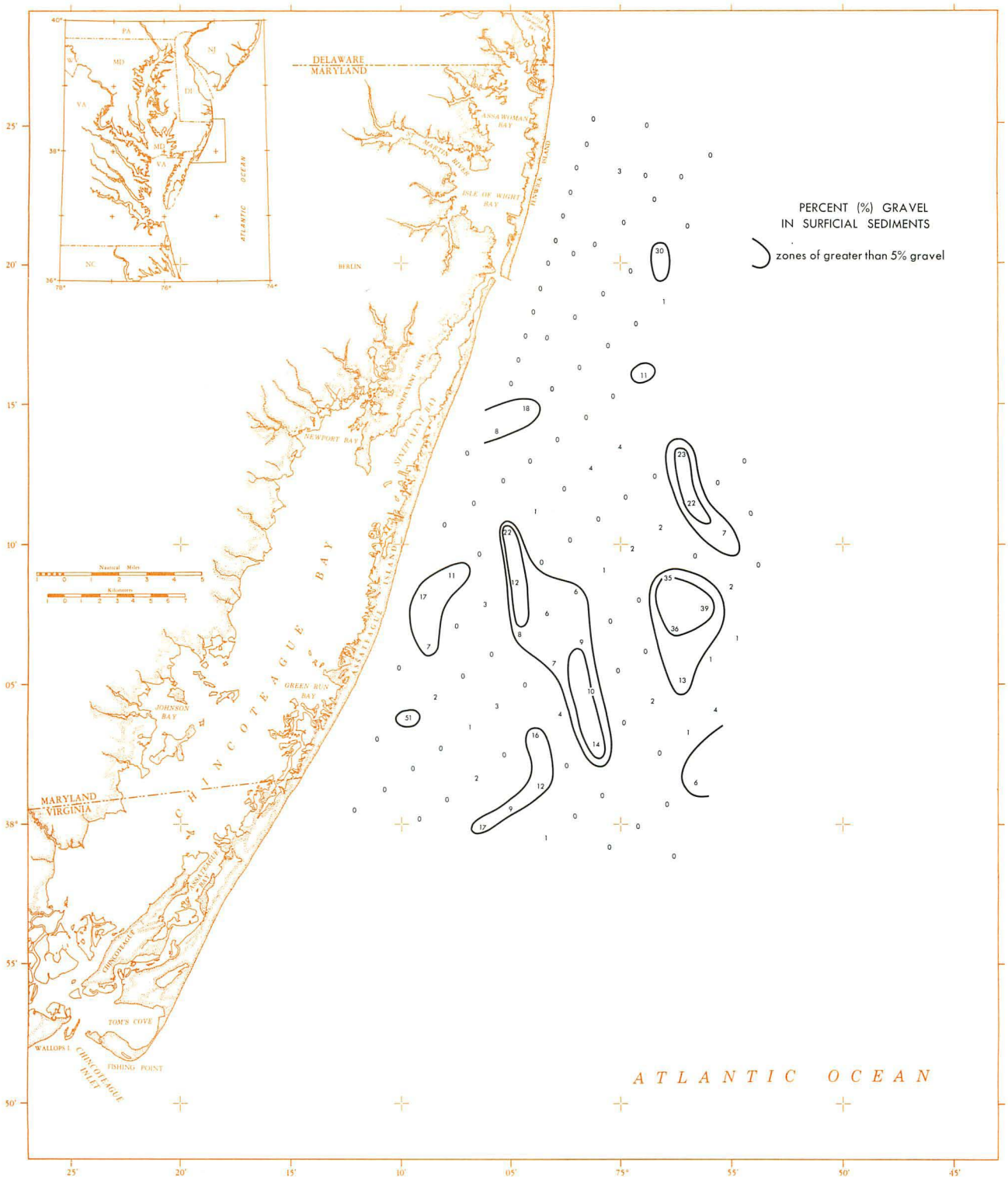

Figure 11.—Percent gravel distribution, Maryland inner continental shelf. Zone lines do not represent contours.

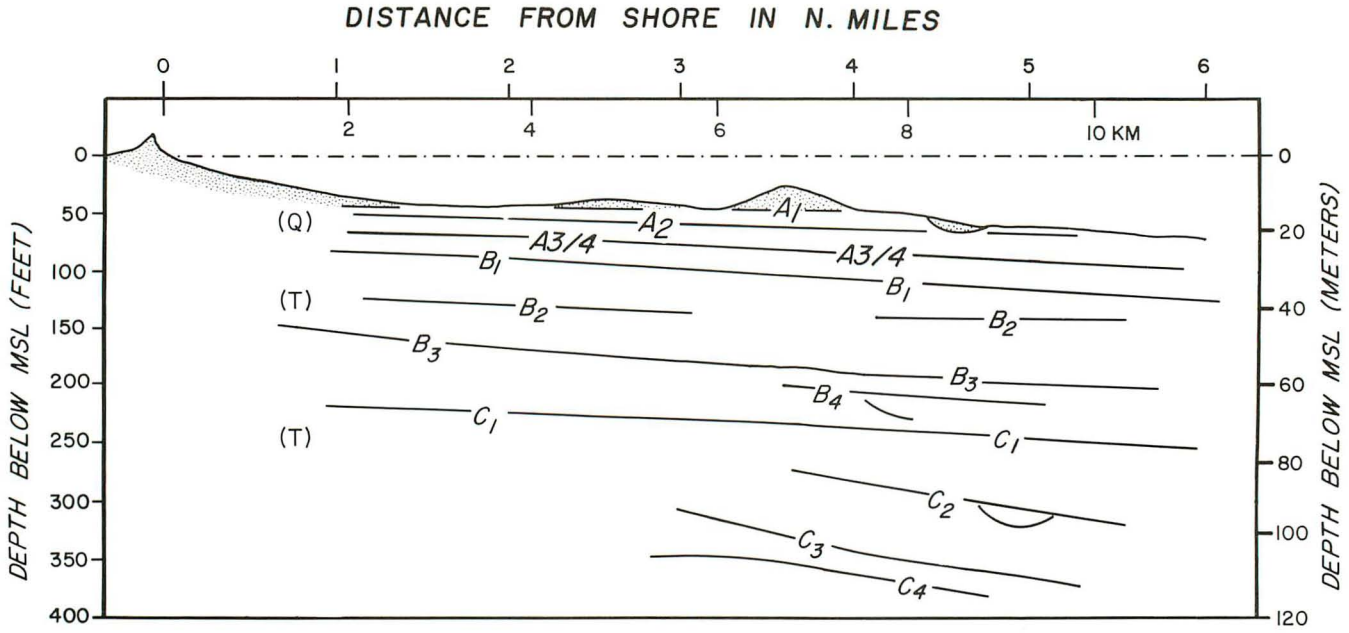

SEDIMENTARY SEQUENCE

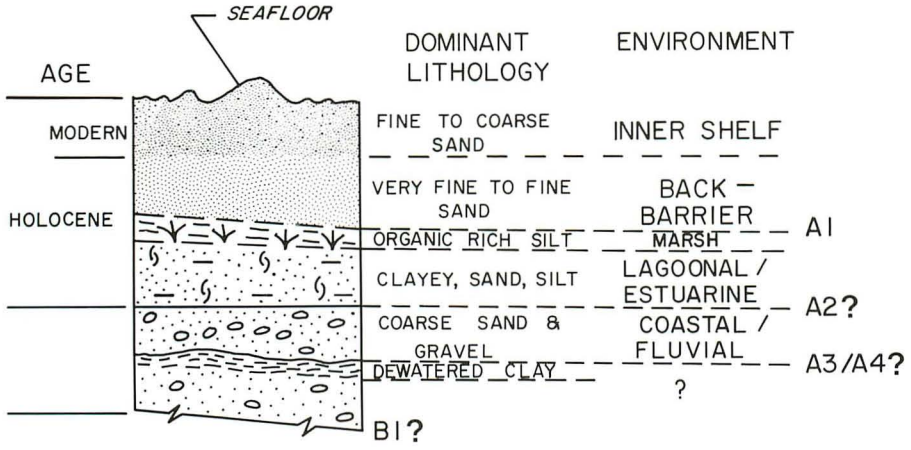

AFTER FIELD, 1976; 1980; & FIELD & DUANE, 1976.

CROSS — SECTION

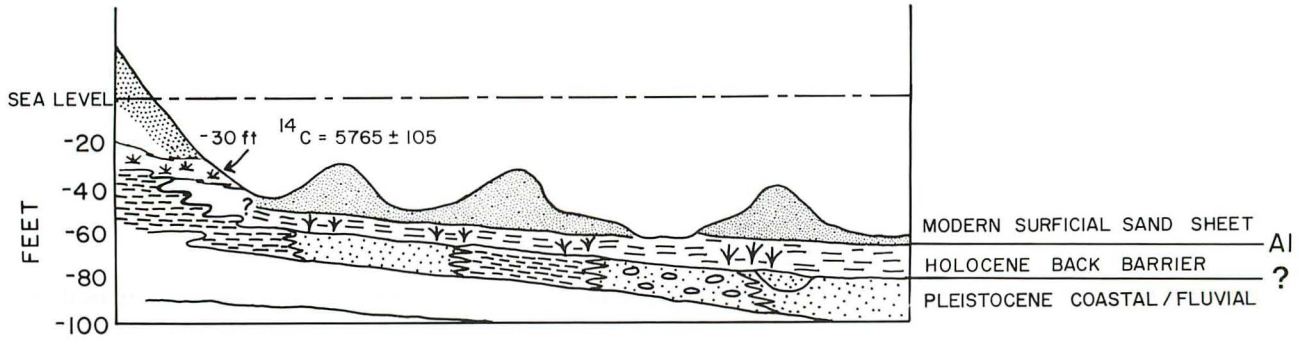

Figure 12.—Maryland inner continental shelf a) subbottom structure; b, c) stratigraphic sequence. After Field (1976; 1980).

MARYLAND SUBSURFACE UNITS — THIS STUDY

Interpretations of selected 1985 seismic-reflection profiles are presented in Figure 13. A scaled, schematic representation of shelf units that extended 40 km east of the coast versus Field's 10 km limit is presented in Figure 14.

Depositional Sequence 1

Unit T1 (Tertiary) —

Only the top boundary of this unit can be delineated. Maximum depth of penetration of our seismic equipment was less than 100 meters, and this combined with the thickness of the unit limited our ability to locate a bottom boundary. The top boundary is marked by a persistent reflector that truncates the high-angle to low-angle clinoforms and channels that characterize the uppermost portion of this unit, which is equivalent to unit B of Shideler *et al.* (1972). This persistent reflector shows a furrowed, eastward sloping surface that was shaped by subaerial erosion at a time of lowered sea level, then reoccupied in places by a later paleofluvial system. Plate III depicts the form and altitude of the reflector, from 21 meters below sea level along the shoreface to 40 meters below sea level at approximately 40 kilometers offshore. The reflector, herein named horizon M1, is prominent throughout the study area. M1 corresponds to horizon R2 (-17 to -39 m MSL) of Shideler *et al.* (1972) south of Cape Henry, Virginia, strongly suggesting that it has a widespread regional character. Our horizon M1 is the most prominent surface seen in all seismic-reflection profiles in this study. The comparable reflector of Field's (1980) study is the composite A3/A4 horizon, which corresponds to the depth range and persistent character of M1.

Depositional Sequence 2

Units Q1 and Q2 (Quaternary) —

The lower boundary of a near-surface tabular unit (units Q1 and Q2) is marked by the persistent reflector (horizon M1) at the top of unit T1. The upper boundary of units Q1 and Q2 (Field's (1976, 1980) A1 horizon) is essentially a ravinement disconformity separating the Pleistocene unit from Holocene shelf sands. Therefore, the A1 surface theoretically underlies the modern shelf linear sand ridges and crops out at the seabed in troughs between the ridges, equivalent to reflector R3 of Shideler *et al.* (1972). Owing to the subaqueous processes forming the ravinement surface and subsequent mixing of different lithologies found along this disconformity, the surface itself is indistinct on our seismic-reflection data. The disconformity between shoal sands and underlying sediment is, however, apparent from vibracores.

Seismic unit Q2 represents approximately the top 5–7 meters of the tabular unit, with a weaker reflector (presumably Field's (1976, 1980) A2 horizon) separating Q2 from Q1. Herein renamed M2, the reflector shows limited but prominent channeling, indicating an erosional (lower sea level) surface. Examples of this M2 channeling occur along line 25 between time fixes 1303-1313, and along line 40 between time fixes 1040-1045 (Figure 13). Horizon M2 is best defined along the inner portion of the study area from the 3.5 kHz records, because the 3.5 kHz signal is reflected by M2 with little or no deeper penetration. Depths to horizon M2 measured from the 3.5 kHz system were used to help distinguish the horizon on the ORE Geopulse records.

For both units Q1 and Q2 the internal seismic reflectors are indicative of concordant strata with parallel to subparallel bedding, becoming slightly subparallel in Q2 in the offshore direction. Along line 20, the uniform parallel-bedding of unit Q2 is cut by a distinct landward-dipping reflector at 20-1350, which grades into less distinguishable reflectors to 20-1415 (Figure 15). Further west, core 20-1430 (Appendix V) may have penetrated this lenticular body in Q2 beneath the reflector. This body gives the appearance of a relict shelf sand ridge analogous to the present shoal sands.

Unit Q3 (Quaternary) —

Deeply incised into units Q1 and Q2 and in some areas cutting into the M1 horizon, are numerous channels, which indicate fluvial erosion of the subaerial shelf during the most recent (late Wisconsin) glacial low sea level stand. Unit Q3 forms much of the fill of these channels, whose geometry is defined by reflector M3. Among many small, steep-sided channels is a prominent, wide, deep (38 meters) main channel that has been located on seismic lines 16, 18, 20, 22, and 43 and whose fill has been cored (16-935 and 16-945). Where the M3 channel has incised into M1, the deepened Tertiary/Quaternary unconformity (M1 surface) becomes the base of the hummocky central channel, with hummocky and chaotic reflectors defining the channel infilling sequence. Internal reflectors in smaller channels exhibit fill structures. Figure 16 depicts the widths and depths of channels traced from seismic-reflection profiles. Several older channels associated with the M2 reflector are indicated by shading. Resolution of channel depths and orientation from clusters or complexes shown in Figure 16 is presented in the Lithology and Stratigraphy section. Appendix VI gives data for individual channels in Figure 16.

Units Q4 and Q5 (Quaternary) —

Q4 represents remnants of Holocene transgressive coastal lithosomes that were preserved below the depth of ravinement erosion because of rapid sea level rise and/or characteristics of the antecedent topography (Belknap and Kraft, 1977; 1981; 1985). Unit Q4 may be defined as having 2 facies-suites, both represented by the upper portions of channel-fill sequences. The first occurs within the outer 13–19 (and possibly 40) kilometers of the study area (especially notable on the offshore ends of lines 16, 18, and 20), and consists of transgressive, leading-edge lithosomes and estuarine phases of Q3 channel infilling. In the inner part of the study area, Q4 is composed of Holocene tidal stream sequences in addition to inlet channel sequences preserved in the shoreface (Field, 1980). Several radiocarbon ages on wood and peat (Table V) between 9000–9700 yrs B.P. from the leading-edge (offshore) suite confirm the Holocene age of Q4 in that area.

Overlying Q2, Q3, and Q4 above the Holocene ravinement surface are the modern trailing-edge sands (unit Q5) forming the linear ridges of the shelf.

LITHOLOGY AND STRATIGRAPHY OF THE SHELF

INTRODUCTION

The 6-meter maximum length of the 29 vibracores (Appendix V) did not allow penetration into unit T1, and only the uppermost section of unit Q1 was reached (Figure 13). Nor could complete penetration of channel infilling sequences in units Q3 and Q4 be achieved with 6 meter vibracores.

TERTIARY UNITS

The upper surface of stratigraphic unit T1 is the persistent mappable horizon M1 (Plate III). As noted earlier the M1 horizon roughly corresponds to the composite A3/A4 of Field (1980). Field (1980) designated his B1 horizon, which is at least 6 meters stratigraphically lower than our M1, as the Tertiary/Quaternary boundary, based on the work of Rasmussen and Slaughter (1955) and Weigle (1974). At the time of those studies the top of the Tertiary was picked as the top of the Yorktown Formation (then assumed to be Miocene in age), while the overlying Beaverdam Sand was assigned to the Pleistocene. Later, however, Owens and Denny (1979) reassigned the Beaverdam Sand to the Tertiary (Pliocene) based on discovery of pollen typifying older Tertiary sediments.

In late Pliocene time (2.4 million years ago) and possibly during the last phases of deposition of the fluviatile Beaverdam Sand, the first major global cooling event occurred (Zimmerman *et al.,* 1984). Evidence of glaciation, in the form of ice-rafted debris and isotopic composition of benthic foraminafera, indicate a glacial maxima similar to those of the late Pleistocene with an accordingly large drop in sea level. Onshore contours of the top of the Beaverdam (Figure 17) are interpreted from published water well logs (Rasmussen and Slaughter, 1955; Weigle, 1974; Hansen, 1973) and from available MGS gamma ray and electric logs (J. Wilson, MD Geological Survey, personal communication) from Worcester County, Maryland and Ocean City.

It is apparent from Figure 17 that, where data are available, onshore contours of the top of the Beaverdam in Maryland and the top of the Pliocene Yorktown in Virginia (Mixon, 1985), meet the offshore M1 surface contours in a smooth transition. We therefore interpret the M1 surface as the offshore extension of the top of Beaverdam Sand and its equivalents, and reassign the Tertiary/Quaternary boundary to the M1 surface, in keeping with the Pliocene age assignment of the Beaverdam (Owens and Denny, 1979). The strong and widespread character of reflector M1 signifies a major erosional event that affected the entire study area and that may be traceable to the shelf edge. The 2.4 m.y. global cooling-glaciation is likely that event. Field's (1980) division of the overlying units into Pleistocene (unit A between M1 and A1) and Holocene (above A1; Figure 12) is essentially correct but warrants subdivision based on data obtained for this study.

QUATERNARY UNITS

Late Pleistocene (Unit Q1)

The upper surface of unit Q1 (M2) is a mappable but weaker horizon than M1. M2 and uppermost unit Q1 were penetrated by several vibracores. On line 16, core 16-835 (2.65 km from shore) contains 0.21 meters of sand at its base, between -19.54 to -19.75 meters MSL. The sand contained numerous transported shells as seen in core X-rays. The positioning of the M2 reflector at -19.54 meters MSL (the top of the sand) is within the depth error range of 1 meter in seismic-reflection data and is therefore uncertain. The sand at the base of

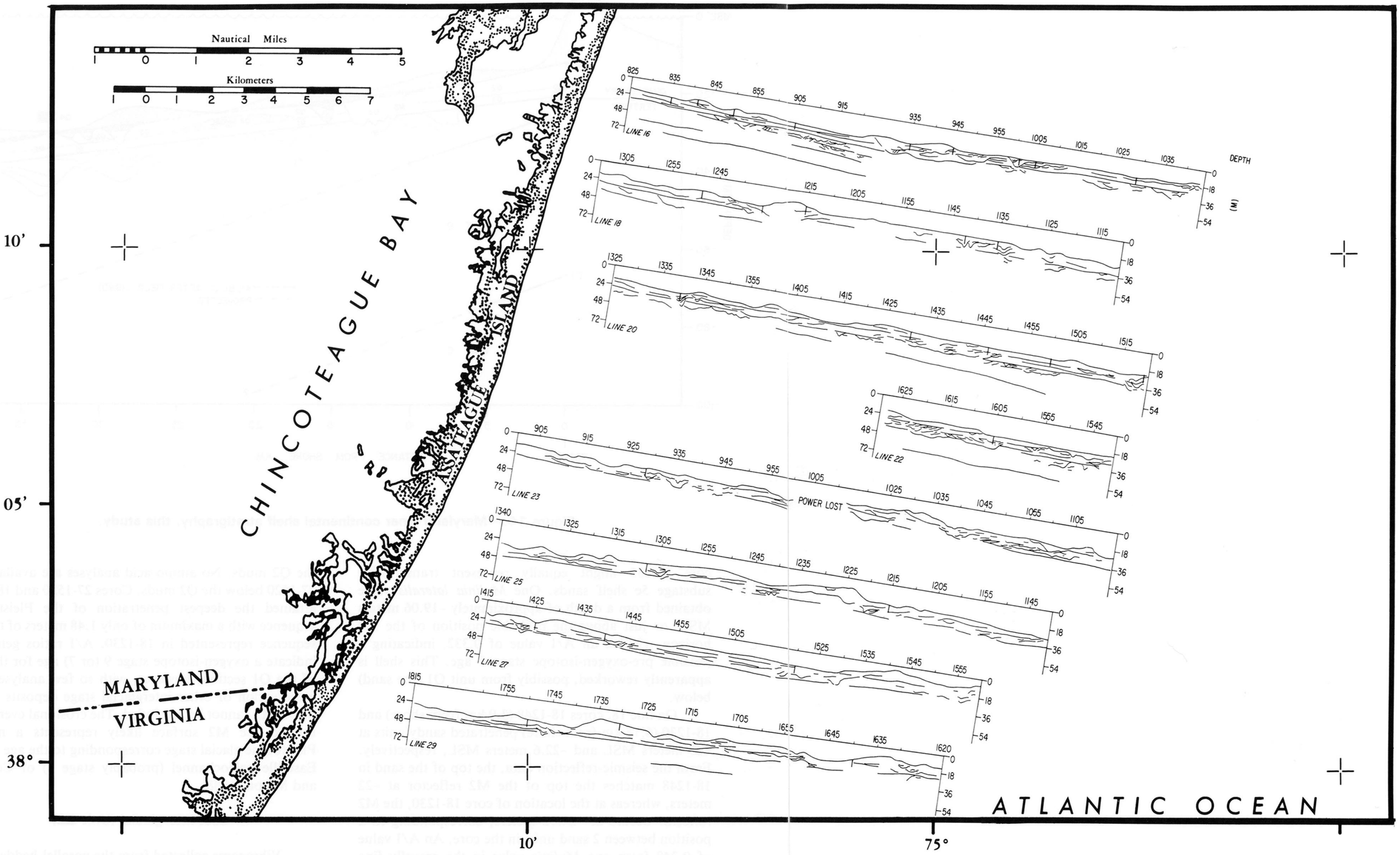

Figure 13.—Interpreted ORE Geopulse 280 joules shore-normal seismic profiles. Selected from 1985 data only. Vertical lines represent vibracore locations. Depth scale assumes 1500 m/s Locations shown in Plate 1.

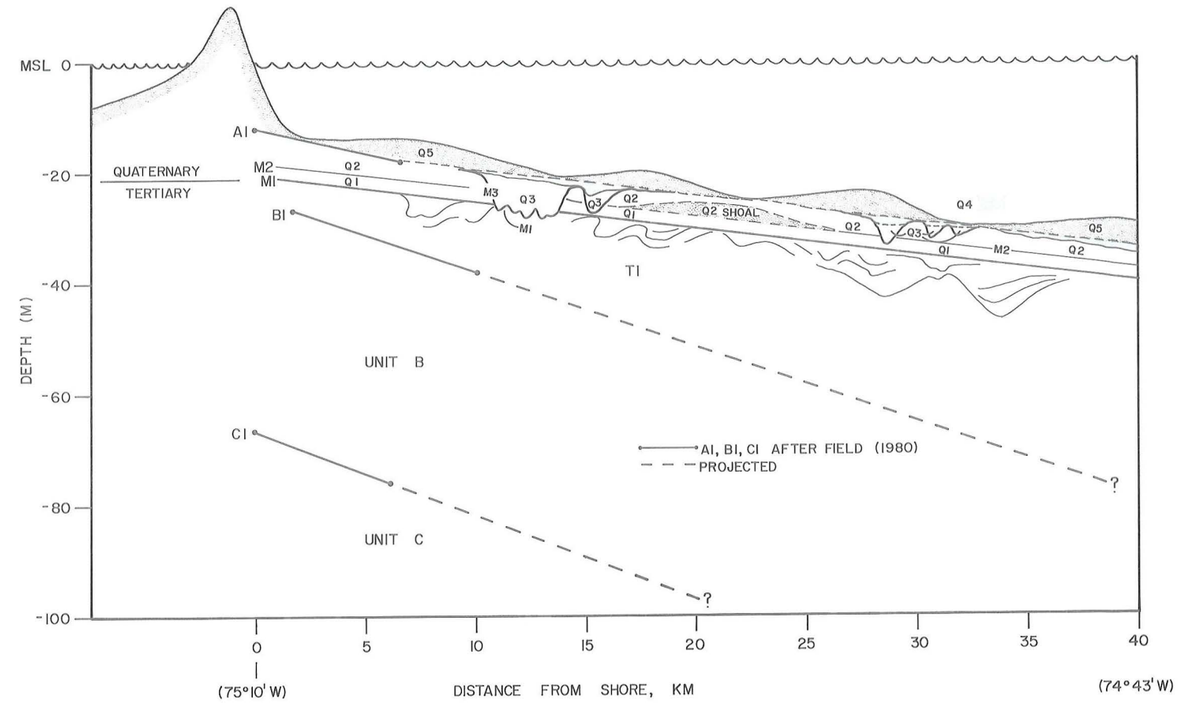

Figure 14.—Maryland inner continental shelf stratigraphy, this study.

core 16-835 might equally represent transgressive substage 5e shelf sands. One *Mulinia lateralis* valve obtained from a depth of approximately -19.06 meters MSL, or just above the probable position of the M2 horizon, yielded an A/I value of 0.332, indicating a possible pre-oxygen-isotope stage 9 age. This shell is apparently reworked, possibly from unit Q1 (the sand) below.

On line 18, cores 18-1248 (3.9 km from shore) and 18-1230 (6.75 km from shore) penetrated sandy units at -22 meters MSL and -22.6 meters MSL, respectively. From the seismic-reflection data, the top of the sand in 18-1248 matches the top of the M2 reflector at -22 meters, whereas at the location of core 18-1230, the M2 reflector occurs at -24.12 meters, corresponding to a position between 2 sand units in the core. An A/I value of 0.248 from one *Mulinia* valve in the gravelly fine sand of unit Q1 in 18-1230 and a mean A/I value of 0.256 from the *Mulinia* valves in the 18-1248 (Q1) gravelly sand suggest an age range within oxygen-isotope stage 9, or possibly early stage 7. Core 27-1520, 12.2 km from shore, may also have penetrated Q1 at a depth of -21 meters MSL, again in a sandy unit below the Q2 muds. No amino acid analyses are available in 27-1520 below the Q2 muds. Cores 27-1520 and 18-1230 attained the deepest penetration of the Pleistocene sequence with a maximum of only 1.48 meters of the Q1 sequence represented in 18-1230. A/I ratios generally indicate a oxygen-isotope stage 9 (or 7) age for the top of the Q1 section; however, with so few analyses, the preservation of other interglacial stage deposits in Q1 below M2 cannot be precluded. The erosional event that formed the M2 surface likely represents a middle Pleistocene glacial stage corresponding to the age of the Eastville paleochannel (probably stage 6) of Colman and Mixon (1988).

Last Interglacial (Unit Q2)

Vibracores collected from the parallel-bedded unit Q2 contained 2.5–6.0 meters of a dark greenish gray, dewatered silty clay with thin, silty, fine sand laminae and numerous *in situ Mulinia lateralis* lenses of varying thicknesses. Bioturbation is virtually absent. Cores 16-835, 16-842, 16-850, 16-905, 18-1230, 18-1248, 25-1308, and 27-1520 (Plate IV) consist entirely (16-905

RI50

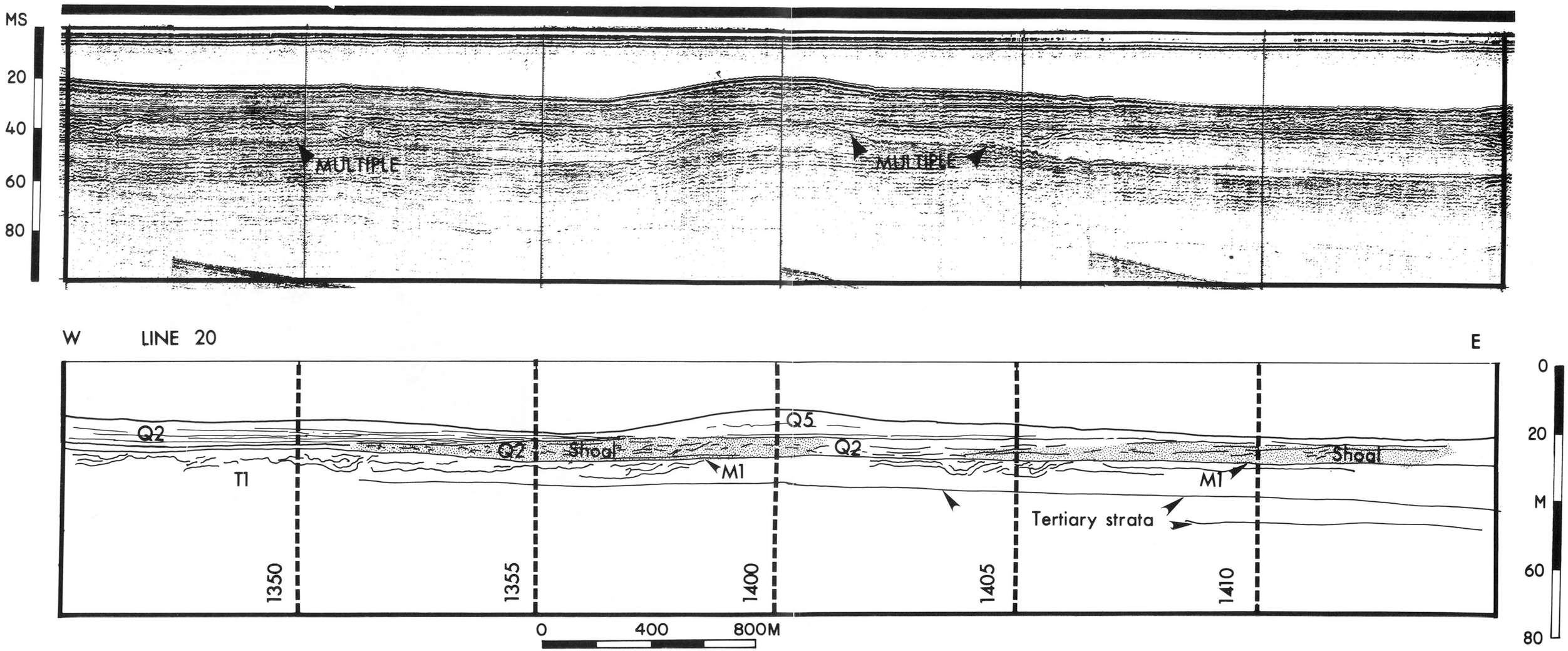

Figure 15.—Evidence of shoal-like sand body remnant in Unit Q2.

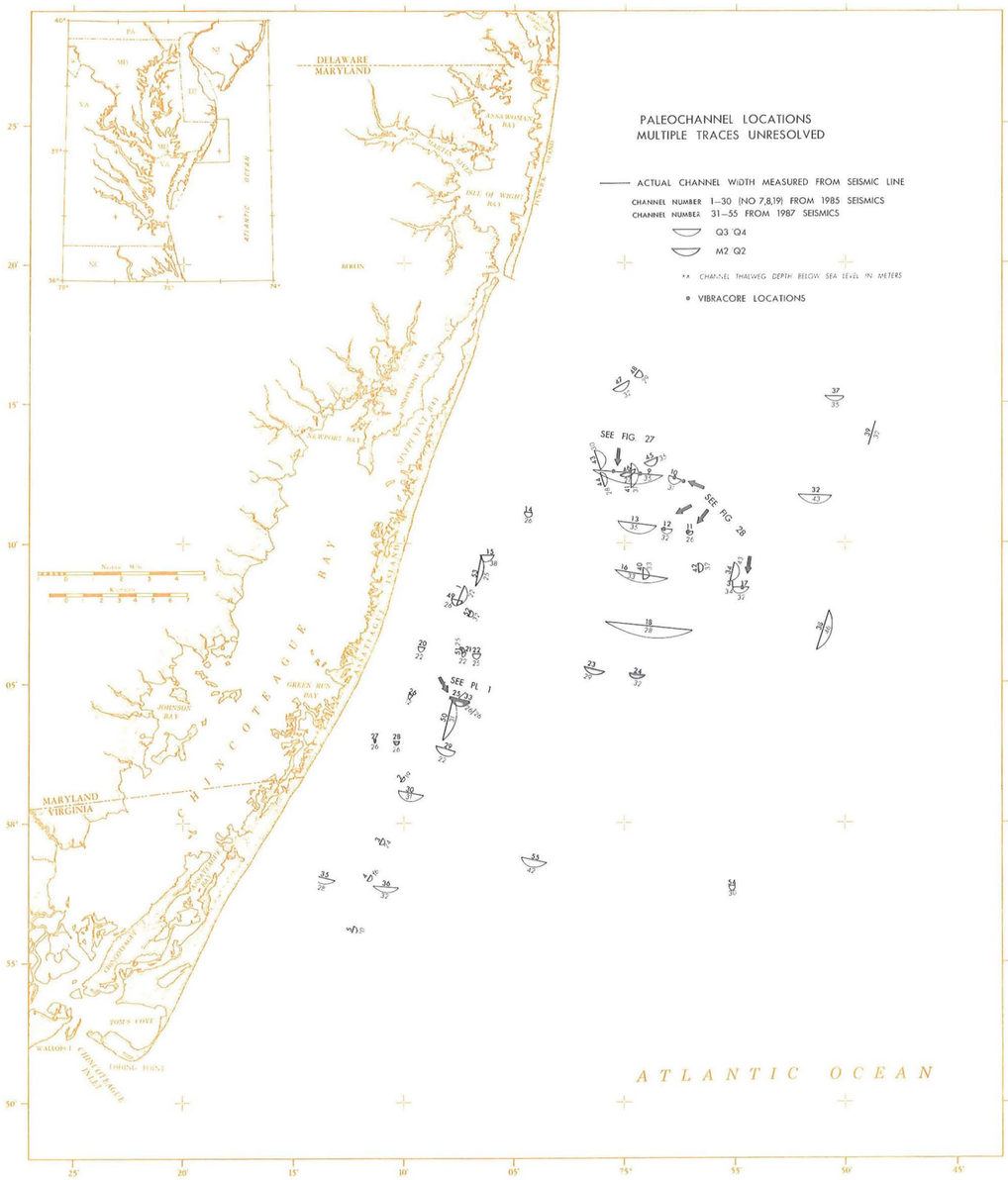

Figure 16.—Buried paleochannel locations from 1985–1987 seismic-reflection data.

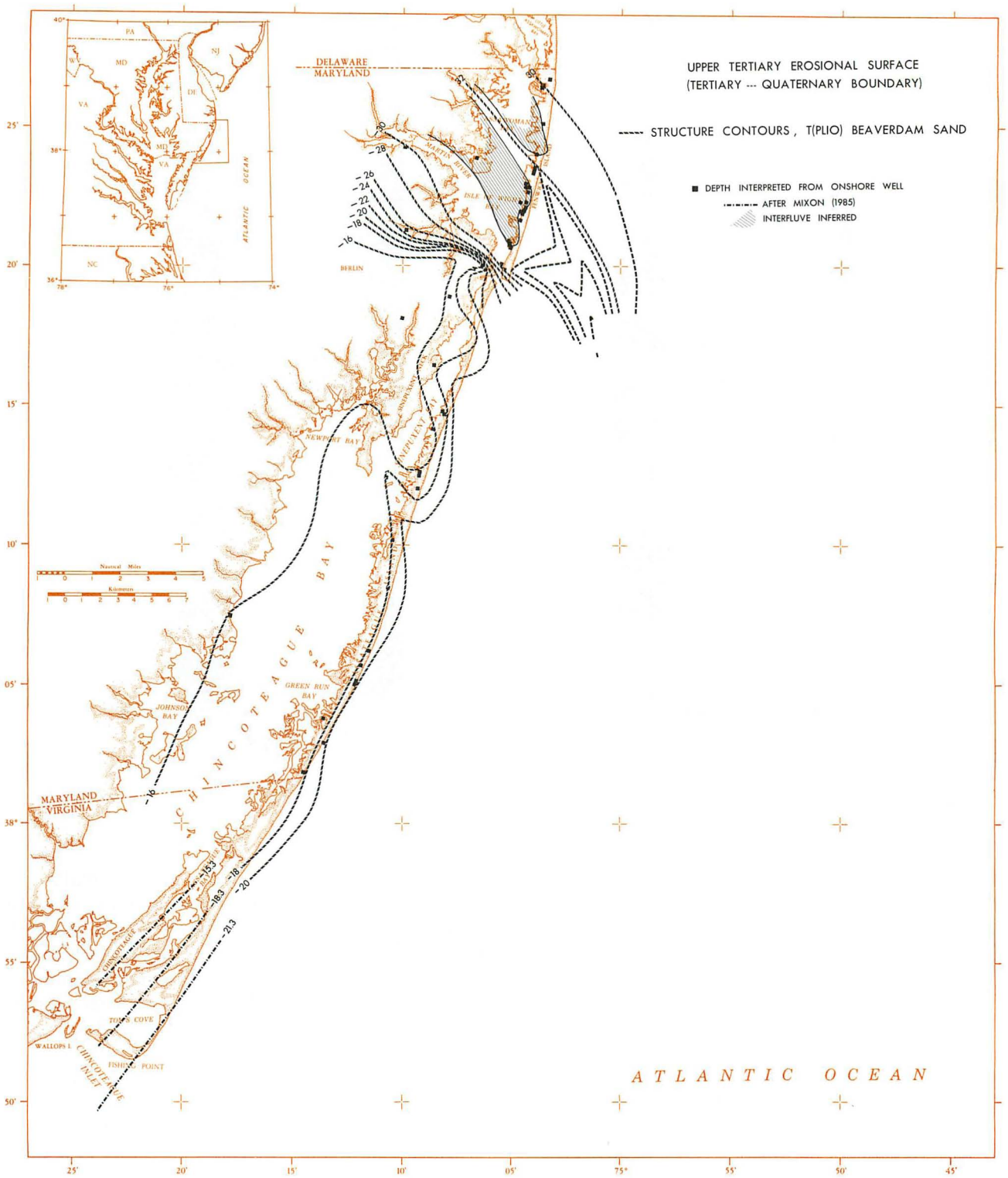

Figure 17.—Depth to top of Pliocene Beaverdam Sand from onshore well data (Maryland), to top of Yorktown Formation (Virginia; Mixon, 1985), and to the M1 reflector offshore. Based on these data, M1 is interpreted as the Tertiary/Quaternary contact.

Figure 18.—Xeroradiographs illustrating the characteristic bedding and shell lenses (Mulinia lateralis) of the Q2 muds.

and 25-1308) or largely of this mud sequence. Shorter mud sequences are preserved in 27-1440 and 27-1425. The cores listed are all located between 2.6 and 6.6 km offshore, with the exception of one at 12.2 km offshore. Modern shelf sands occur at the tops of 16-850 (≈ 1.8 meters), 16-842 (0.3 meters), 18-1248 (0.4 meters), 27-1520 (0.4 meters), 27-1425 (0.9 meters), and 27-1440 (0.6 meters). A/I ratios of 0.00 *(Mulinia)* in the top of core 16-850 indicate a modern age for these surficial sands. The top of the Q1 sands below the Q2 mud unit in 27-1520, 18-1248, 18-1230, and 16-835 marks the level of the oxygen-isotope stage 5/pre-stage 5 boundary (Plate IV). In core 18-1230 a sand unit occurs above the M2 surface (unconformity). This sand may grade into the muds above with no actual depositional hiatus, suggesting an early stage 5 age for the sand. The mud unit is ubiquitous across the shelf, from line 16 south to line 27, and attains thicknesses of 3.5–6.0 meters. It appears that the mud unit extends further eastward, on the basis of seismic-reflection data; however, the majority of cores taken further seaward were located in channeled areas or in shoals, and did not reach the parallel-bedded Q2 unit. Extrapolation of the Q2 mud seaward is inferred from seismic-reflection data, and the unit may include unknown facies (lithologic) changes offshore. Selected xeroradiographs (Figure 18) illustrate the characteristic thin bedding of the mud with silty sand laminae and *Mulinia lateralis* lenses. Such intact bedding indicates a lack of biogenic disturbance, possibly attributable to a high sedimentation rate, a quantity which cannot be measured without actual radiometric dating of the unit. Lithologically the unit C mud of Shideler *et al.* (1972) is similar to unit Q2 on the Maryland shelf. Core 20-1430 contains less than 1 meter of Q2 muds, but penetrated the lenticular unit in Q2, which is represented by over 2 meters of sands in this core. The sand body is herein interpreted as a remnant of a transgressive shelf sand body.

Ostracode Paleoclimatic Zones — Q2 —

The most significant faunal changes within unit Q2 occur in cores 16-905, 27-1520, and 18-1230. Figures 19, 20, and 21 depict percentages of key ostracode species in 16-905, 27-1520, and 18-1230, respectively, derived from the raw data in Appendix IV. Four distinct climatic zones are distinguished in unit Q2 on the basis of these quantitative occurrence data.

Zone 1 occurs in the lower sandy unit of core 18-1230 and the lower sandy unit of 27-1520, and contains a mild-temperate ostracode assemblage similar to that living in the region today. It is a typical interglacial assemblage with high percentages of *Pseudocytheretta edwardsi, Pontocythere* sp., *Muellerina ohmerti* (Figures 20 and 21) and *M. canadensis* and several species of *Bensonocythere.* It lacks warm water subtropical species that today inhabit regions south of Cape Hatteras and that sometimes occur in interglacial assemblages in the Pleistocene of the Norfolk area. Thus, approximately the present annual bottom temperature range for the region (13-27°C) is inferred. There is no evidence in these cores for bottom waters warmer than today.

A faunal change that represents the transition from Zone 1 to Zone 2 at approximately -21 to -22 meters MSL is found between 490 and 440 cm in core 27-1520 and between 328 and 330 cm in core 18-1230. A complete record of Zone 2 is well represented in core 16-905 between the lowermost sample (624-626 cm) and 411-413 cm. Ostracodes are generally not as abundant in Zone 2 as in Zones 1 and 3, but diagnostic cold water species consistently occur in Zone 2 and make up large percentages of the assemblages where ostracodes are common. *Elofsonella concinna* is the most abundant, comprising between 8% and 35% of total assemblages. Several other species *(Cytheropteron nodosum, Hemicythere villosa, Hemicytherura clathrata, Palmenella limicola, Sarsicytheridea bradii,* and *Robertsonites tuberculatus)* occur between 546 and 626 cm in core 16-905. These species are rarely if ever found south of Nova Scotia today. They indicate substantially cooler bottom water temperatures off Maryland during the deposition of sediments of lower Zone 2. Within Zone 2, the interval in core 16-905 between 546 and 626 cm also contains higher percentages of *Cytheridea* than the 446-546 cm interval. Although the significance of this distribution is not clear, it also seems to support the idea that the middle of Zone 2 had colder waters than upper Zone 2. The interval between 150 and 292 cm in core 18-1230 contains a typical upper Zone 2 assemblage. Assemblages correlative with upper Zone 2 of core 16-905 can also be recognized in the lowermost 30 cm of core 16-850 and in core 18-1248 at 409-411 cm. At least some facies of the Wachapreague Formation studied by Mixon (1985) in Exmore, Virginia also contain a Zone 2 assemblage (Mixon, 1985; core Ex-24). The approximate annual range of bottom water temperatures inferred from Zone 2 assemblages was less than 4 to 15°C.

A very sharp faunal change between the samples at 382 and 411 cm in core 16-905 separates Zones 2 and 3 (at approximately -20.5 meters MSL). This boundary is also found between 61 and 150 cm in core 18-1230. Subfrigid-cold temperate species mentioned above disappear and the percentages of *Cytheridea, Loxoconcha,* and *Muellerina* increase rapidly. Zone 3 consists of the uppermost 400 cm of core 16-905 and contains a relatively monotonous, low diversity assemblage that lacks the typically mild temperate species *(Pontocythere* sp. *Pseudocytheretta edwardsi)* abundant in Zone 1 and the cold water species that occur in lower Zone 2. The predominant species is *Cytheridea* sp., which accounts for between 50% and 90% of each sample. Empty carapaces of *Cytheridea* occur in only a few modern samples off the Delmarva Peninsula and its modern climatic tolerance is not well known. Because no modern specimens having soft parts have been found, it is not even certain whether it is extant. *Cytheridea,* however, is generally a temperate genus. The absence of other typical mild temperate species and the rare occurrence of cold water *Elofsonella* towards the top of core 16-905 suggests water temperature in Zone 3 were slightly cooler than today's situation but warmer than Zone 2. A rough estimate of the range of annual temperatures would be 8-20°C. Based on comparison of the percentages of the common ostracode species in core 16-905, the following core intervals appear correlative with Zone 3 (Figure 22): core 18-1230 at 59-61 cm, core 16-835 at 90–92 cm (upper Zone 3), core 27-1520 at 234–241 cm, core 16-842 at 530–540 cm (lower Zone 3), and core 18-1248 at 300–302 cm. The sample in core 18-1248 at 409–411 cm was transitional between Zones 2 and 3, perhaps representing uppermost Zone 2.

Zone 4 is defined in core 27-1440 and is also found in 27-1520 and 18-1230. It appears to represent a warm interval subsequent to the cool period of Zone 3.

Previous Age Estimates — Q2 —

Both Field (1976, 1980) and Shideler *et al.* (1972) attempted to date the Quaternary muds beneath the shelf shoal sands. Within his unit A (our Q2), Field (1980) described a "widespread" Holocene mud deposit, an assumed back-barrier lithosome, overlying various Pleistocene low sea level deposits (Figure 12C). The Holocene age assigned by Field to the entire mud deposit was based on a single radiocarbon date on peaty material in his core 13, 10.8 meters below sea level, of 5765 ± 105 yr B.P. Field (1976; 1980) did not specify the distance of the sample from shore; however, the depth indicates a shoreface outcrop of Holocene back-

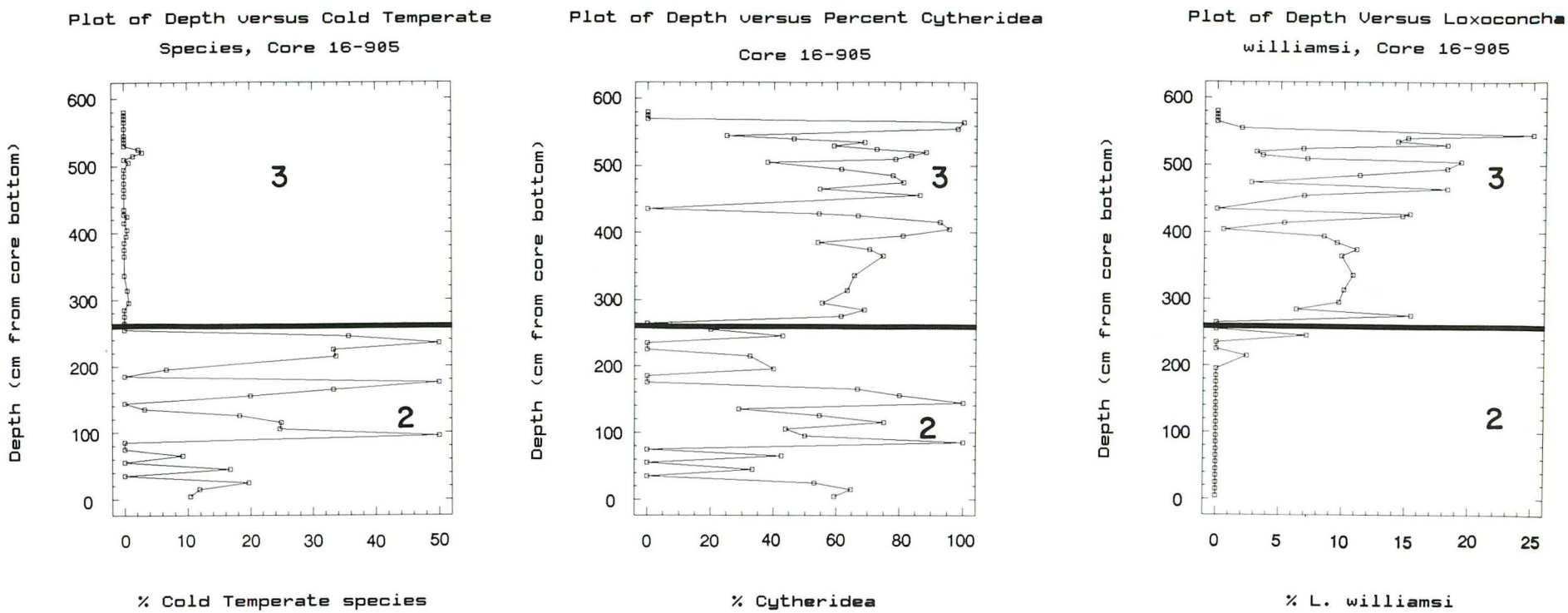

Figure 19.—Percentages of climatically significant ostracodes, core 16-905. One 2-cm sample taken every 5 cm downcore was analyzed (see Appendix IV). Zones 2 and 3 present in this core.

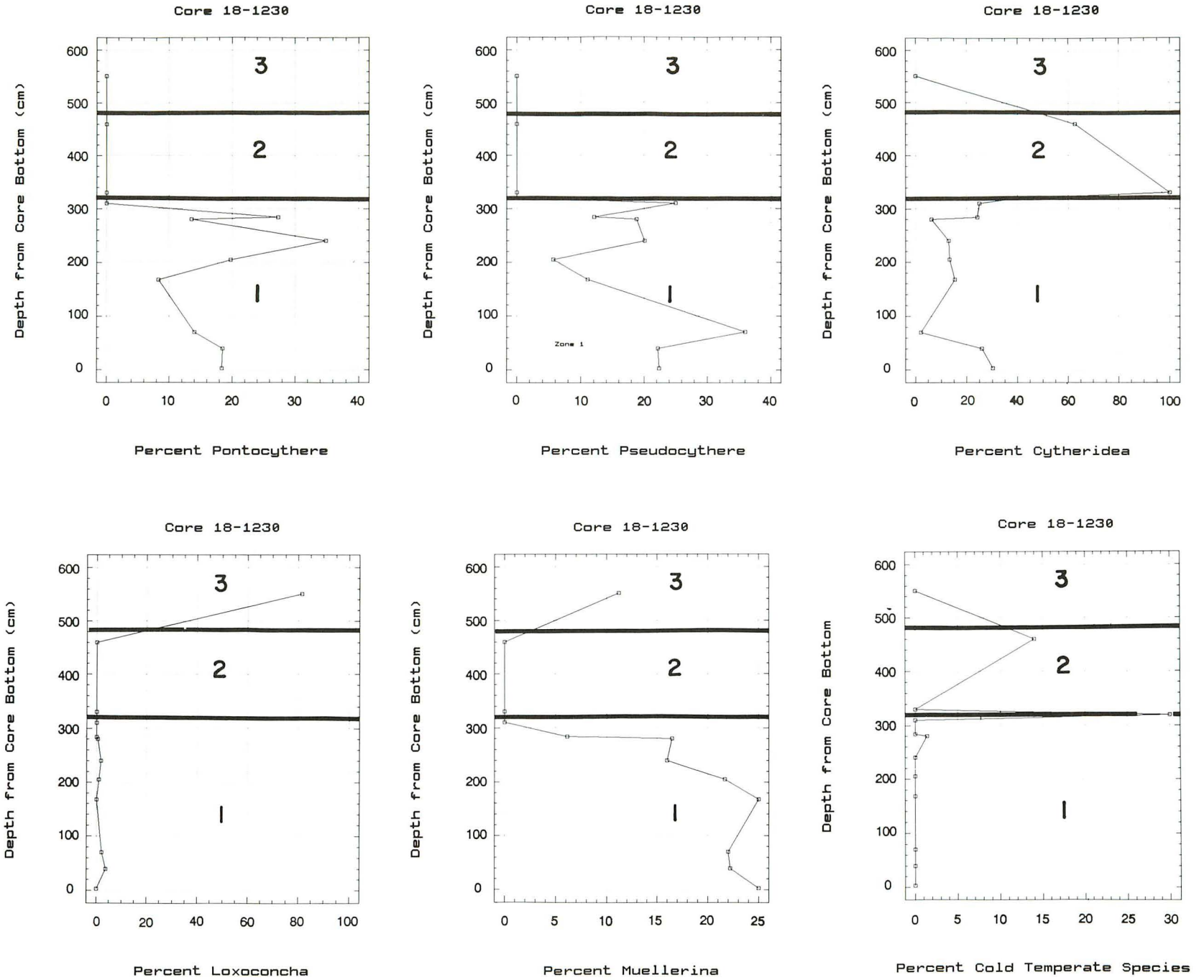

Figure 20.—Percentages of climatically significant ostracode genera in core 18-1230. Zones 1, 2, and 3 present in this core.

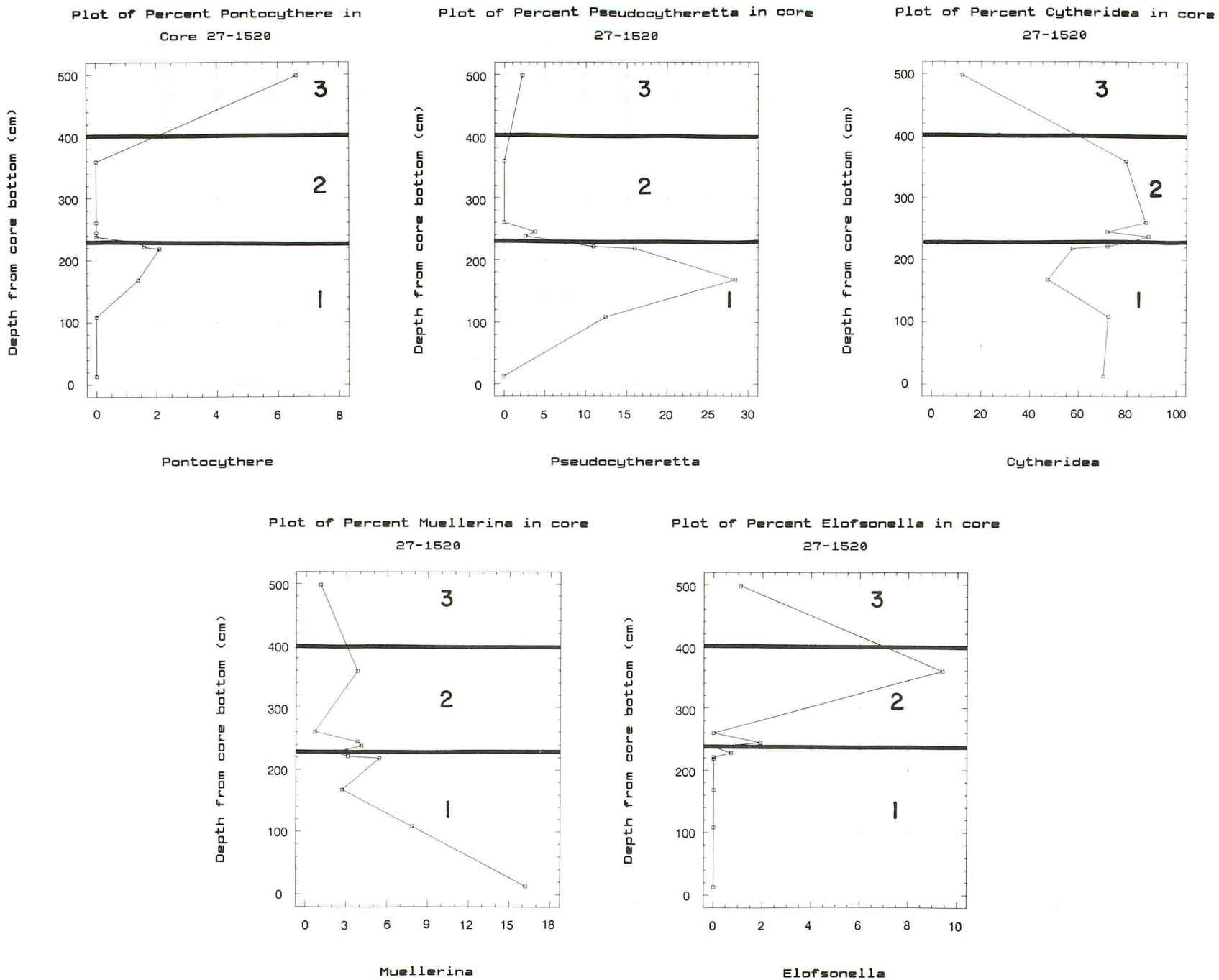

Figure 21.—Percentages of climatically significant ostracode genera in core 27-1520. Zones 1, 2, and 3 present in this core.

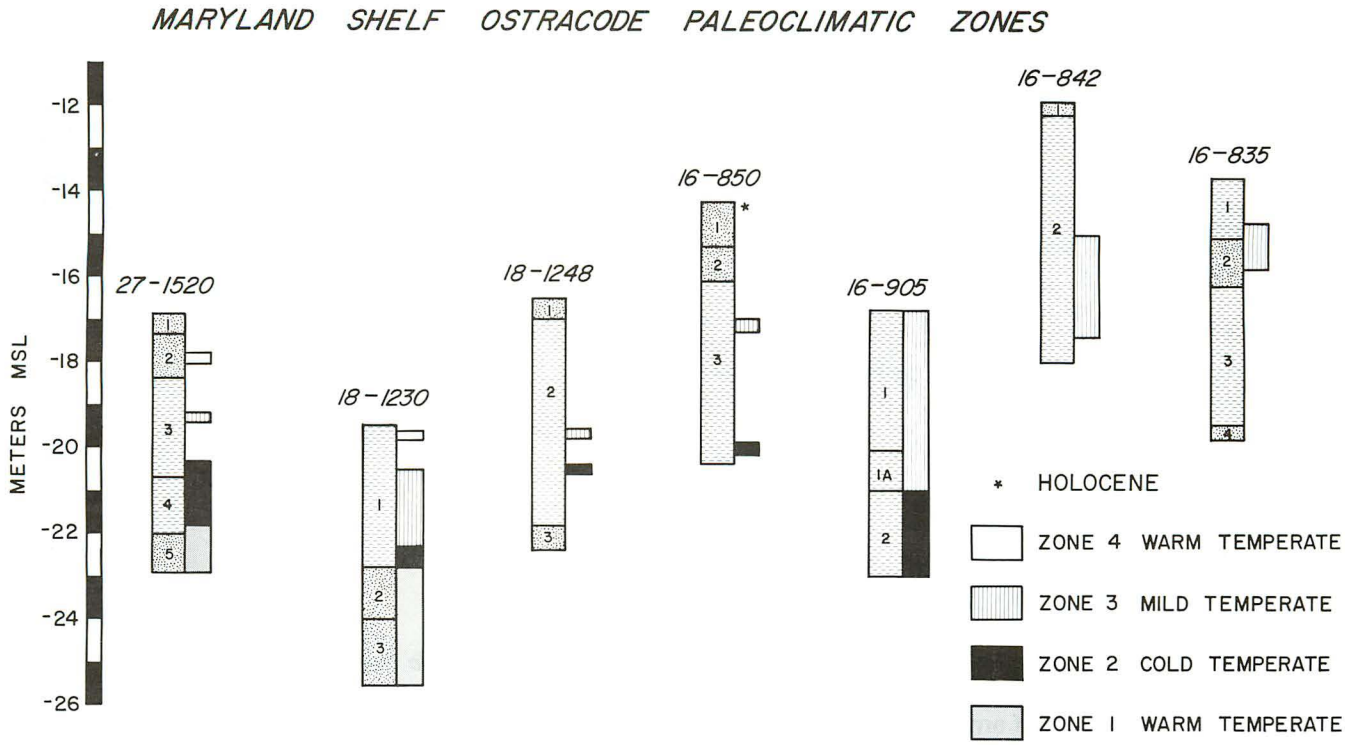

Figure 22.—Generalized ostracode paleoclimatic zones in stratigraphic sequence for studied cores. Numbers inside cores refer to successive downcore lithologic units shown in detail in Appendix V.

barrier marsh. Field (1976; 1980) inferred that this probable shoreface marsh outcrop was continuous with the near-surface shelf muds below the base of the shoreface, stating that a Holocene mud unit is the dominant lithology at approximately 4 meters below the surface in cores (assuming overlying shoal sands). However, a Holocene unit at 4 meters below the sea floor conflicts with Field's (1980) designation of A1 reflector at the top of the mud unit, just underlying the shoals as the Pleistocene/Holocene boundary. Dewatered muds were described earlier in this report; however, Field (1976; 1980) noted dewatered muds in only 5% of his cores, and none of the muds he reported were exposed at the sea floor.

Similarly, Shideler *et al.* (1972) obtained several radiocarbon analyses from their units B (our T1) and C (our Q1/Q2), from bulk sand-gravel sized shell fragments (2 cases) and "total carbonate extracted from the sample" (in one sample that had insufficient shell material). The resulting ages, ranging between 37 and 20 ka, are likely to be gross underestimates of the true ages of units B and C due to the high susceptibility of shell material to modern carbon contamination.

Amino Acid Age Estimates — Q2 —

Figure 23 summarizes, in cross-section, the mean alloisoleucine/isoleucine (A/I) *Mulinia* ratios for bracketed intervals in cores containing Q2 sequences. Individual analyses from which these mean ratios were calculated are listed in Appendix II. Table I gives depth intervals and value ranges represented by each mean A/I value.

No definitive trend of lower ratios up core or upsection in the mud unit as a whole is apparent. The precision of multiple analyses of *Mulinia* from single horizons is poorer than for other molluscan genera such as *Mercenaria* (Wehmiller *et al.*, 1988; York *et al.*, 1989. The variability in the *Mulinia* analyses is reflected in the coefficient of variation (c.v.) values (Table I), ranging from 2–19%, and averaging 10.05%. Accordingly, in any core the standard deviation of each analyzed interval overlaps those of one or more other intervals (Table II).

The mean A/I and standard deviation data plotted against latitude on Figure 24 indicate the degree of overlap of A/I ranges between cores.

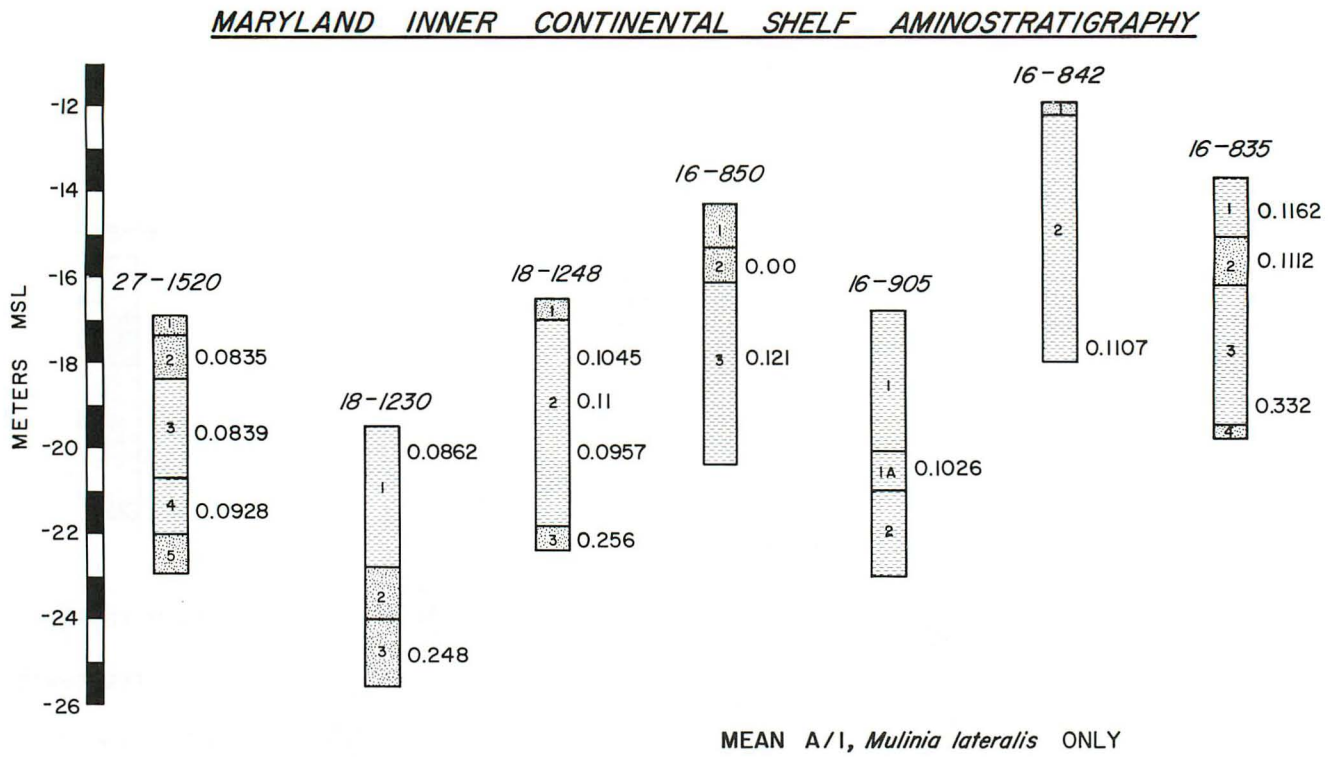

Figure 23.—Cross-shelf aminostratigraphy. Numbers inside cores refer to successive downcore lithologic units shown in detail in Appendix V.

Table I.—Mulinia Amino Acid Data Summary.

Core #	Sample Depth in Core (cm)	No. Valves	A/I Range	Mean A/I ± STD. DEV.	C.V.%	Unit
16-835	54-110	6	0.095–0.125	0.1162 ± 0.011	9.47	Q2
	135-228	13	0.072-0.136	0.1112 ± 0.0167	15.02	Q2
		1	0.332	0.332	—	Q2/Q1?
16-842	560-568	4	0.097–0.118	0.1107 ± 0.0095	8.58	Q2
16-850	140-143	1	0.00	0.00	—	Q5
	271-510	3	0.119–0.124	0.1212 ± 0.0026	2.15	Q2
16-905	344-373	14	0.078–0.127	0.1026 ± 0.0153	14.91	Q2
18-1230	15-39	6	0.073–0.103	0.0862 ± 0.0127	14.73	Q2
	490-495	1	0.248	0.248	—	Q2
18-1248	141-152	6	0.092–0.118	0.1045 ± 0.0095	9.15	Q2
	185-218	2	0.106–0.114	0.11 ± 0.0056	5.14	Q2
	344-398	3	0.081–0.116	0.0957 ± 0.0182	19.02	Q2
		2	0.256	0.256	—	Q1
27-1520	85-141	2	0.081–0.086	0.0835 ± 0.0035	4.19	Q2
	160-350	15	0.072–0.100	0.0839 ± 0.00977	11.64	Q2
	380-430	4	0.086–0.100	0.0928 ± 0.0057	6.14	Q2

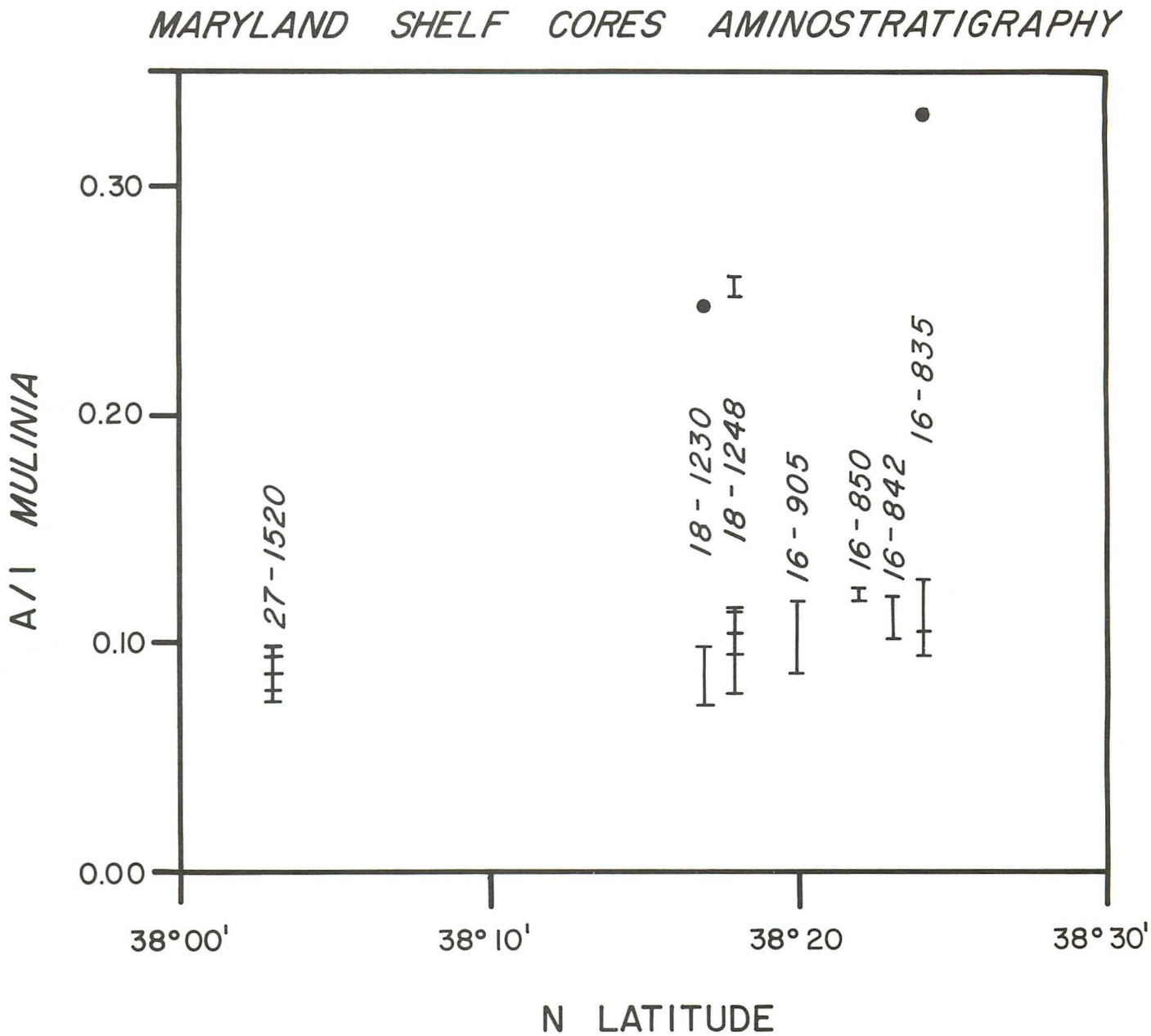

Figure 24.—A/I Mulinia values versus latitude in Maryland shelf cores analyzed. Vertical ranges of A/I values for each core are plotted using the standard deviation about the mean A/I value. Cores 27-1520, 18-1248, 16-905, and 16-835 show overlapping value ranges. Single analyses are shown as points.

Table II.—Overlap of Standard Deviations of Mean A/I Ratios in Three Portions of Unit Q2 in Core 18-1248.

Interval	Mean A/I ± STD DEV.	Value Range	Interval	Ranges in Order
TOP	.1045	.095	BOTTOM	.0774
	± .0095	.1140		.1138
MIDDLE	.11	.1044	TOP	.095
	± .0056	.1156		.1140
BOTTOM	.0956	.0774	MIDDLE	.1044
	± .0182	.1138		.1156

Numerical age estimates can be made for the amino acid data through the use of a kinetic model equation (Bada and Schroeder, 1972) and a calibration point. We used oxygen-isotope stage 5e, the peak of last interglacial at 125 ka and a mean A/I ratio of 0.1162 (an approximation of a mean value for our mean A/I ratios ranging from 0.10 to 0.12) as our calibration point. Kinetic model age calculations, which depend on effective Quaternary temperatures (EQT), are explained in detail in Appendix III. Correlations for broad groups of amino acid data are shown in Figure 25 in the regional framework of Wehmiller *et al.* (1988). Three Delmarva localities (BN — Bell Neck, VA; TI — Tingles Island, MD; BB — Bethany Beach, DE) contain marine sediments that are likely to be the onshore continuation of the Q2 muds. Core samples from all three localities have been previously analyzed for the D/L leucine ratio (MacDonald, 1982; Belknap, 1979; Mixon, 1985), and locality BN has a supporting Th/U date on *Mercenaria* of 128 ka (Mixon, 1985). This onshore data is summarized in Table III. Additional *Mulinia* samples from these same cores have recently been analyzed for other studies in the University of Delaware amino acid laboratory. In Appendix II, Table VII contains the A/I *Mulinia* values that are used as the basis of our stratigraphic correlations for the region.

The four aminozones for Region II shown in Figure 25 represent probable correlations of the A/I *Mulinia* data with original Region II aminozones based on *Mercenaria* D/L leucine ratios (Wehmiller, *et al.*, 1988). Slopes of the aminozone boundaries are based on latitudinal gradients of temperature and their effect on racemization rates. The localities of Stetson Pit (SP), North Carolina, Gomez Pit (GP), Virginia, and Sankaty Head (SH), Massachusetts have associated U/Th coral dates and are used as calibrations for the aminozone age assignments. Aminozone IIa (Figure 25) represents late oxygen-isotope stage 5 (substages 5c–a?) while IIb represents early stage 5 (substage 5e), having an estimated age range of 120–130 ka (Wehmiller *et al.*, 1988). Wehmiller *et al.* (1988) give a more detailed discussion of the methods used in these age assignments. The Maryland shelf data fit into and overlap regional aminozones IIa and IIb, indicating that these data span a large portion of stage 5. The numerical ages calculated for the *Mulinia* samples from the Maryland shelf are shown in Appendix III and fall into the range of 79-137 ka. This broad range reflects both the variability in the *Mulinia* data as well as some uncertainties involved with the age calculations of the data (Appendix III).

Finally, the *Mulinia* recently analyzed from BN core EX-24 (Mixon, 1985) with an A/I ratio of 0.103 are supported by a U-series date of 128 ka on *Mercenaria* and a D/L leucine ratio interpreted (by Belknap, 1979) as indicating an age of 82 ka for a *Mesodesma* sample. For locality BB the A/I range for *Mulinia* (0.097–0.123; Table 3) is essentially the same as that for the shelf cores. The D/L leucine data provide a kinetic model age estimate of 100 ka ± 25 ka (McDonald, 1982). Both these localities support our age interpretations and, based on their A/I values, are correlative with the shelf samples of unit Q2. Samples from locality TI are also correlative with BN, BB, and unit Q2 of the Maryland inner shelf on the basis of *Mulinia* A/I values (0.106–0.113).

Mulinia A/I values clearly lack resolving power for small age differences, such as those between the substages of oxygen-isotope stage 5 (see Wehmiller *et al.*, 1987). Paleoclimatic zones based on ostracode assemblages provide the information necessary to divide the Q2 mud unit into stage 5 substages, and the amino acid ratios provide a regionally consistent general time frame.

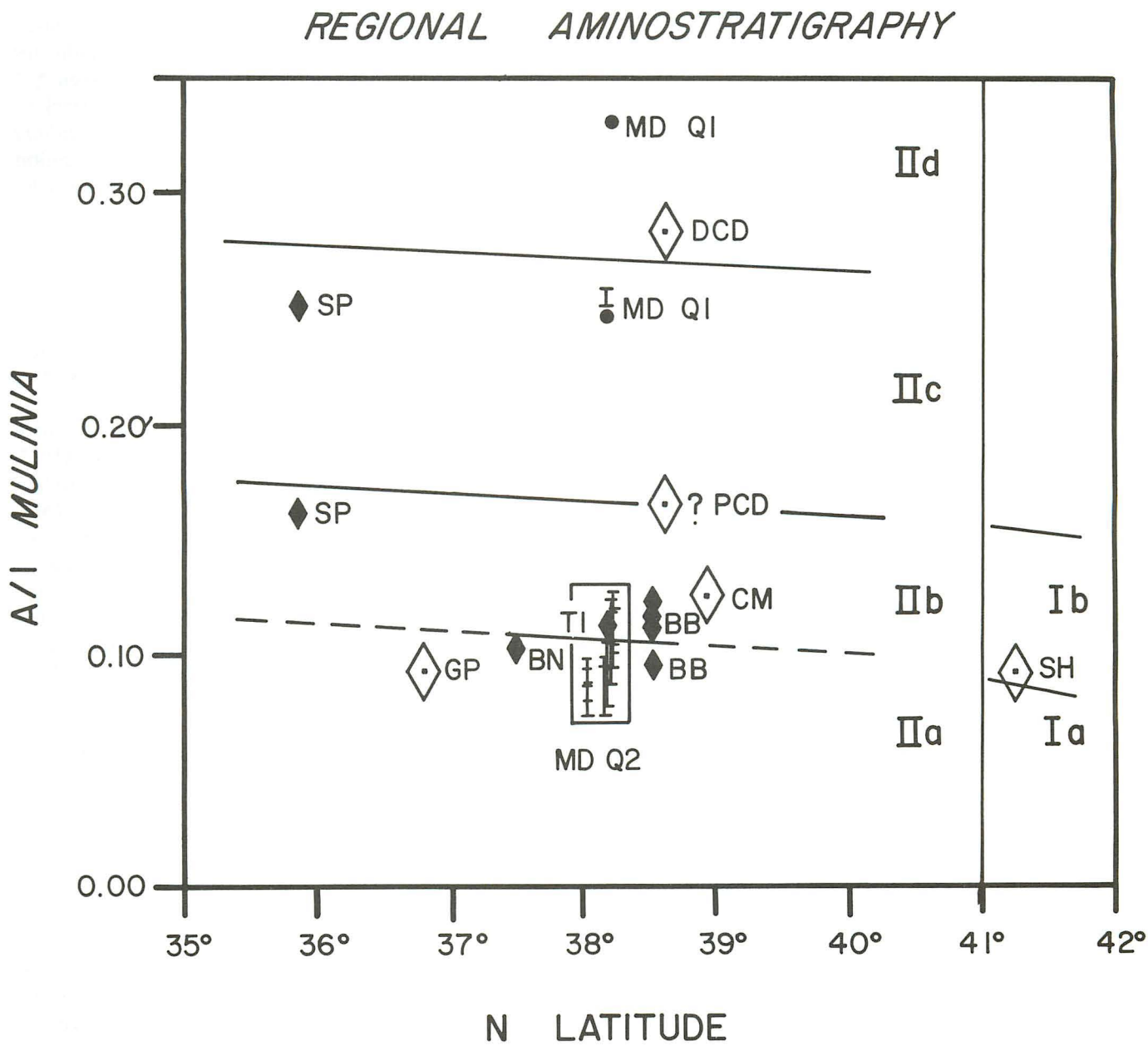

Figure 25.—Continental shelf A/I Mulinia data shown (Maryland Q1 and Maryland Q2) shown in the Region II aminozone framework of Wehmiller et al. (1988). Region II includes southern New Jersey (CM — Cape May), Delaware (BB — Bethany Beach; PCD — Pepper Creek Ditch; DCD — Dirickson Creek Ditch), Maryland (TI — Tingles Island), Virginia (BN — Bell Neck; GP — Gomez Pit), and northeastern North Carolina (SP — Stetson Pit). Open symbols represent Mercenaria D/L leucine values converted to A/I Mulinia data. Size of symbols reflects relative uncertainty in A/I values between localities. The conversion of Mercenaria D/L to Mulinia A/I ratios involves a large amount of uncertainty due to a somewhat ambiguous Mulinia/Mercenaria intergeneric conversion factor, which may be related to the variability in Mulinia data.

Unit Q2 — Age and Correlation —

Plate V incorporates the ostracode climatic zones 1–4 with amino acid ratios and lithostratigraphy of Q2 and Q1. Each paleoclimatic zone is found in at least two cores, allowing cross-shelf correlations to be made. Warm Zone 1 corresponds to the sandy units beneath the muds in 18-1230 and 27-1520, and contains sedimentologic evidence of reworked, older shells (A/I ratio of 0.248 in 18-1230). Where the sand occurs it overlies the M2 reflector (18-1230), and it is interpreted as the transgressive shelf sands of oxygen-isotope substage 5e which reached a maximum relative sea level of +6 meters MSL, at about 125 ka (Martinson *et al.,* 1987). Where unit Q1 sands underlie M2 (27-1520, 18-1248, 16-835) the transgressive shelf sand interpretation appears to apply, however the sediments of Q1 represent pre-stage 5 shelf sands (stages 7-13?). A transition from transgressive (5e) to regressive (5e-5d) deposition is suggested by samples in core 27-1520, at least one of which may be climatically transitional between warm Zone 1 and cold Zone 2. This transition is interpreted as the end of substage 5e and the beginning of interstadial substage 5d.

The majority of Zone 2, interpreted as a regressive unit correlative with substage 5d, a cool, probably brief interval of lower sea level within the last interglacial, is correlated across the shelf from core 27-1520 through cores 18-1248 and 18-1230 to core 16-905 where it was originally defined. The very cold bottom water temperatures on the shelf inferred for lower Zone 2 are difficult to explain except by a brief but relatively intense cooling. The only other fossil occurrence at these latitudes of the subfrigid species in lower Zone 2 is in submarine canyons in sediment most likely deposited during peak glacial climates and low sea levels (Hazel, 1968).

Zone 3, representing a warmer interval not quite as warm as Zone 1, lies stratigraphically above cold Zone 2 and is separated from Zone 2 by a sharp break, as noted in core 16-905. Some of the upper Zone 2 record may therefore be missing depending on the depth of sea level minima during substage 5d. Such a break may indicate a drop in sea level below -20 to approximately -20.5 meters MSL at the substage 5d minima. Zone 3 is documented across the shelf (Plate V) and most likely represents a regressive shelf mud of substages 5c-a, whose sea levels may have approached present sea level, but not the higher water temperatures of 5e or of the present regime. Zone 3 appears to correlate with many other late Pleistocene deposits between Nantucket and North Carolina that contain cool water faunas of the last interglaciation (Cronin, 1988). These faunas commonly occur in the youngest pre-Holocene marine units in this part of the Atlantic coast, signifying slightly cooler conditions than those that exist today.

Zone 4 may represent the peak of stage 5a especially if the 80 ka sea level reached the present level. The tendency for lower A/I ratios (0.0835–0.0862) in Zone 4 compared to Zone 2 suggests an age younger than that of substage 5e; however, cross-shelf correlations based on the ostracode paleoclimatic zones (Plate V) indicates that there is no consistent age relationship between A/I ratios and ostracode zones in unit Q2. Again, the lack of resolving power of amino acid analyses of *Mulinia lateralis* whole valves is demonstrated in a situation where numerous analyses are available for a single, spatially confined, stratigraphic unit. Nevertheless, the A/I ratios as a group constrain the stage 5 age of the entire Q2 unit most reliably and consistently.

In regional terms, unit Q2 lithologically corresponds to the unit C sediments of Shideler *et al.* (1972) offshore of Virginia below the mouth of the Chesapeake Bay. Shideler *et al.* (1972) described their unit C as a regressive paralic-neritic sequence, consistent with the suite of characteristics of the unit and with the data presented here for Q2. In addition, Shideler *et al.* (1972) observed a sand unit beneath the muds in their unit C, equivalent to the sand penetrated by cores 27-1520, 18-1230, 18-1248, and 16-835. We therefore correlate our unit Q2 with their unit C, their basal sequence bounding reflector R2 with our M1, and place the mud sequences in the age range of 118-75 ka. The Quaternary/Tertiary boundary, according to Shideler *et al.* (1972) was originally designated as the deeper (-30 to -75 meters MSL) R1 reflector (equivalent to the B1 of Field (1976; 1980)). Our conclusion that Shideler *et al.*'s (1972) Wisconsinan age assignments were based on erroneous ^{14}C dates and the depth equivalence of Shideler *et al.*'s (1972) R2 with our M1 supports reassignment of the Virginia Quaternary/Tertiary boundary to the R2 reflector.

Last Glacial (Unit Q3)

The numerous channels shown in Figure 16 have similar channel configurations and thalweg depths (Figure 26). Most of the channels likely represent the downcutting that occurred during the last glacial (Wisconsin) period (oxygen-isotope stages 4, 3, and 2). These channels contain depositional sequences that begin at the base with fluvial sediment (Q3) grading upsection into estuarine or tidal stream sediments deposited during the Holocene transgression (Q4). Channels would have first been cut into unit Q2 during low sea level associated with glacial oxygen-isotope stage 4 (60–70 ka) and may have been aggraded somewhat during oxygen-isotope stage 3 when sea level reached between -35 and -45 meters MSL (Bloom and Yonekura, 1985; Bloom *et al.,* 1974; Chappell, 1974; Chappell and Shackleton, 1986). Deposition during stage 3 in the study area was most likely confined to the channels, then eroded during the ensuing low sea level,

full-glacial episode related to oxygen-isotope stage 2. Subsequent aggradation and estuarine filling of these channels began between 18 and 13 ka and continued until the shoreline of the Holocene transgression passed over each. Estuarine materials have been recovered in cores in several channels (23-928, 20-1518, 18-1142, 18-1135, 20-1430, 16-1005). Seismic characteristics are typical of infilling and vary depending on the orientations of the seismic lines.

A trunk fluvial channel is identified on Figure 26 based on its width and depth. M3 thalwegs have depths that exceed the depth of the M1 surface, which is the top of the Beaverdam Sand (Plate III), and cut into it slightly, making the deepened M1 the base of the channel. The depression in the top of the Beaverdam that extends into the Fenwick Island/West Ocean City area suggests that the fluvial channel offshore is the ancestral St. Martin River (Figure 17). The cross section of the ancestral St. Martin channel in Figure 27 is derived directly from the seismic reflection records on line 16 between 16-929 and 16-955. Field's (1980) postulation of such a paleofluvial system (in the absence of seismic-reflection evidence) was correct; however the channel is unequivocally traceable to the St. Martin River. It is too small to be one of the ancestors of the Susquehanna River that cross the Delmarva Peninsula (Colman *et al.*, in press).

Core samples collected from the low sea level-fluvial sequence designated as Q3 (cores 16-935 and 16-945; Figure 27; and possibly core 16-1002; Figure 28) consist of light orange silty fine sands or clean, coarser sands with slight to intense iron-oxide staining. These sands contain no microfauna (Appendix IV, Table XII).

Based on amino acid A/I ratios, all mollusca *(Spisula)* from the top two units of core 16-935 are interpreted to be Holocene in age (Appendix II, Table VII). Unit 1 is a thin sandy unit (Q5), while unit 2, a sandy mud, may be a preserved remnant of the Holocene transgression (Q4). A sample taken at 70-73 cm (unit Q4) contains an ostracode assemblage typical of normal marine conditions of the inner to middle continental shelf, with several species occupying the northern limits of their ranges. As such, the sample appears to be Holocene in age and may represent slightly warmer bottom water than present. Below unit 2 the entire core consists of light orange silty fine sand (unit Q3) which is devoid of shells and microfauna, supporting a fluvial rather than estuarine origin.

Cursory petrologic analysis of the light mineral fraction of unit Q3 sands show a downcore variation in the feldspar to feldspar + quartz $((f/f+q) \times 100)$ percentages (Milliman, 1972). The upper sections of cores 16-935 and 16-945 consist of Q5 surficial shelf sediment, and are relatively quartz rich, as indicated by average

Table III.—Comparison of D/L, Leucine, Radiometric, and A/I Mulinia Data for Delmarva Localities TI, BN, and BB and Previous Age Estimates.

Locality (Latitude)	Core #	Sample Depth MSL	D/L	Previous Age Est.	A/I Mulinia	Radiometric Age
BN (37°51′) Wachapreague Formation	EX-24	-15 to -25m	0.284*	82 ka	0.103	128 ka U-series on *M. merc*
TI (38°19′) Sinepuxent Formation	unident. USGS borehole	16m?	0.147**	≈58 ka**	0.106 0.113	—
BB (38°53′) Omar Formation	KAM-MB-80	-9.5m	0.27-0.29***	100 ± 25ka***	0.123 0.117	^{14}C shell 45 ka
— Bethany Paralic Unit	KAM-NOV-80	-9m	0.22***	100 ± 25ka***	0.113 0.097	> 45 ka

* Mixon, 1985; ** Belknap, 1979; *** McDonald, 1982.

f/f + q ratios of 35.5 and 38.8. Beneath the Q5 sediments (120 cm in core 16-935 and 170 cm in 16-945) a marked increase occurs in the f/f + q ratios, averaging 50.1 and 45.7, respectively, as orthoclase and plagioclase become more important (Table IV).

The arkosic sands below unit Q5 in cores 16-935 and 16-945 suggest a proximal source area that has a relatively high feldspathic content. The probable source is the Beaverdam Sand, which is feldspathic and outcrops along the adjacent coastal plain in Maryland (Owens and Denny, 1979). Arkosic sand deposits would have been transported onto the shelf during the last glacial low sea level stand by any fluvial system that drained those coastal plain sediments (Milliman, 1972).

The distribution of unit Q3 derived from the seismic-reflection data, iron-staining and high feldspar content of the unit Q3 sands, and lack of marine microfauna in the unit, support the interpretation that unit Q3 is the subsurface fill of the ancestral St. Martin River. The river apparently drained the feldspathic Beaverdam sand, then flowed across and incised into the exposed continental shelf during Wisconsin time. This ancestral system is analogous to the Indian River tributaries of the Delaware paleochannel system described by Sheridan *et al.* (1974), but is unlikely to be any way connected to the tributary system of the ancestral Delaware River (Sheridan *et al.*, 1974).

Core 16-1002 (Figure 28) was taken from a solitary channel just east of core 16-945 and just out of the main stem of the M3-Q3 channel. The small channel is interpreted to be a tributary of the M3-Q3 system. A dense unit of imbricated shells of several genera were analyzed for amino acid racemization, and assigned a Pleistocene age based on the A/I ratios (Appendix II). These would appear to be older (stage 7) shells that were transported up the stream valley during early stages of transgression and chanel aggradation during oxygen-isotope stage 3 or 1.

Core 16-1029 (17.45 km offshore) is situated in what appears to be shallow, near-surface channeling under present shelf sands, and penetrates a unit of oxidized sands and gravels near its base. Field's (1976) core 33 is located the same distance offshore approximately 10 km northeast of core 16-1029, and contains a similar

Table IV.—Light Mineral Petrology, Cores 16-935 and 16-945.

Core 16-935 Depth in Core (cm)	Percent quartz (qtz)	Percent feldspar (f)	f/(f + qtz) × 100	Core 16-945 Depth in Core (cm)	Percent quartz (qtz)	Percent feldspar (f)	f/(f + qtz) × 100
40-43	48	31	39	15-20	53	31	36
52-55	52	26	33	53-55	47	36	43
63-67	49	34	40	75-80	52	30	36
95-100	37	26	41	110-115	43	36	45
105-110	50	20	28	163-166	43	23	34
116-120	40	19	32	191-194	38	40	51
130-135	37	29	43	198-203	24	32	56
165-170	41	19	31	240-245	36	38	50
190-195	30	28	48	290-295	38	30	34
255-260	36	36	50	310-315	35	35	50
295-300	33	37	52	341-345	30	28	48
348-352	33	49	59	370-375	35	24	40
425-430	27	49	64	451-457	32	24	42
525-530	25	49	66	465-470	42	24	36
565-570	37	29	43	520-526	38	27	41
608-610	31	28	45	570-575	34	36	51
				590-595	32	34	51

feldspars — orthoclase > plagioclase > microline
Heavy minerals — garnet, zircon, tourmaline, with epidote, hornblende, micas, glauconite, rutile
200 grain point count in 3.0 to 4.0 phi size class

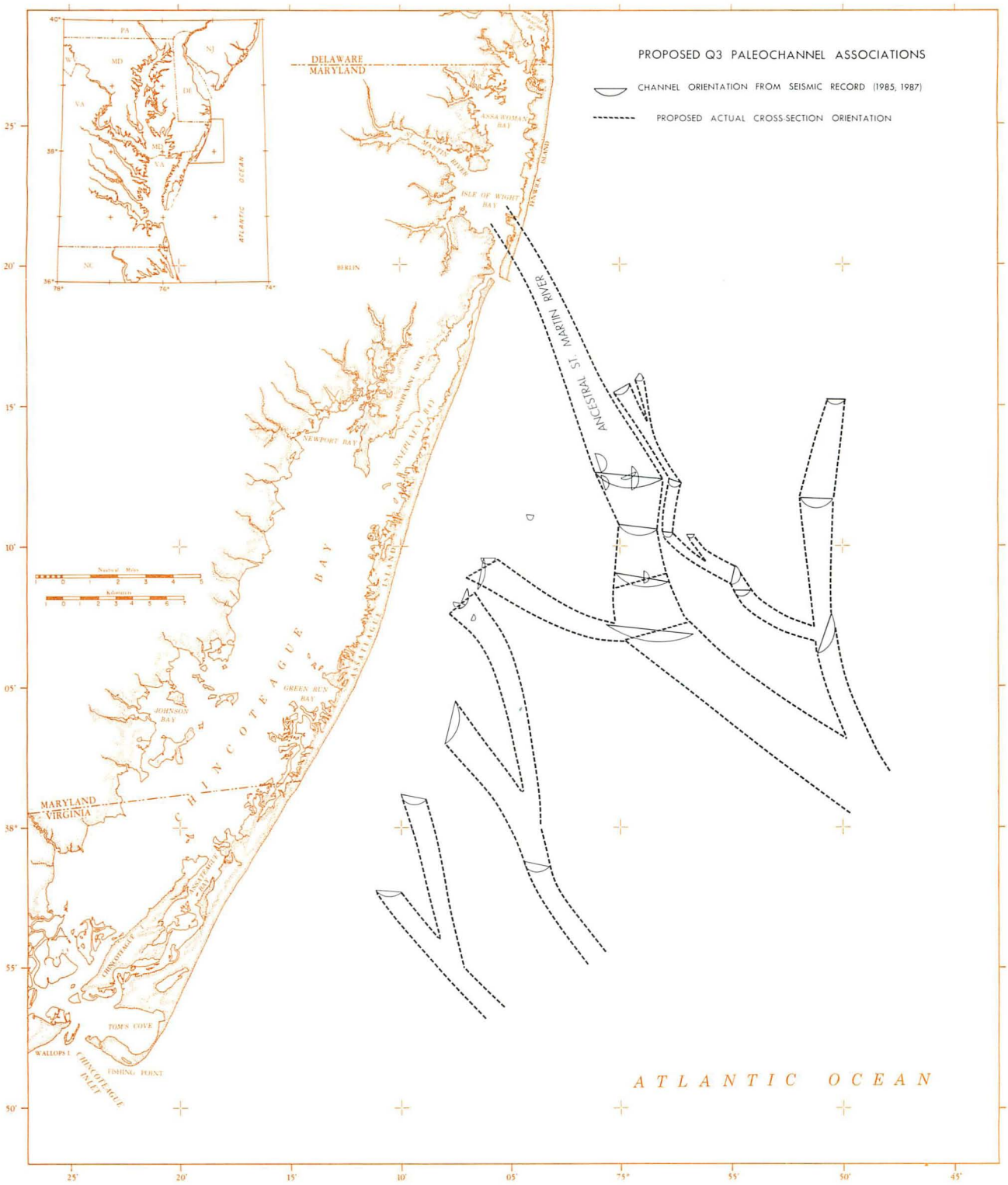

Figure 26.—Reconstruction of drainage system associated with channels (M3-M1) filled by unit Q3.

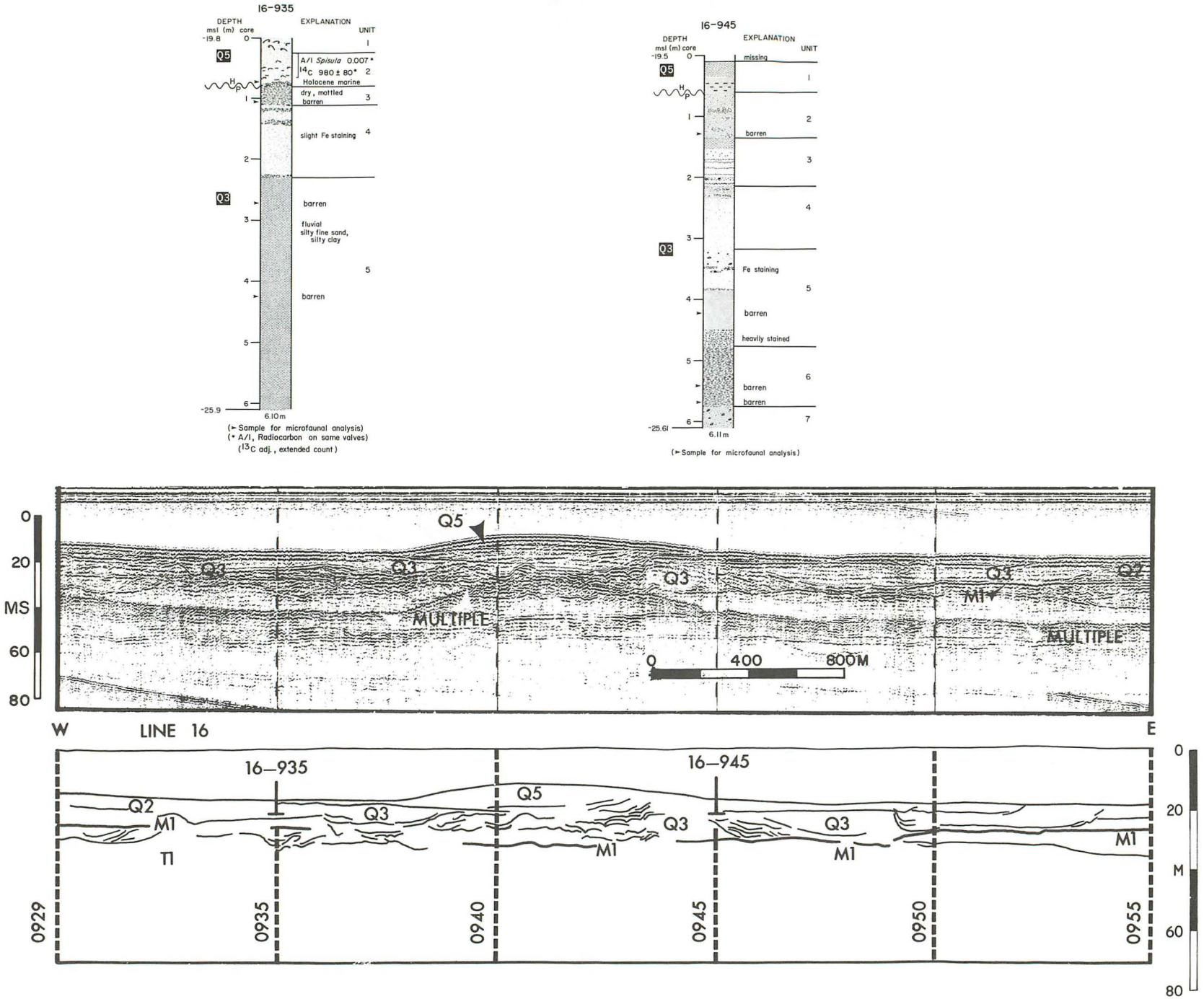

Figure 27.—Area of line 16 showing cross section of M3 channel feature and 2 vibracores (16-935 and 16-945) that penetrated fluvial sediments (Q3) in the channel fill.

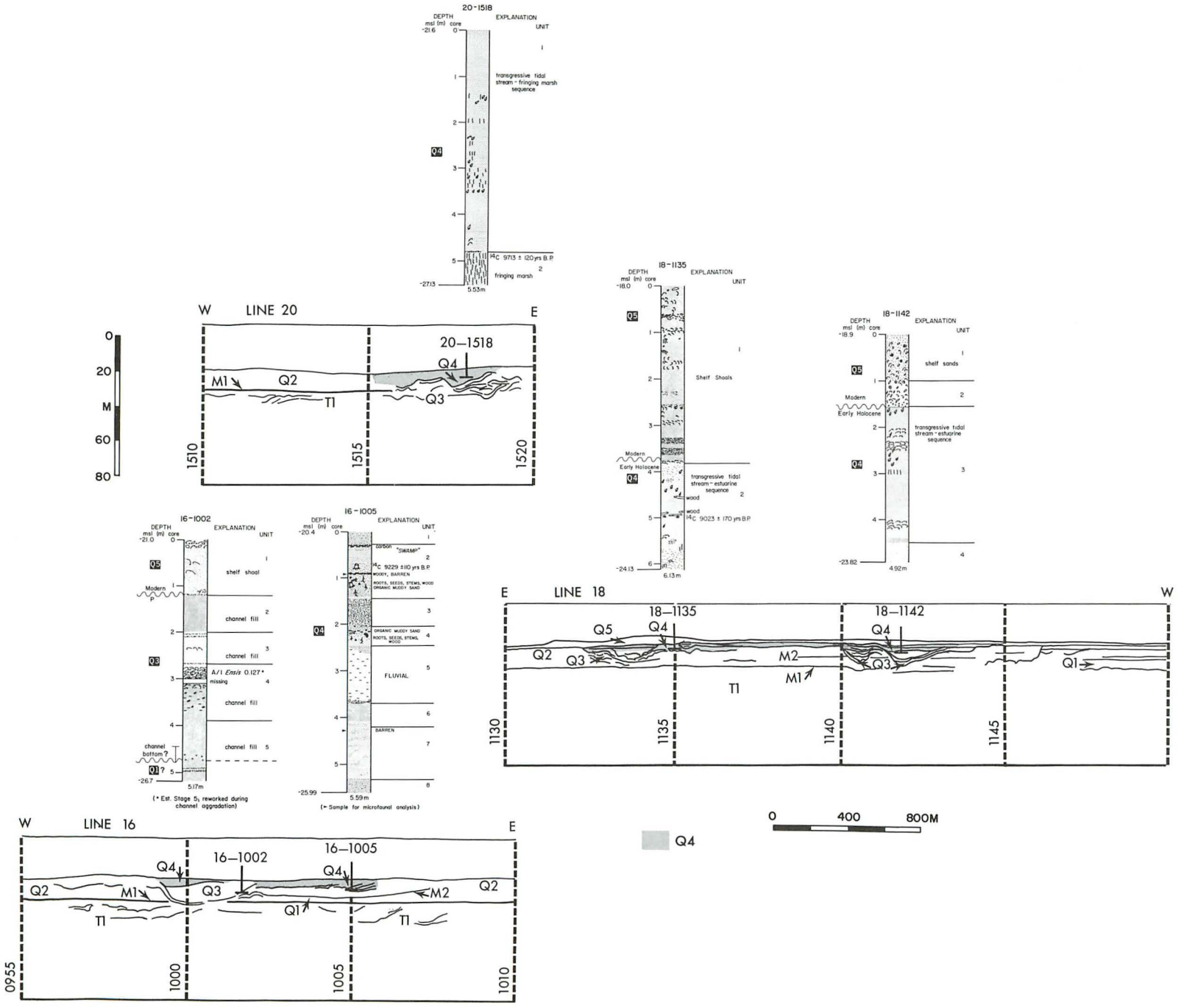

Figure 28.—Smaller channels, tributary to the main M3 channel, in which Holocene estuarine sediments (Q4) have been cored and radiocarbon-dated, with the exception of 16-1002, which contains reworked late Pleistocene shells beneath Holocene shelf sands.

iron-stained lowest unit, interpreted by Field (1976) as a fluvial deposit. In the absence of clear seismic-reflection evidence of a discrete channel, core 16-1029 is interpreted as having penetrated a marginal-fluvial unit that is equivalent to unit Q3 beneath shelf sands.

Early Holocene (Unit Q4)

The record of Holocene transgressive coastal lithosomes (unit Q4), both leading edge (lagoon perimeter, estuarine, coastal swamp environments) and trailing edge (inlet channels, barrier environments) is sparse and almost exclusively restricted to locations with relict channeled topography. Antecedent topography as a control on preservation of the transgressive sequence has been demonstrated (Belknap and Kraft, 1985), and the data presented here further exemplify that control in terms of rate of sea level rise and resulting depth of shoreface erosion (Swift, 1968).

A belt lying between 13 and 19 kilometers east of Assateague Island contains one suite of the Holocene Q4 section, consisting of early Holocene leading-edge lithosomes. Cores 18-1142, 1135, and 20-1518 are characterized by transgressive tidal-stream or estuarine channel-fill deposits, analogous to those in the present back-barrier estuaries. Core 18-1135 contained a Q4 sequence consisting of muds overlain by sands in which *Quercus* stems (U.S.D.A. Forest Products Laboratory, written comm., 1987; Figure 28) were found at a depth of -22.95 meters (MSL). These stems yielded a ^{14}C age of 9023 yr B.P. (Table V). Likewise, a transgressive tidal-channel sequence is recorded in core 20-1518, consisting of a basal meter of peaty mud, the peat being fringing marsh peat (R.P. Stumpf, NOAA, pers. comm., 1987). This unit is topped by uniform gray mud with additional scattered plant remains, deposited in what appears to be a central tidal channel. The lower, concentrated peat (Figure 29), at a depth of -26.5 m (MSL), gave a ^{14}C age of 9713 yr B.P. (Table V). The greater depth and greater age of this sample relative to that of 18-1135 is consistent with Holocene sea level history (Belknap and Kraft, 1977). Both of these cores were obtained from well-defined channel features identified on seismic-reflection records (Figure 28). These muds and plant remains comprise the upper portion of the transgressive, channel-bound succession of lithosomes, beginning with basal fluvial deposits of oxygen-isotope stage 2, grading up to estuarine or leading-edge tidal-stream muds encroaching a coastal upland swamp/marsh setting. These channels probably were initially cut during oxygen-isotope stage 4, and may have aggraded slightly during stage 3. If so, these deposits were eroded during the subsequent oxygen-isotope stage 2 and associated downcutting. Fluvial aggradation, probably beginning shortly after the 18 ka sea level minimum, should have proceeded virtually uninterrupted to estuarine sedimentation as the post-glacial transgression progressed.

Core 16-1005 was obtained from what appears on the Datasonics 3.5 kHz seismic-reflection record as a very shallow channeled section with low relief, 14.3 kilometers from shore. Core 16-1005 contains the extremely rare case of preserved, freshwater coastal wetland/swamp deposits and is characterized at its top by 2.5 meters of organic muddy sands, wood chunks, seeds, carbonaceous matter, roots, and twigs (Figure 28). The swamp sequence is twice punctuated by probable fluvial gravels, and is underlain by approximately 3 meters of light bluish gray muddy sands and sandy muds barren of microfauna, possibly of fluvial origin (Figure 28). A block of wood, tentatively identified as the common coastal genus *Fraxinus* (U.S.D.A. Forest Products Laboratory, written comm., 1986) gave a ^{14}C age of 9229 yr B.P. (Table V) at a depth of -21.0 meters (MSL), which is again consistent with local early Holocene sea level history. The well-documented local-relative Holocene sea level curve for Delaware (Belknap and Kraft, 1977) is used as a framework in which to place these three ages and from which to evaluate the sea level history of the Holocene shelf record (Figure 30).

Both wood samples plot just higher than the interpolated curve. *In situ* wood will lie above sea level; therefore, the *in situ Fraxinus* age is judged to be accurate. *Quercus* stems from core 18-1135 were deposited in a tidal stream setting, i.e., somewhat lower than *in situ;* however, they still plot above the curve. *In situ* fringing marsh peat (from a tidal stream setting) bears a direct relationship to sea level. Sample 20-1518 is likely *in situ* or not far removed from its source, and plots very close to the Delaware curve. Its ^{14}C date is therefore judged to be reasonably accurate (Figure 30).

With the accuracy of the ages supported in the context of the Delaware sea level curve, we may consider the effects of the varying rate of sea level rise, as shown by the curve, on stratigraphic preservation or erosion. During the period in which these samples were deposited, the rate of sea level rise was at least 29.6 cm/century, more than double the present rate of 12.5 cm/century. According to Swift (1968), rate of sea level rise relates directly to the depth of ravinement (shoreface erosion) at the trailing edge of the barrier system. Slower rates of sea level rise allow time in which to achieve greater depths of erosion, and vice versa. The remarkable preservation of coastal swamp in core 16-1005 can be attributed to the relatively fast rate of sea level rise at 9200 yrs B.P. and the resulting incomplete erosion. The sediments in cores 18-1142, 1135, and 20-1518 are preserved in the deeper parts of channels and owe their preservation mainly to antecedent topography. However, offshore channels may preserve more complete Holocene sections because of the rela-

Table V.—Summary of Radiocarbon Data, Early Holocene Continental Shelf Samples, Maryland.

Beta Lab No.	Core No. & Sect.	Depth in Core (cm)	Depth (m) MSL	Distance from Shore N.miles	km	Material	Age: 5568-yr Halflife yr B.P. + 1σ	Age:** 5730-yr Halflife yr B.P.
19963	20-1518D	490-500	-26.55	12.7	19.5	peat	9430 ± 120	9713***
19964	16-1005A	71-79 cm	-21.0	8.9	14.3	*Fraxinus*	8960 ± 110	9229***
21348	18-1135D	491-495 cm	-22.95	9.4	15.1	*Quercus*	8730 ± 170	9023***

*Beta Analytic, Inc.
**5730-year half-life obtained by multiplying the yr. B.P. age by 1.030 (Ralph *et al.*, 1973) used in Figure 30.
***beyond range of MASCA correction (Ralph *et al.*, 1973).

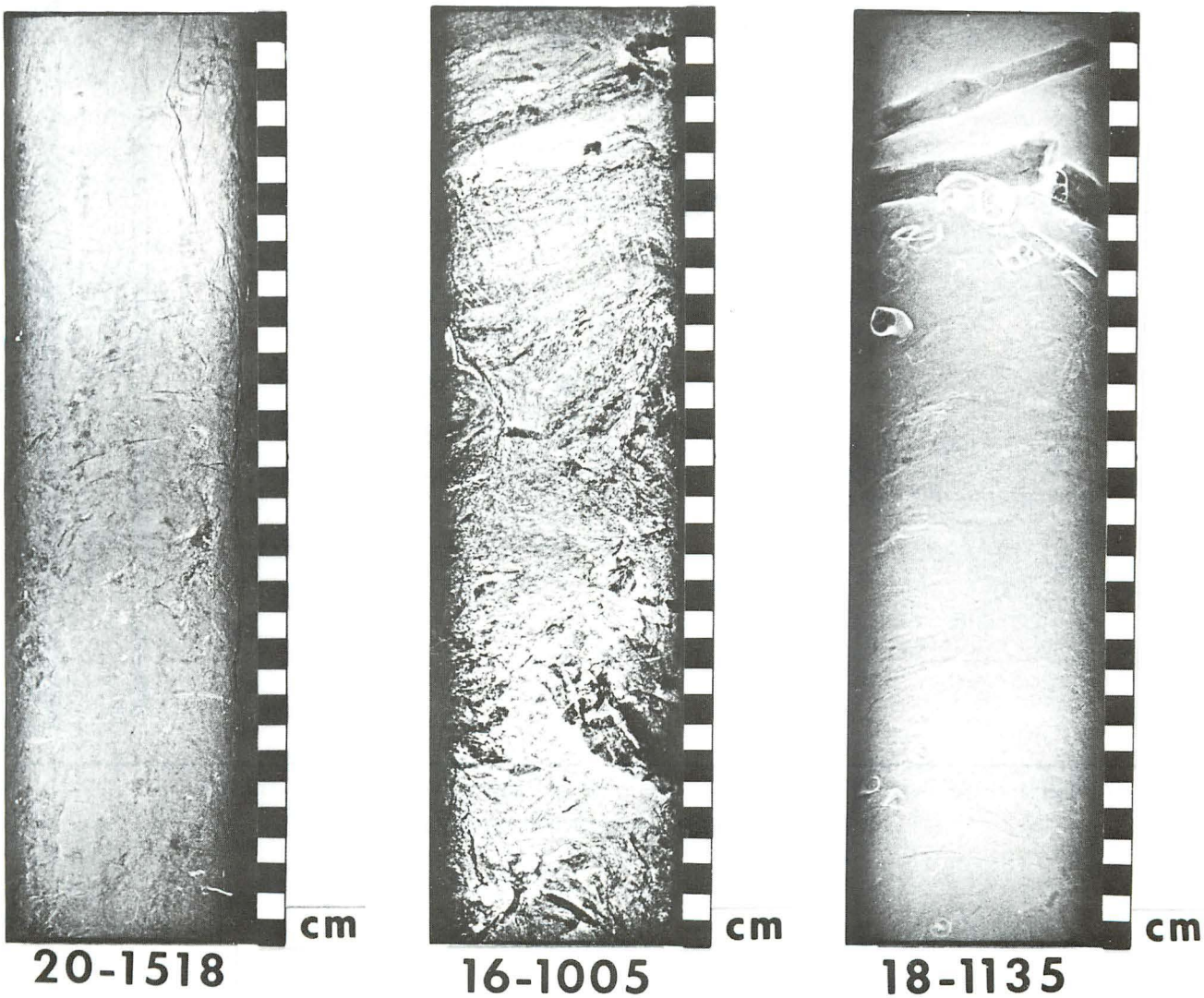

Figure 29.—Selected xeroradiographs showing radiocarbon-dated woody materials in 3 Holocene estuarine sequences, from 13–19 km offshore.

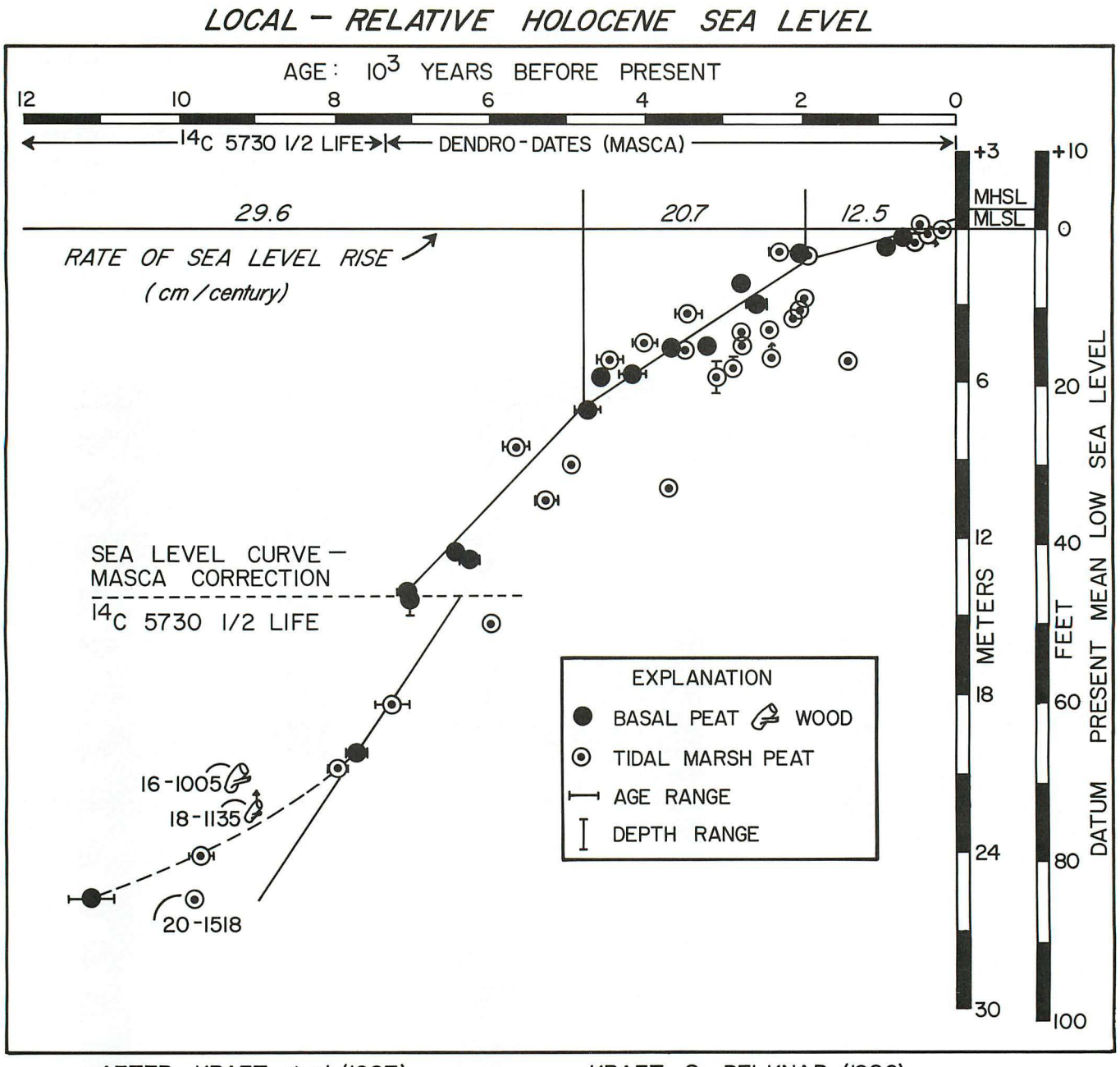

AFTER KRAFT et al (1987); ----- KRAFT & BELKNAP (1986); BELKNAP & KRAFT (1977)

Figure 30.—Local-relative Holocene sea level curve derived from basal peats, Delaware. Preservation of estuarine and swamp lithosomes on the outer shelf is attributed to the fast rate of sea level rise for the interval represented by the dated samples.

tively fast rate at which they were transgressed, compared to inshore channels, transgressed at a later time and slower rate.

Between 13 and 5 kilometers from shore no Holocene sediments were cored. Within 4.8 kilometers of shore other channels with probable Holocene fill have been noted in seismic-reflection data by Field (1976, 1980) and in this study (Figure 16). Cores 20-1340 and 23-928 penetrated two channel-fill sections, 4.3 and 4.8 kilometers from shore, respectively. No reliably datable material was found in either core; however, characteristics of the muds, including the gray coloration, soft consistency, and high water content point to Holocene ages for each. Core 23-928 contains a typical soft, wet, and pure (not olive-) gray estuarine mud with articulated *Crassostrea,* overlain by uniform sands with thin mud lenses and clasts, deposited in a wide, shallow channel seen in seismic-reflection profiles. This sequence is analogous to those in offshore cores 18-1135, 1142, and 20-1518. Core 20-1340 records a deep, more complex channel which may trend parallel to shore, and which exhibits infilling, perhaps point bar, structure prograding in which appears to be a landward direction (Figure 31). Coarse sediment interbedded with mud in the lower portion of this core may represent a fluvial-estuarine transition during transgression.

The apparent lack of a preserved Holocene back-barrier section between 6.6 and 13 km from shore is in direct contrast to Field's (1980) stratigraphic cross section (Figure 12C). As stated earlier, it is highly likely that the sample from Field's (1976) core 13, dated at 5765 ± 105 yr B.P., represents a Holocene marsh remnant outcropping in the shoreface, based on its depth below MSL and its apparent proximity to shore (less than 1.6 km). Our core coverage on lines 16, 18, and 20 is concentrated enough to have documented the occurrence of a widespread mud unit of Holocene age if it existed. Our unit Q2 is apparently equivalent to Field's (1976; 1980) widespread mud unit, but is of Pleistocene rather than Holocene age. It appears that the slowing rate of sea level rise between 7 ka and 2 ka was responsible for increased shoreface erosion and loss of the Holocene back-barrier record. The only Holocene section found inshore of 13 km, with the exception of shoreface outcrops and modern shelf sands, is contained in the uppermost portions of channel sequences, in contrast to Field's (1980) interpretation (Figure 12C) of widespread Holocene deposits.

Modern Shelf Sands (Unit Q5)

Overlying units Q2, Q3, and Q4 are transgressive, trailing-edge shelf sands on which ridge and swale topography is developed. This discontinuous sand body is termed unit Q5 (Holocene/modern), and is believed to be generated in the shoreface as a direct result of ravinement processes. Initially shoreface-connected, shoals detach and evolve with rising sea level and shoreface retreat (McBride, 1986; Swift and Field, 1981). Cores 18-1215, 29-1730, and 29-1640 were collected from shoal axes and contain 4.6-6 meters of sands, shells and gravel. Cores collected near shoal flanks (cores 16-850, 20-1430, 25-1215) commonly contain 1-3 meters of shoal sands underlain by stiff Q2 muds. Field (1976) encountered this same pattern in a cross section of cores taken in Isle of Wight shoal. Three of his cores (15, 4, 5) along that ridge crest produced all sand, whereas two (19 and 20) on the flank penetrated an underlying mud unit. Cores collected in this study in troughs between shoals (cores 16-905, 16-935, 18-1230, 18-1248, 25-1308, 27-1520) consist of thick mud sequences topped by thin (≈ .33 meters) sand units, or have no surficial sand, indicating that mud is outcropping in some trough areas. This disconformity is physical evidence of a time-transgressive ravinement surface that by its nature and mode of formation may not always have an acoustically profound or persistent character due to probable mixing of different lithologies along the surface. Field's (1980) seismic-reflection data indicated that the shelf sand body's flat bottom was formed by a reflection surface represented by the top of the mud unit beneath the sands. This reflector (A1 of Field, 1980) (assumed but not mapped in this study), appears to outcrop at the seafloor in ridge troughs, exposing muds of unit Q2 at the surface. The lowermost (Q2) cored sand unit interpreted as oxygen-isotope stage 5e transgressive shelf shoal remnants, appears to be analogous to unit Q5.

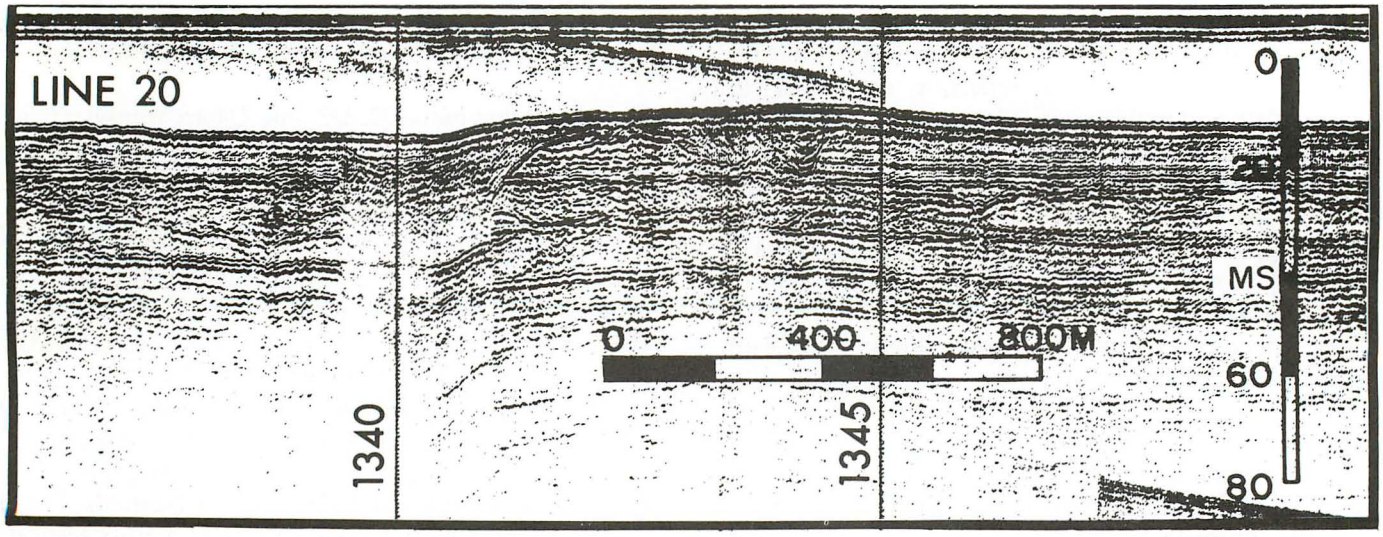

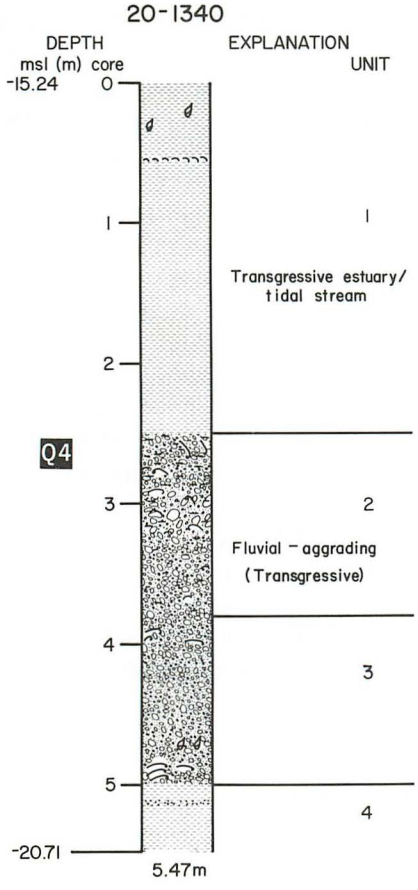

Figure 31.—Core 20-1340 and seismic cross-section of near-shore channel feature.

CONCLUSIONS

Above the Tertiary/Quaternary unconformity, late Pleistocene sediments record several glacial-interglacial sea level fluctuations. The thickest deposits (Q2) reflect the long period (50 ka) of relatively high sea level (+6 to -21 meters MSL) during marine oxygen-isotope stage 5. This unit was deposited in a unique, predominantly regressive shelf environment that has no modern analog. The source of the large quantities of fine sediment making up this unit (seemingly ubiquitous from North Carolina to New Jersey) can only be postulated. Sea level may have been low enough to cause a seaward shift of the limit of deposition of fluvial fine-grained sediment in major estuaries such as Delaware and Chesapeake Bays, resulting in a net export of mud to the adjacent inner shelves. The nearshore shelf regime may also be surmised as a quiet, low energy system due to the widespread occurrences of *in situ M. lateralis* in undisturbed beds. The thickness (>6 meters) and lack of biogenic alteration of the mud unit suggest a high sedimentation rate.

In terms of barrier island formation, oxygen-isotope stages 5e and 5c attained sea level elevations high enough (6 meters and 0 meters MSL) to have maintained barriers through headland erosion and shoreface retreat. Deposits containing such barrier sequences, such as the Nassawadox, Ironshire, and Wachapreague Formations, have been mapped on the Delmarva peninsula. Lower sea levels, such as oxygen-isotope stage 5a (-7 meters MSL) may never have reached an elevation at which a headland sediment source extended far enough out on the shelf to supply a barrier. Nearshore deposition may have occurred as widespread tidal-marshes or mudflats, a possible explanation for those marsh layers cored in the Sinepuxent Formation.

Figure 32 summarizes the Quaternary shelf deposits in Maryland in their isotopic stage and sea level framework. Oxygen-isotope stage 6 is represented by the erosion surface M2, and substage 5e is represented by transgressive shelf sands and relict shoals of unit Q1. Substages 5d-5a are represented by a regressive shelf mud that accounts for intervals between deposition of peak transgressive units onshore and establishes a continuum of a complete transgressive-regressive interglacial-glacial cycle previously undocumented in this area. No available data support a high sea level stand during the period of approximately 30–40 ka. No deposits, only a fluvial erosional surface, represent oxygen-isotope stages 4, 3, and 2 on the Maryland shelf. The oxygen-isotope stage 2-1 transition is marked by fluvial-estuarine fill (unit Q3) sequences in M3 paleo-channels. The limited Holocene record indicates that previous theories of remnant backbarrier deposits left beneath transgressing barriers are unfounded, at least during periods of slow sea level rise. Such deposits may exist on the outer shelf, where they were transgressed during early Holocene episodes of much faster sea level rise and shallower shoreface erosion.

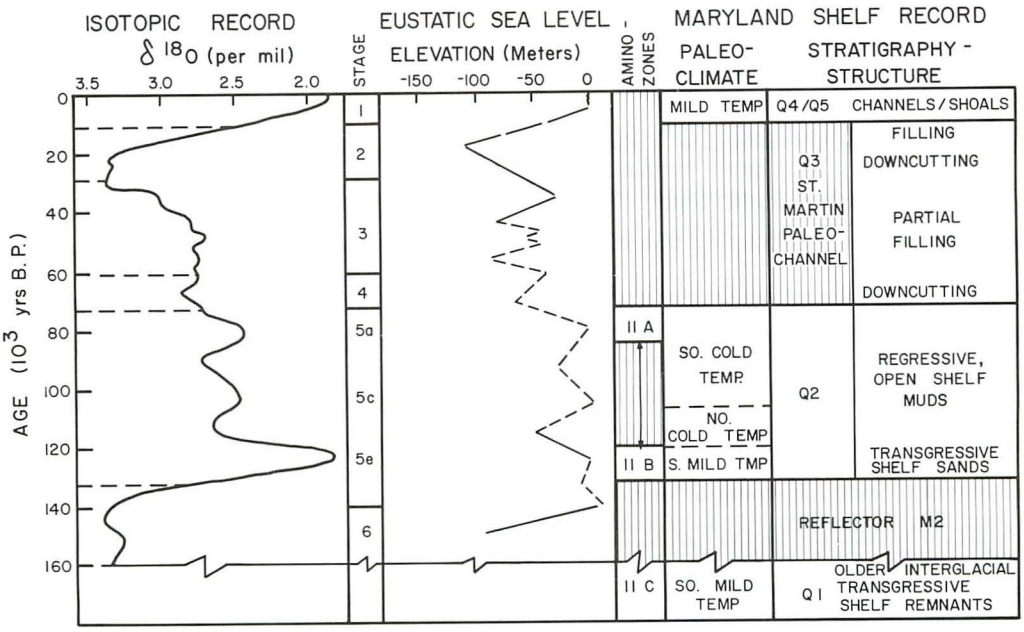

Figure 32.—Assignment of Maryland shelf lithologic units and erosional surfaces to appropriate time frames based on consistency of amino acid ratios, correlations to onshore dated units, and the context of global glacioeustatic ice volume and sea level records.

REFERENCES CITED

Bada, J.L. and Schroeder, R.A., 1972, Racemization of isoleucine in calcareous marine sediments: Kinetics and mechanism. Earth and Planetary Science Letters, vol. 15, p. 1-11.

Bartberger, C.E., 1976, Sediment sources and sedimentation rates, Chincoteague Bay, Maryland and Virginia: Jour. Sed. Petrology, vol. 46, p. 326-336.

Belknap, D.F., 1979, Applications of amino acid geochronology to stratigraphy of the Late Cenozoic marine units of the Atlantic coastal plain: Ph.D. Dissertation, Dept. of Geology, Univ. of Delaware, Newark, DE, 550 pp.

_____, 1981, Preservation potential of transgressive coastal lithosomes on the U.S. Atlantic shelf: Marine Geology, vol. 42, p. 429-442.

_____, 1985, Influence of antecedent geology on stratigraphic preservation potential and evolution of Delaware's barrier systems: Marine Geology, vol. 63, p. 235-262.

Belknap, D.F., and Kraft, J.C., 1977, Holocene relative sea-level changes and coastal stratigraphic units on the northwest flank of the Baltimore canyon trough geosyncline: Jour. Sed. Petrology, vol. 47, p. 610-629.

Belknap, D.F., and Wehmiller, J.F., 1980, Amino acid racemization in Quaternary mollusks: Examples from Delaware, Maryland, and Virginia, *in,* P.E. Hare (ed.), Biogeochemistry of amino acids, John Wiley and Sons, Inc. p. 401-414.

Bender, M.L., Fairbanks, R.G., Taylor, F.W., Matthews, R.K., Goddard, J.G., and Broecker, W.S., 1979, Uranium-Series dating of Pleistocene reef tracks of Barbados, West Indies: Geol. Soc. American Bull., vol. 90, p. 577-594.

Biggs, R.B., 1970, The origin and geological history of Assateague Island, Maryland and Virginia, *in,* Assateague Ecological Studies, Final Report, Part 1: University of Maryland, Natural Resources Inst., Contr. No. 446, p. 8-41.

Bloom, A.L., 1983, Sea level and coastal morphology of the United States through the late Wisconsinan glacial maximum, *in,* Porter, S.C., ed., Late Quaternary environments of the United States, Vol. 1, The Late Pleistocene, University of Minnesota Press, Minneapolis, MN, p. 215-229.

Bloom, A.L., Broecker, W.S., Chappell, M.A., Matthews, R.K., and Mesolella, K.J., 1974, Quaternary sea level fluctuations on a tectonic coast: New 230Th/234U dates from the Huon Peninsula, New Guinea: Quaternary Research, vol. 4, p. 185-205.

Bloom, A.L., and Yonekura, N., 1985, Coastal terraces generated by sea-level change and tectonic uplift, *in,* M.J. Woldenberg, ed., Models in Geomorphology, Allen and Unwin, Inc., Winchester, MA, p. 139-154.

Bowen, D.Q., Sykes, G.A., Reeves, A., Miller, G.H., Andrews, J.T., Brew, J.S., and Hare, P.E., 1985, Amino acid geochronology of raised beaches in southwest Britain: Quaternary Science Reviews, vol. 4, p. 297-318.

Chappell, J., 1974, Geology of coral terraces, Huon Peninsula, New Guinea: A study of Quaternary tectonic movements and sea-level changes: Geol. Soc. America Bull., vol. 85, p. 553-570.

_____, **and Veeh, H.H.**, 1978, Late Quaternary tectonic movements and sea-level changes at Timor and Atauro Island: Geol. Soc. America Bull., vol. 89, p. 356-368.

_____, **and Shackleton, N.J.**, 1986, Oxygen isotopes and sea level: Nature, vol. 324, no. 13, p. 137-140.

Climap Project, Members, Ruddiman, W.F., et al., 1984, The last interglacial ocean: Quaternary Research, vol. 21, p. 123-224.

Colman, S.M., and Hobbs, C.H., III, 1987, Quaternary geology of the southern Virginia part of the Chesapeake Bay: U.S. Geol. Survey, Misc. Field Studies Map MF 1948A, 2 sheets.

_____, **and Mixon, R.B.**, The record of major Quaternary sea-level changes in a large coastal plain estuary, Cheseapeake Bay, eastern United States: Paleao., Paleao., Paleao., in press.

_____, **Mixon, R.B., Ruben, M., Bloom, A.L., and Johnson, G.H.**, 1989, A dilemma revisited: comment on "Late Pleistocene barrier island sequence along the southern Delmarva Peninsula: Implications for Middle Wisconsin sea levels.": Geology, vol. 17, p. 84-85.

_____, **Halka, J.P., Hobbs, C.H. III, Mixon, R.B., and Foster, D.S.**, Ancient channels of the Susquehanna River beneath Chesapeake Bay and the Delmarva Peninsula: Geol. Soc. America Bull., in press.

Cronin, T.M., 1981, Rates and possible causes of neotectonic vertical crustal movements of the emerged southeastern United States Atlantic coastal plain: Geol. Soc. America Bull., vol. 92, p. 812-833.

_____, 1983, Rapid sea level and climate change: evidence from continental and island margins: Quaternary Science Reviews, vol. 1, p. 177-214.

_____, 1987, Quaternary sea-level studies in the Eastern United States of America: A methodological perspective; *in,* M.J. Tooley and I. Shennan, eds., Sea Level Changes: Institute of British Geographers Special Paper, Oxford, Basil Blackwell, p. 225-248.

_____, 1988, Evolution of marine climates of the U.S. Atlantic coast during the past four million

years: Phil. Trans. Royal Soc. London, B 318, p. 661-678.

Cronin, T.M., Szabo, B.J., Ager, T.A., Hazel, J.E., and Owens, J.P., 1981, Quaternary climates and sea levels of the U.S. Atlantic coastal plain: Science, vol. 211, no. 4479, p. 233-240.

Demarest, J.M., 1981, Genesis and preservation of Quaternary paralic deposits on Delmarva Peninsula: Ph.D. Dissertation, Dept. Geology, University of Delaware, Newark, DE, 240 pp.

Demarest, J.M., Biggs, R.B., and Kraft, J.C., 1981, Time-stratigraphic aspects of a formation: Interpretation of surficial Pleistocene deposits by analogy with Holocene paralic deposits, southeastern Delaware: Geology vol. 9, p. 360-365.

Demarest, J.M., and Leatherman, S.P., 1985, Mainland influence on coastal transgression: Delmarva Peninsula: Marine Geology, vol. 63, p. 19-33.

Duane, D.B., Field, M.E., Meisburger, E.P., Swift, D.J.P., and Williams, S.J., 1972, Linear shoals on the Atlantic inner shelf, Florida to Long Island; *in,* D.J.P. Swift, D.B. Duane, and O.H. Pilkey, eds., Shelf Sediment Transport: Process and Pattern: Dowden, Hutchinson and Ross, Stroudsberg, PA, p. 447-449.

Field, M.E., 1976, Quaternary evolution and sedimentary record of a Coastal Plain Shelf: Central Delmarva Peninsula, Mid-Atlantic Bight, U.S.A.: Ph.D. Dissertation, Dept. Geology, George Washington Univ., Washington, D.C., 200 pp.

_____, 1979, Sediments, shallow subbottom structure, and sand resources of the inner continental shelf, central Delmarva Peninsula: Technical Paper 79-2, USACE Coastal Engineering Research Center, Ft. Belvoir, VA, 122 pp.

_____, 1980, Sand bodies on coastal plain shelves: Holocene record of the U.S. Atlantic inner shelf of Maryland: Jour. Sed. Petrology, vol. 50, p. 505-528.

Finkelstein, F., and Kearny, M.S., 1988, Late Pleistocene barrier-island sequence along the southern Delmarva Peninsula: Implications for middle Wisconsin sea levels: Geology, vol. 16, p. 41-45.

Fisher, J.J., 1967, Origin of barrier island chain shoreline, Middle Atlantic states: Geol. Soc. America Spec. Paper 115, p. 66-67.

Folk, R.L., 1954, The distinction between grain size and mineral composition in sedimentary rock nomenclature: Jour. Geology, vol. 62, p. 344-359.

Halsey, S.D., 1978, Late Quaternary geologic history and morphologic development of the barrier island system along the Delmarva Peninsula of the mid-Atlantic bight: Ph.D. Dissertation, Dept. Geology, University of Delaware, Newark, DE., 592 pp.

Hansen, H.J., 1973, Stratigraphic discussion in support of a major unconformity separating the Columbia Group from the underlying Upper Miocene aquifer complex in eastern Maryland: Southeastern Geology, vol. 22, p. 123-138.

Harmon, R.S., Schwarcz, H.P., and Ford, D.C., 1978, Late Pleistocene sea level history of Bermuda: Quaternary Research vol. 9, p. 205-218.

Harmon, R.S., Mitterer, R.M., Kriausaku, N., Land, L.S., Schwarcz, H.P., Garrett, P., Larson, G.J., Vacher, H.L., and Rowe, M., 1983, U-series and amino acid racemization geochronology of Bermuda: Implications for eustatic sea-level fluctuations over the past 250,000 years: Paleao., Paleao., Paleao., vol. 44, p. 41-70.

Hazel, J.E., 1968, Pleistocene ostracode zoogeography in Atlantic submarine canyons: Jour. Paleontology, vol. 42, p. 1264-1271.

_____, 1970, Atlantic continental shelf and slope of the United States — Ostracode zoogeography in the southern Nova Scotian and northern Virginian faunal provinces: U.S. Geol. Survey Prof. Paper 529-E, 21 pp.

Imbrie, J., Hays, J.D., Martinson, D.G., McIntyre, A., Mix, A.C., Morley, J.J., Pisias, N.G., Prell, W.L. and Shacklelton, N.J., 1984, The orbital theory of Pleistocene climate: support from a revised chronology of the marine 180 record, *in,* A.L. Berger, J. Imbrie, J. Hays, G. Kukla, and B. Saltzman, eds., Milankovitch and Climate, Part 1. D. Reidel Publishing Co., Boston, MA, p. 269-305.

Kerhin, R.T., and Williams, S.J., 1987, Surficial sediments and later Quaternary sedimentary framework of the Maryland inner continental shelf: Proceedings, Coastal Sediments '87, Am. Soc. Civil Engineers, New Orleans, LA, vol. II, p. 2126-2140.

Kraft, J.C., 1971, Sedimentary facies patterns and geologic history of a Holocene marine transgression: Geol. Soc. America Bull., vol. 82, p. 2131-2158.

Ku, T.-L., Kimmel, M.A., Easton, W.H., and O'Neil, T.J., 1974, Eustatic sea level 120,000 years ago on Oahu, Hawaii: Science, vol. 183, p. 959-962.

Leatherman, S.P., 1979, Migration of Assateague Island, Maryland, by inlet and overwash processes: Geology, v. 7, p. 104-107.

Martinson, D.G., Pisias, N.G., Hays, J.D., Imbrie, J., Moore, T.C., and Shackleton, N.J., 1987, Age dating and the orbital theory of the ice ages: Development of a high-resolution 0 to 300,000-year chronostratigraphy: Quaternary Research, vol. 27, p. 1-29.

McBride, R.A., 1986, The origin, evolution, orientation, and distribution of shoreface-attached sand ridges and their relationship to tidal inlets, North Atlantic Shelf, USA. M.S. Thesis, Dept. Geog. and Antropology, Louisiana State University, Baton Rouge, LA, 180 pp.

McDonald, K.A., 1982, Three-dimensional analysis of

Pleistocene and Holocene coastal sedimentary units at Bethany Beach, Delaware. M.S. Thesis, Dept. of Geology, Univ. of Delaware, Newark, DE., 205 pp.

Miller, G.H., and Mangerud, J., 1985, Aminostratigraphy of European marine interglacial deposits: Quaternary Science Reviews, vol. 4, p. 215–278.

Milliman, J.D., 1972, Atlantic continental shelf and slope of the United States — Petrology of the sand fraction of sediments, northern New Jersey to southern Florida: U.S. Geol. Survey Prof. Paper 529-J, 137 pp.

Mixon, R.B., 1985, Stratigraphic and geomorphic framework of uppermost Cenozoic deposits in the southern Delmarva Peninsula, Virginia and Maryland: U.S. Geol. Survey Prof. Paper 1067-G, 53 pp.

Mixon, R.B., Szabo, B.J., and Owens, J.P., 1982, Uranium-series dating of mollusks and corals, and age of Pleistocene deposits, Chesapeake Bay area, Virginia and Maryland: U.S. Geol. Survey Prof. Paper 1067-E, 18 pp.

Neumann, A.C., and Moore, W.S., 1975, Sea level events and Pleistocene coral ages in the northeastern Bahamas: Quaternary Research, vol. 5, p. 215–224.

Newman and Rusnak, G.A., 1965, Holocene submergence of the eastern shore of Virginia: Science, vol. 148, p. 1464–1466.

Owens, J.P., and Denny, C.S., 1979, Upper Cenozoic deposits of the Central Delmarva Peninsula, Maryland and Delaware: U.S. Geol. Survey Prof. Paper 1067-A, 28 pp.

Peebles, P.C., 1984, Late Cenozoic landforms, stratigraphy and history of sea level oscillations of southeastern Virginia and northeastern North Carolina: Ph.D. Dissertation, College of William and Mary, School of Marine Science, Williamsburg, VA., 149 pp.

Peebles, P.C., Johnson, G.H., and Berquist, C.R., 1984, The middle and late Pleistocene stratigraphy of the outer coastal plain, Southeastern Virginia: Virginia Minerals, v. 30, no. 2, p. 13–22.

Ralph, E.K., Michael, H.N., and Han, M.C., 1973, Radiocarbon dates and reality: M.A.S.C.A. Newsletter, Museum Applied Science Center for Archeology, Univ. of PA, vol. 9, p. 1–20.

Rasmussen, W.C., and Slaughter, T.H., 1955, The water resources of Somerset, Wicomico, and Worcester counties: MD Geol. Survey Bull. 16, 533 pp.

Rine, J.M., Tillman, R.W., Stubblefield, W.L., and Swift, D.J.P., 1986, Lithostratigraphy of Holocene sand ridges from the nearshore and middle continental shelf of New Jersey, U.S.A., *in,* T.F. Moslow and E.G. Rhodes, eds., Modern and Ancient Shelf Clastics: A Core Workshop: S.E.P.M. Core Workshop No. 9, p. 1–72.

Shackleton, N.J., and Opdyke, N.D., 1973, Oxygen isotope and paleomagnetic stratigraphy of Equatorial Pacific core V28-238: Oxygen isotope temperatures and ice volumes on a 10^5 year and 10^6 year scale: Quaternary Research, vol. 3, p. 39–55.

Sheridan, R.E., C.E. Dill, Jr., and J.C. Kraft, 1974, Holocene sedimentary environments of the Atlantic inner shelf off Delaware: Geol. Soc. America Bull., vol. 85, p. 1319–1328.

Shideler, G.L., Swift, D.J.P., Johnson, G.H., and Holliday, B.W., 1972, Late Quaternary Stratigraphy of the inner Virginia continental shelf: A proposed standard section: Geol. Soc. America Bull., vol. 83, p. 1787–1804.

Shideler, G.L., Ludwick, J.C., Oertel, G.F., and Finkelstein, K., 1984, Quaternary stratigraphic evolution of the southern Delmarva Peninsula coastal zone, Cape Charles, Virginia: Geol. Soc. America Bull., v. 95, p. 489–502.

Stahl, L., Kocgan, J., and Swift, D.J.P., 1974, Anatomy of a shoreface-connected sand ridge on the New Jersey shelf: Implications for the genesis of the surficial sand sheet: Geology, vol. 2, p. 117–120.

Stubblefield, W.L., McGrail, D.W., and Kersey, D.G., 1984, Recognition of transgressive and post-transgressive sand ridges on the New Jersey continental shelf; *in,* Siliclastic Shelf Sediments, R.W. Tillman and C.T. Siemers, eds., S.E.P.M. Spec. Pub. No. 34, p. 1–24.

Stuvier, M., and Daddario, J.J., 1963, Submergence of the New Jersey Coast: Science, vol. 140, p. 951.

Swift, D.J.P., 1968, Coastal erosion and transgressive stratigraphy: Jour. Geology, vol. 76, p. 444–456.

_____, 1973, Delaware Shelf valley: Estuary retreat path, not drowned river valley: Geol. Soc. America Bull., vol. 84, p. 2743–2748.

Swift, D.J.P., and M. Field, 1981, Evolution of a classic sand ridge field, Maryland sector, North America inner shelf: Sedimentology, vol. 28, p. 462–482.

Szabo, B.J., 1985, Uranium-series dating of fossil corals from marine sediments of southeastern United States Atlantic Coastal Plain: Geol. Soc. America Bull., vol. 96, p. 398–406.

Toscano, M.A., 1989, Comment on "Late Pleistocene barrier island sequence along the southern Delmarva Peninsula: Implications for middle Wisconsin sea levels": Geology, vol. 17, p. 85–86.

Truitt, R.V., 1968, High winds — high tides: a chronicle of Maryland's coastal hurricanes: Univ. of Maryland, Nat. Res. Inst., Ed. Ser. No. 77, 35 pp.

Valentine, P.C., 1971, Climatic implication of a late Pleistocene ostracode assemblage from southeastern Virginia: U.S. Geol. Survey Prof. Paper 683-D, 28 pp.

Van Donk, J., 1976, O^{18} record of the Atlantic Ocean for the entire Pleistocene epoch: Geol. Soc. America Memoir 145, p. 147–163.

Ward, L.W., and Blackwelder, B.W., 1980, Strati-

graphic revision of upper Miocene and lower Pliocene beds of the Chesapeake Group, Middle Atlantic coastal plain: U.S. Geol. Survey Bull. 1482-D, 61 pp.

Wehmiller, J.F., 1984, Relative and absolute dating of Quaternary mollusks with amino acid racemization: Evaluation, application, questions; *in,* Quaternary Dating Methods, W.C. Mahaney, ed., Elsevier, Amsterdam, p. 171-193.

_____, 1986, Amino acid racemization geochronology; *in,* Dating Young Sediments, A.J. Hurford, E. Jager, and J.A.M. Ten Cate, eds., United Nations, CCOP Techn. Publ. No. 16, Bangkok, p. 139-158.

Wehmiller, J.F., and Belknap, D.F., 1982, Amino acid age estimates, Quaternary Atlantic coastal plain: Comparison with U-series dates, biostratigraphy, and paleomagnetic control: Quaternary Research, vol. 18, p. 311-336.

Wehmiller, J.F., Belknap, D.F., and York, L.L., 1987, Discussion on Corrado and others (1986), Capabilities and limitations of applied aminostratigraphy as illustrated by analysis of *Mulinia lateralis* from the Late Cenozoic marine beds near Charleston, South Carolina. South Carolina Geology, vol. 31, no. 2, p. 109-118.

Wehmiller, J.F., Belknap, D.F., Boutin, B.S., Mirecki, J.E., Rahaim, S.D., and York, L.L., 1988, A review of the aminostratigraphy of Quaternary mollusks from United States Atlantic coastal plain sites; *in,* D.L. Easterbrook, ed., Dating Quaternary Sediments, Geol. Soc. America Spec. Paper #227, p. 69-110.

Weigle, J.M., 1974, Availability of fresh ground water in northeastern Worcester County, Maryland: Maryland Geol. Survey, Rept. Invests. 24, 64 pp.

York, L.L., Wehmiller, J.F., Cronin, T.M. and Ager, T.M., 1989, Stetson Pit, Dare County, North Carolina: An integrated chronologic faunal, and floral record of subsurface coastal sediments; *in,* G. Kukla and D. Adam, eds., 1987 INQUA Proceedings Volume, Long Continental Records: Paleao., Paleao., Paleao., vol. 72, p. 115-132.

York, L.L. and Wehmiller, J.F., 1987, Aminostratigraphy of subsurface Quaternary marine sediments, Dare Co., NC (abstract). Geological Society of America Abstracts with Programs, vol. 19, no. 2, p. 138.

York, L.L., Aminostratigraphy of the U.S. Mid-Atlantic Pleistocene Coastal Plain: Norfolk, VA to Charleston, SC: Ph.D. Dissertation, Dept. of Geology, Univ. of Delaware, Newark, DE, in prep.

Zimmerman, H.B., Shackleton, N.J., Backman, J., Kent, D.V., Baldauf, J.G., Kaltenback, A.J., and Morton, A.C., 1984, History of Plio-Pleistocene climate in the northeastern Atlantic, Deep Sea Drilling Project hole 552A: Initial Reports of the Deep Sea Drilling Project, vol. 81, U.S. Govt. Print. Off., Washington, D.C., p. 861-875.

APPENDICES

APPENDIX I

SURFICIAL SEDIMENT SAMPLES

Table VI.—Textural Parameters of the Surficial Sediment Samples. See Figure 7 for Location. Water Depth is in Meters. Mean Grain Size and Sorting are in Phi (ϕ) Units for Only the Sand Fraction.

No.	Date	Latitude	Longitude	Water Depth (m)	Percents Gravel	Sand	Mud	Mean Grain Size	Sort
1	7/25/84	38°22′20″	75°01′21″	7.9	0	100	0	1.92	0.39
2	7/25/84	38°22′59″	74°58′45″	18.0	0	97	4	3.58	0.50
3	7/25/84	38°23′06″	74°59′59″	11.6	3	97	0	0.79	0.66
4	7/25/84	38°24′06″	75°01′26″	12.8	0	97	3	2.46	0.43
5	7/25/84	38°24′56″	76°00′45″	14.3	0	98	2	2.46	0.27
6	7/25/84	38°24′46″	74°58′42″	17.7	0	93	8	2.46	0.30
7	7/25/84	38°25′50″	75°00′52″	12.2	1	99	0	1.24	0.56
8	7/25/84	38°26′41″	75°00′28″	13.7	0	99	1	2.11	0.33
9	7/25/84	38°24′58″	75°01′08″	9.1	0	100	0	2.30	0.31
10	7/25/84	38°23′15″	75°01′53″	13.1	0	45	55	2.50	0.76
11	7/25/84	38°22′24″	75°02′10″	11.3	0	100	0	1.13	0.41
12	7/25/84	38°21′33″	75°02′31″	12.2	0	52	48	2.82	0.57
13	7/25/84	38°20′41″	75°02′53″	6.1	0	100	0	1.73	0.22
14	7/25/84	38°19′50″	75°03′12″	7.9	0	100	0	1.73	0.33
15	7/25/84	38°18′58″	75°03′33″	11.3	0	97	3	2.64	0.41
16	7/25/84	38°18′08″	75°03′52″	12.2	0	58	42	2.60	0.63
17	7/25/84	38°17′16″	75°04′15″	12.8	0	11	89	2.69	1.02
18	7/25/84	38°16′25″	75°04′34″	12.8	0	100	0	1.48	0.55
19	7/25/84	38°15′34″	75°04′54″	13.7	0	88	12	6.69	0.45
20	7/26/84	38°13′06″	75°06′54″	12.2	0	63	37	2.90	0.80
21	7/26/84	38°10′33″	75°07′55″	12.2	0	87	13	2.55	0.75
22	7/26/84	38°08′00″	75°08′57″	11.0	17	82	1	0.45	0.46
23	7/26/84	38°05′27″	75°09′57″	12.5	0	97	3	1.02	0.72
24	7/26/84	38°02′55″	75°10′59″	12.8	0	99	1	1.74	0.53
25	7/26/84	38°00′23″	75°11′59″	14.0	0	98	2	2.36	0.69
26	7/26/84	38°01′07″	75°10′39″	12.8	0	100	0	1.90	0.44
27	7/26/84	38°01′52″	75°09′23″	13.1	0	98	2	2.28	0.44
28	7/26/84	38°00′04″	75°09′04″	17.7	0	99	1	1.99	0.25
29	7/26/84	38°00′48″	75°07′47″	7.9	0	100	0	1.74	0.41
30	7/26/84	38°01′33″	75°06′28″	10.1	2	98	0	0.88	0.60
31	7/26/84	37°59′45″	75°06′12″	14.6	17	83	0	0.94	0.65
32	7/26/84	38°00′29″	75°04′54″	12.8	9	91	0	0.82	0.72
33	7/26/84	38°01′15″	75°03′35″	12.2	12	88	0	1.08	0.62
34	7/26/84	37°59′26″	75°03′17″	19.2	1	98	0	1.62	0.73
35	7/26/84	38°00′11″	75°01′59″	21.3	0	99	1	2.26	0.48
36	7/26/84	38°00′55″	75°00′44″	20.7	0	85	15	2.36	0.33
37	7/26/84	37°59′05″	75°00′25″	14.0	0	100	0	1.83	0.42
38	7/26/84	37°59′51″	74°59′08″	14.9	0	100	0	1.79	0.28
39	7/26/84	38°00′36″	74°57′50″	20.1	0	100	0	1.41	0.58
40	7/26/84	37°58′46″	74°57′31″	26.8	0	97	3	0.229	0.38
41	7/26/84	38°01′22″	74°56′33″	21.9	6	94	0	1.03	0.66
42	7/26/84	38°03′12″	74°56′55″	22.6	1	98	0	1.26	0.77
43	7/26/84	38°03′57″	74°55′39″	25.6	4	96	0	1.11	0.58
44	7/26/84	38°05′46″	74°55′55″	21.9	1	98	0	1.68	0.64
45	7/26/84	38°06′33″	74°54′43″	20.7	1	99	0	0.93	0.63
46	7/26/84	38°08′22″	74°54′59″	22.9	2	98	0	1.00	0.71

Table VI.—Textural Parameters of the Surficial Sediment Samples. See Figure 7 for Location. Water Depth is in Meters. Mean Grain Size and Sorting are in Phi (ϕ) Units for Only the Sand Fraction, continued.

No.	Date	Latitude	Longitude	Water Depth (m)	Percents Gravel	Sand	Mud	Mean Grain Size	Sort
47	7/26/84	38°09′09″	74°53′46″	20.7	0	100	0	1.44	0.39
48	7/26/84	38°10′58″	74°54′05″	24.1	0	99	1	2.64	0.28
49	7/26/84	38°11′44″	74°52′49″	21.3	0	100	0	2.39	0.30
50	7/27/84	38°17′12″	75°03′16″	7.9	0	100	0	1.46	0.28
51	7/27/84	38°17′58″	75°02′01″	8.2	0	100	0	2.10	0.26
52	7/27/84	38°18′46″	75°00′43″	15.2	0	100	0	2.36	0.33
53	7/27/84	38°19′34″	74°59′27″	16.5	0	98	2	2.52	0.26
54	7/27/84	38°20′17″	74°58′15″	19.5	30	69	0	1.16	0.68
55	7/27/84	38°21′11″	74°56′53″	20.7	0	98	2	2.10	0.62
56	7/27/84	38°23′42″	74°55′52″	20.1	0	100	0	0.94	0.52
57	7/27/84	38°22′56″	74°57′11″	19.5	0	99	1	1.94	0.68
58	7/27/84	38°22′06″	74°58′23″	12.2	0	100	0	1.78	0.26
59	7/27/84	38°21′18″	74°59′45″	16.5	0	100	0	1.11	0.66
60	7/27/84	38°20′31″	75°01′03″	15.5	0	98	2	2.47	0.28
61	7/27/84	38°20′12″	75°02′03″	11.3	0	100	0	2.20	0.36
62	7/31/84	38°18′29″	74°57′59″	19.5	0	99	1	1.03	0.77
63	7/31/84	38°17′42″	74°59′13″	15.2	0	100	0	1.77	0.46
64	7/31/84	38°16′56″	75°00′30″	17.1	0	99	1	1.94	0.37
65	7/31/84	38°16′09″	75°01′46″	14.9	0	100	0	1.68	0.47
66	7/31/84	38°15′23″	75°03′02″	17.1	0	97	3	2.16	0.27
67	7/31/84	38°14′38″	75°04′19″	15.8	18	57	25	0.69	0.87
68	7/31/84	38°13′52″	75°05′33″	14.6	8	90	2	1.12	0.84
69	7/31/84	38°11′18″	75°06′36″	11.3	0	100	0	1.52	0.41
70	7/31/84	38°12′04″	75°05′20″	17.1	0	88	12	2.29	0.64
71	7/31/84	38°12′49″	75°04′03″	17.7	0	60	40	2.60	0.66
72	7/31/84	38°13′35″	75°02′48″	16.5	0	100	0	2.07	0.62
73	7/31/84	38°14′22″	75°01′29″	18.9	0	95	5	2.62	0.27
74	7/31/84	38°15′07″	75°00′14″	21.3	0	87	13	2.75	0.39
75	7/31/84	37°15′54″	74°58′58″	18.9	11	89	0	1.02	0.71
76	7/31/84	38°13′20″	74°59′58″	18.6	4	96	0	1.11	0.69
77	7/31/84	38°12′33″	75°01′14″	17.7	4	96	0	1.19	0.80
78	7/31/84	38°11′48″	75°02′29″	20.7	0	66	34	2.52	1.02
79	7/31/84	38°11′02″	75°03′47″	18.3	1	98	1	1.24	0.59
80	7/31/84	38°10′16″	75°05′04″	16.2	22	78	0	0.81	0.50
81	7/31/84	38°09′31″	75°06′21″	18.3	0	80	20	2.86	0.50
82	7/31/84	38°08′45″	75°07′39″	14.6	11	87	1	0.44	0.54
83	7/31/84	38°06′12″	75°08′39″	14.0	7	92	1	0.40	0.37
84	7/31/84	38°06′57″	75°07′22″	17.7	0	37	63	1.61	0.45
85	7/31/84	38°07′43″	75°06′04″	17.7	3	89	8	1.81	0.60
86	7/31/84	38°08′29″	75°04′48″	15.8	12	87	1	0.87	0.69
87	7/31/84	38°09′13″	75°03′30″	15.8	0	99	1	2.72	0.29
88	7/31/84	38°09′59″	75°02′14″	18.9	0	90	10	2.14	0.48
89	7/31/84	38°10′45″	75°00′58″	20.1	0	82	18	0.175	0.70
90	7/31/84	38°12′17″	74°58′24″	20.1	0	99	1	2.17	0.48
91	7/31/84	38°12′17″	74°58′24″	20.1	0	99	1	2.17	0.48
92	7/31/84	38°13′03″	74°57′11″	20.1	23	71	6	0.76	0.73

Table VI.—Textural Parameters of the Surficial Sediment Samples. See Figure 7 for Location. Water Depth is in Meters. Mean Grain Size and Sorting are in Phi (ϕ) Units for Only the Sand Fraction, continued.

No.	Date	Latitude	Longitude	Water Depth (m)	Percents Gravel	Sand	Mud	Mean Grain Size	Sort
93	7/31/84	38°12′48″	74°54′24″	21.6	0	100	0	2.31	0.43
94	7/31/84	38°12′01″	74°55′35″	21.0	0	100	0	1.91	0.50
95	8/1/84	38°11′14″	74°56′51″	16.5	22	78	0	1.53	1.18
96	8/1/84	38°10′28″	74°58′08″	18.3	2	98	0	1.22	0.58
97	8/1/84	38°09′42″	74°59′24″	18.3	2	98	0	1.0	0.59
98	8/1/84	38°08′57″	75°00′41″	15.2	1	99	0	1.28	0.53
99	8/1/84	38°08′11″	75°01′55″	18.0	6	94	1	0.85	0.61
100	8/1/84	38°07′25″	75°03′14″	16.2	6	94	0	0.98	0.51
101	8/1/84	38°06′39″	75°04′31″	18.3	8	40	52	0.85	0.65
102	8/1/84	38°05′55″	75°05′48″	14.9	0	99	1	2.21	0.34
103	8/1/84	38°05′09″	75°07′05″	14.6	0	77	23	2.14	0.35
104	8/1/84	38°04′25″	75°08′22″	15.5	2	97	1	1.37	0.62
105	8/1/84	38°03′40″	75°09′40″	14.6	51	47	2	0.42	0.59
106	8/1/84	38°02′36″	75°08′06″	15.2	0	98	2	2.49	0.26
107	8/1/84	38°03′22″	75°06′48″	12.8	1	99	0	1.12	0.59
108	8/1/84	38°04′06″	75°05′31″	11.6	3	97	0	0.69	0.66
109	8/1/84	38°04′52″	75°04′13″	16.8	0	99	1	1.62	0.42
110	8/1/84	38°05′37″	75°02′55″	13.4	7	93	0	0.87	0.49
111	8/1/84	38°06′22″	75°01′40″	13.1	9	91	0	0.79	0.52
112	8/1/84	38°07′07″	75°00′23″	18.3	0	100	0	1.12	0.46
113	8/1/84	38°07′54″	74°59′05″	18.6	0	100	0	1.70	0.43
114	8/1/84	38°08′39″	74°57′51″	20.7	35	64	0	0.92	0.57
115	8/1/84	38°09′26″	74°56′34″	23.8	0	99	1	2.36	0.41
116	8/1/84	38°10′12″	74°55′18″	21.6	7	93	0	1.18	0.65
117	8/2/84	38°07′36″	74°56′15″	19.8	39	60	0	0.78	0.68
118	8/2/84	38°06′50″	74°57′32″	20.1	36	61	2	1.25	0.98
119	8/2/84	38°06′04″	74°58′47″	18.6	0	100	0	1.49	0.54
120	8/2/84	38°05′18″	75°00′04″	11.6	0	100	0	1.52	0.43
121	8/2/84	38°04′34″	75°01′19″	11.3	10	90	0	0.63	0.46
122	8/2/84	38°03′48″	75°02′38″	12.2	4	96	0	1.00	0.54
123	8/2/84	38°03′02″	75°03′54″	13.4	16	83	0	0.85	0.70
124	8/2/84	38°02′17″	75°05′11″	14.0	0	100	0	1.79	0.50
125	8/2/84	38°01′59″	75°02′19″	17.7	0	100	0	2.20	0.43
126	8/2/84	38°02′45″	75°01′02″	15.2	14	86	0	0.73	0.48
127	8/2/84	38°03′30″	74°59′45″	17.1	0	100	0	1.86	0.32
128	8/2/84	38°04′16″	74°58′29″	18.9	2	98	0	0.93	0.57
129	8/2/84	38°05′01″	74°57′13″	19.5	13	87	0	1.02	0.68
130	8/2/84	38°02′26″	74°58′11″	19.5	0	100	0	1.33	0.55
131	8/2/84	38°01′40″	74°59′26″	20.7	0	99	1	2.12	0.33

APPENDIX II

List of samples analyzed for extent of amino acid racemization in selected vibracores.

Table VII.—List of Samples Analyzed for Extent of Amino Acid Racemization in Selected Vibracores. Depth in Core Refers to Depth From Top of Sediments in the Core.

Core 16-835

Core Unit 1: *Mulinia* shells

Sample #	Depth in core (cm)	A/I Ratio	
MT16-835-1T1	54-59	0.12	$\overline{X}$ = 0.1162 ± 0.011
MT16-835-2T1	54-59	0.116	c.v. = 9.47%
MT16-835-3T1	76-81	0.117	
MT16-835-4T1	76-81	0.095	
MT16-835-6AT1	106-110	0.124	
MT16-835-6BT1	106-110	0.125	

Core Unit 2: *Mulinia* shells

Sample #	Depth in core (cm)	A/I Ratio	
MT16-835-7T1	135-138	0.108	$\overline{X}$ = 0.1112 ± 0.0167
MT16-835-8T1	147	0.11	c.v. = 15.02%
MT16-835-9AT1	150-160	0.101	
MT16-835-9BT1	150-160	0.105	
MT16-835-10T1	142	0.128	
MT16-835-11AT1	148-151	0.13	
MT16-835-11BT1	148-151	0.072	
MT16-835-12AT1	150-160	0.096	
MT16-835-13AT1	160-170	0.119	
MT16-835-13BT1	160-170	0.122	
MT16-835-14AT1	170-180	0.108	
MT16-835-15AT1	200-205	0.11	
MT16-835-16AT1	223-228	0.136	

Core Unit 2: *Ensis* shells

Sample #	Depth in core (cm)	A/I Ratio
MT16-835-13CT1	160-170	0.131
MT16-835-14BT1	170-180	0.131
MT16-835-15BT1	200-205	0.188
MT16-835-17AT1	241-245	0.095

Core Unit 3: *Mulinia* shells

Sample #	Depth in core (cm)	A/I Ratio
MT16-835-18AT1	533-539	0.332

Core 16-842

Core Unit 2: *Mulinia* shells

Sample #	Depth in core (cm)	A/I Ratio	
MT16-842-7A1	560-568	0.097	$\overline{X}$ = 0.1107 ± 0.0095
MT16-842-7B1	560-568	0.112	c.v. = 8.58%
MT16-842-8A1	560-568	0.116	
MT16-842-8B1	560-568	0.118	

Core 16-850

Core Unit 1: *Spisula* shells

Sample #	Depth in core (cm)	A/I Ratio
MT16-850-1AT1	7-20	0.010
MT16-850-2AT1	30-40	0.00
MT16-850-3AT1	70-80	0.00
MT16-850-4AT1	80-90	0.010
MT16-850-4BT1	80-90	0.007

Core Unit 2: *Mulinia* shells

Sample #	Depth in core (cm)	A/I Ratio
MT16-850-5CT1	140-143	0.00

Core Unit 2: *Spisula* shells

Sample #	Depth in core (cm)	A/I Ratio
MT16-850-5AT1	140-143	0.00
MT16-850-5BT1	140-143	0.00
MT16-850-6AT1	152-162	0.00
MT16-850-6BT1	152-162	0.00

Core Unit 3: *Mulinia* shells

Sample #	Depth in core (cm)	A/I Ratio	
MT16-850-7AT1	271-274	0.124	$\overline{X} = 0.121 \pm 0.0026$
MT16-850-9AT1	509-510	0.119	c.v. = 2.15%
MT16-850-9BT1	509-510	0.120	

Core Unit 3: *Spisula* shells

Sample #	Depth in core (cm)	A/I Ratio
MT16-850-8AT1	500-501	0.00
MT16-850-8BT1	500-501	0.013

Core 16-905

Core Unit 1A: *Mulinia* shells

Sample #	Depth in core (cm)	A/I Ratio	
MT16-905-16A1	344-346	0.1005	$\overline{X} = 0.1026 \pm 0.0153$
MT16-905-16B1	344-346	0.113	c.v. = 14.91%
MT16-905-17A1	349-352	0.078	
MT16-905-17B1	349-352	0.0955	
MT16-905-17C1	349-352	0.0907	
MT16-905-9AT1	349-352	0.125	
MT16-905-9BT1	349-352	0.118	
MT16-905-2T1	357-358	0.082	
MT16-905-10T1	357-358	0.127	
MT16-905-18A1	358-362	0.098	
MT16-905-18B1	358-362	0.093	
MT16-905-11AT1	358-362	0.117	
MT16-905-11BT1	358-362	0.095	
MT16-905-13T1	372-373	0.103	

Core 16-935

Core Unit 1: *Spisula* shells

Sample #	Depth in core (cm)	A/I Ratio
MT16-935-1AT1	0-24	0.007
MT16-935-1BT1	0-24	0.011
MT16-935-1CT1	0-24	0.008

Core Unit 2: *Spisula* shells

Sample #	Depth in core (cm)	A/I Ratio
MT16-935-2AT1	43	0.000
MT16-935-3AT1	60	0.007
MT16-935-4AT1	65	0.007
MT16-935-5AT1	70-75	0.000

Core Unit 2: *Ensis* shells

Sample #	Depth in core (cm)	A/I Ratio
MT16-935-4BT1	65	0.000

Core 16-1002

Core Unit 1: *Ensis* shells

Sample #	Depth in core (cm)	A/I Ratio
MT16-1002-3T1	46-50	0.091
MT16-1002-4T1	66-72	0.177
MT16-1002-7T1	120	0.11

Core Unit 1: *Mercenaria?* shells

Sample #	Depth in core (cm)	A/I Ratio
MT16-1002-2T1	1-20	0.249

Core Unit 1: *Astarte?* shells

Sample #	Depth in core (cm)	A/I Ratio
MT16-1002-1T1	1-20	0.144

Core Unit 1: *Anadara* shells

Sample #	Depth in core (cm)	A/I Ratio
MT16-1002-6T1	120	0.113

Core Unit 3: *Ensis* shells

Sample #	Depth in core (cm)	A/I Ratio
MT16-1002-5T1	237-238	0.127

Core Unit 4: *Anadara* shells

Sample #	Depth in core (cm)	A/I Ratio
MT16-1002-10T1	280-300	0.141
MT16-1002-11T1	280-300	0.098

Core Unit 4: *Astarte* shells

Sample #	Depth in core (cm)	A/I Ratio
MT16-1002-9T1	280-300	0.16
MT16-1002-12T1	308-316	0.16

Core Unit 4: *Spisula* shells

Sample #	Depth in core (cm)	A/I Ratio
MT16-1002-8T1	280-300	0.159

Core 18-1230

Core Unit 1: *Mulinia* shells

Sample #	Depth in core (cm)	A/I Ratio
MT18-1230-1A1	15-16	0.076
MT18-1230-1B1	15-16	0.079
MT18-1230-2A1	16-17	0.073
MT18-1230-3A1	37-38	0.100
MT18-1230-4A1	38-39	0.103
MT18-1230-4B1	38-39	0.086

$\overline{X} = 0.0862 \pm 0.0127$
c.v. = 14.73%

Core Unit 1: *Mercenaria* shells

Sample #	Depth in core (cm)	A/I Ratio
MT18-1230-5AT1	330	0.124

Core Unit 2: *Ensis* shells

Sample #	Depth in core (cm)	A/I Ratio
MT18-1230-6A1	350	0.061
MT18-1230-7B1	420	0.054

Core Unit 2: *Spisula* shells

Sample #	Depth in core (cm)	A/I Ratio
MT18-1230-7A1	420	0.082

Core Unit 3: *Mulinia* shells

Sample #	Depth in core (cm)	A/I Ratio
MT18-1230-9AT1	490-495	0.248

Core Unit 3: *Ensis* shells

Sample #	Depth in core (cm)	A/I Ratio
MT18-1230-10AT1	545-550	0.074

Core 18-1248

Core Unit 2: *Mulinia* shells

Sample #	Depth in core (cm)	A/I Ratio	
MT18-1248-2A1	141-142	0.107	$\overline{X}$ = 0.1045 ± 0.0095
MT18-1248-2B1	141-142	0.118	c.v. = 9.09%
MT18-1248-3A1	143-144	0.106	
MT18-1248-3B1	143-144	0.109	
MT18-1248-4A1	151-152	0.095	
MT18-1248-4B1	151-152	0.092	
MT18-1248-5A1	185-186	0.106	$\overline{X}$ = 0.11 ± 0.0056
MT18-1248-6A1	217-218	0.114	c.v. = 5.09%
MT18-1248-7A1	344-345	0.090	$\overline{X}$ = 0.0957 ± 0.0182
MT18-1248-8A1	392-393	0.116	c.v. = 19.02%
MT18-1248-9A1	397-398	0.181	

Core Unit 2: *Mercenaria* shells

Sample #	Depth in core (cm)	A/I Ratio
MT18-1248-10AT1	400	0.149
MT18-1248-11AT1	513-514	0.181

Core Unit 3: *Mulinia* shells

Sample #	Depth in core (cm)	A/I Ratio
MT18-1248-12AT1	550-560	0.253
MT18-1248-13AT1	560-570	0.259

Core Unit 3: *Mercenaria* shells

Sample #	Depth in core (cm)	A/I Ratio
MT18-1248-14AT1	580-588	0.132

Core 27-1520

Core Unit 1: *Spisula* shells

Sample #	Depth in core (cm)	A/I Ratio
MT27-1520-1AT1	6-10	0.007

Core Unit 2: *Spisula* shells

Sample #	Depth in core (cm)	A/I Ratio
MT27-1520-2AT1	85-95	0.107

Core Unit 2: *Mulinia* shells

Sample #	Depth in core (cm)	A/I Ratio	
MT27-1520-2B1	85-95	0.086	$\overline{X}$ = 0.0835 ± 0.0035
MT27-1520-3A1	141	0.081	c.v. = 4.19%

Core Unit 3: *Mulinia* shells

Sample #	Depth in core (cm)	A/I Ratio	
MT27-1520-4A1	160-164	0.077	$\overline{X} = 0.0839 \pm 0.00977$
MT27-1520-4BT1	160-164	0.085	c.v. = 11.64%
MT27-1520-5A1	170-171	0.077	
MT27-1520-6A1	184-185	0.077	
MT27-1520-6B1	184-185	0.080	
MT27-1520-7A1	193-195	0.080	
MT27-1520-7B1	193-195	0.095	
MT27-1520-8A1	211	0.093	
MT27-1520-9A1	247	0.100	
MT27-1520-10A1	255-256	0.097	
MT27-1520-10B1	255-256	0.097	
MT27-1520-11A1	309-310	0.072	
MT27-1520-12A2	341-342	0.079	
MT27-1520-13B2	340-350	0.077	
MT27-1520-13CR	340-350	0.072	

Core Unit 4: *Mulinia* shells

Sample #	Depth in core (cm)	A/I Ratio	
MT27-1520-14A2	380-390	0.086	$\overline{X} = 0.0928 \pm 0.0057$
MT27-1520-15A2	390	0.093	c.v. = 6.14%
MT27-1520-16A2	410-420	0.092	
MT27-1520-17A2	420-430	0.10	

Core Unit 4: *Spisula* shells

Sample #	Depth in core (cm)	A/I Ratio
MT27-1520-18AT2	468-47:	0.127
MT27-1520-19AT2	490-505	0.110

Core Unit 4: *Ensis* shells

Sample #	Depth in core (cm)	A/I Ratio
MT27-1520-18BT2	468-475	0.144

APPENDIX III

NUMERICAL AGE ASSIGNMENTS CALCULATED FROM AMINO ACID RACEMIZATION A/I RATIOS

To calculate numerical ages for the Maryland shelf core *Mulinia* samples, the kinetic model equation

$$\ln [(1 + A/I)/(1-.77(A/I))] = 1.77\ kt$$

was used where k = first order rate constant and t = sample age in years, and A/I is the alloisoleucine-isloeucine ratio of the sample. This equation is based on first order reversible racemization kinetics and is discussed in detail in Bada and Schroeder (1972). Table VIII lists previous data assigning numerical ages to A/I ratios.

When the mean A/I value of 0.1162 (representing approximately the mean value for A/I values of this study ranging from 0.10 to 0.12) is calibrated to 125,000 years, then k can be calculated as 9.2×10^{-7} by using the above equation. Once the rate constant (k) is known, then ages (t) can be calculated for other A/I ratios (assuming all have the same rate constant).

The rate constant can be related to temperature by the equation

$$\log k = 15.77 - 5939/T$$

where $T = T_{eff}$ or effective Quaternary temperature (EQT). This equation is also discussed in Bada and Schroeder (1972). With an A/I ratio of 0.1162 = 125,000 years, and $k = 9.2 \times 10^{-7}$, then T_{eff} = 272.35°K or -0.79°C (Table IX).

It is reasonable to assume that samples originating during early Sangamon time (stage 5e) would have a slightly higher T_{eff} than samples originating during the latter (and cooler) substages of stage 5, since the middle to late Sangamon samples would have spent a greater proportion of their history at glacial temperatures. Therefore, if T_{eff} or EQT is 1.0° colder than the value used above (or -1.79°C) then a new rate constant can be calculated: $k = 7.7 \times 10^{-7}$.

Using the new k value, ages can again be calculated for the A/I ratios. A lower k value results in greater ages for the same A/I ratios. See Table X.

A third alternative is to use the lower rate constant ($k = 7.7 \times 10^{-7}$) for A/I ratios of 0.0835 to 0.0926 (younger samples) and to use the higher rate constant (9.2×10^{-7}) for the A/I ratios of 0.1017 to 0.121. The major difficulty with this is a resulting overlap in the age estimates. See Table XI.

The numerical ages listed in Tables IX, X, and XI are meant to demonstrate the most reasonable range of ages that can be calculated for each mean A/I ratio. Table IX represents probable minimum age estimates for each mean A/I ratio, while Table X represents probable maximum estimates for each mean A/I ratio.

Table VIII.—Previous Data and Re-analyzed Data for Numerical Age Assignments from A/I Ratios.

McDonald (1982) cores, Bethany Beach, Delaware

Locality BB
KAM-MB-80 (9 and 10 meters)
University of Delaware Sample JW80-148
D/L leucine 0.27-0.29 *(Mulinia)*
*Age estimate 100,000 ± 25,000 yrs

Re-analyzed 1988
University of Delaware Sample 80-148A, 80-148B
A/I 0.123, 0.117 *(Mulinia)*
*Age estimate 125,000

KAM-NOV-80 (9 and 10 meters)
University of Delaware Sample JW80-147
D/L leucine 0.22 *(Mulinia)*
*Age estimate 100,000 ± 25,000 yrs

Re-analyzed 1988
University of Delaware Sample 80-147A, 80-147B
A/I 0.1135, 0.096 *(Mulinia)*
*Age estimate 100,000-125,000 yrs

Mixon, 1985 Bell Neck, VA, Wachapreague Formation, Southern Delmarva peninsula

Locality BN
Core EX-24 (3.5-5 meters MSL)
^{14}C *Mulinia* = >33 ka (beyond range of ^{14}C)
Th/U *Mercenaria* = 128,000 ± 1000 yrs B.P.
D/L leucine *Mesodesma* = 0.284
*Age estimate 82 ka (Belknap, 1979)

Re-analyzed 1988
University of Delaware Sample 80-181AT
A/I *(Mulinia)* 0.103
*Age estimate ≈ 110,000 (stage 5c)

Belknap, 1979 Assateague Island, Maryland Tingles Island Quadrangle

(locality not precisely specified — J.P. Owens, USGS)
Locality TI.
USGS borehole — unidentified
Depth 50-55′ in core (≈-15 to -16 m MSL)
D/L leucine 0.147, probably *M. mercenaria*
*Age estimate 58ka

Re-analyzed 1988, York (in prep.)
University of Delaware Sample 80-182A, 80-182B
A/I *Mulinia* 0.106, 0.113
*Age estimate 115,000-125,000

* Racemization-derived age estimate

Table IX.—Age Calculations Where First Order Rate Constant (K) is 9.2×10^{-7} and the Effective Quaternary Temperature (T_{eff}) is −0.79°C.

Core	Unit	A/I Ratio Mean	A/I Ratio Std Dev.	Numerical Ages Mean	Numerical Ages Max	Numerical Ages Min	FINAL: Mean ±	FINAL: Max Min
27-1520	2	0.0835	0.0035	90,009	93,758	86,258	90,009	+3749 -3751
	3	0.0839	0.00977	90,437	100,933	79,931	90,437	+10,496 -10,506
	4	0.0928	0.0057	99,970	106,071	93,866	99,970	+6101 -6104
18-1230	1	0.0862	0.0127	92,902	106,499	79,288	92,902	+13,597 -13,614
18-1248	2	0.1031	0.0119	110,992	123,749	98,224	110,992	+12,757 -12,748
16-905	1A	0.1026	0.0153	110,410	126,763	94,040	110,410	+16,353 -16,370
16-850	3	0.121	0.0026	130,130	132,908	127,351	130,130	+2778 -2779
16-842	2	0.1107	0.0095	119,120	129,275	108,959	119,120	+10,155 -10,161
16-835	1	0.1162	0.011	125,000	136,755	113,238	125,000	+11,755 -11,762
	2	0.1112	0.0167	119,655	137,503	101,789	119,655	+17,848 -17,866

Table X.—Age Calculations Where First Order Rate Constant (K) is 7.7×10^{-7} and the Effective Quaternary Temperature (T_{eff}) is −1.79°C.

Core	Unit	A/I Ratio Mean	A/I Ratio Std Dev.	A/I Ratio Min	A/I Ratio Max	Numerical Ages Mean	Numerical Ages Min	Numerical Ages Max
27-1520	2	0.0835	0.0035	0.081	0.086	107,602	103,118	112,085
	3	0.0839	0.00977	0.072	0.100	108,115	95,555	120,662
	4	0.0928	0.0057	0.086	0.100	119,510	112,213	126,804
18-1230	1	0.0862	0.0127	0.073	0.103	111,061	94,786	127,316
18-1248	2	0.1031	0.0119	0.081	0.118	132,688	117,424	147,938
16-905	1A	0.1026	0.0153	0.087	0.118	132,330	112,709	151,929
16-850	3	0.121	0.0026	0.119	0.124	155,566	152,245	158,888
16-842	2	0.1107	0.0095	0.097	0.118	142,404	130,258	154,544
16-835	1	0.1162	0.011	0.095	0.125	149,433	135,373	163,486
	2	0.1112	0.0167	0.072	0.136	143,043	121,686	164,380

Table XI.—Age Calculations Where First Order Rate Constant (K) is 7.7×10^{-7} for A/I Ratios Between 0.0875 to 0.0928 and 9.2×10^{-7} for A/I Ratios Between 0.1017 to 0.121. A/I Ratio 0.1162 Equals 125,000 Years.

Core	Unit	A/I Ratio Mean	A/I Ratio Std Dev.	A/I Ratio Min	A/I Ratio Max	Numerical Ages Mean	Numerical Ages Min	Numerical Ages Max
27-1520	2	0.0835	0.0035	0.081	0.186	107,603	103,118	112,085
	3	0.0839	0.00977	0.072	0.100	108,115	95,555	120,662
	4	0.0928	0.0057	0.086	0.100	119,510	112,213	126,804
18-1230	1	0.0862	0.0127	0.073	0.103	111,061	94,786	127,316
18-1248	2	0.1031	0.0119	0.081	0.118	110,992	98,224	123,749
16-905	1A	0.1026	0.0153	0.0873	0.118	110,410	94,040	126,763
16-850	3	0.121	0.0026	0.119	0.124	130,130	127,351	132,908
16-842	2	0.1107	0.0095	0.097	0.118	119,120	108,959	129,275
16-835	1	0.1162	0.011	0.095	0.125	125,000	113,238	136,755
	2	0.1112	0.0167	0.072	0.136	119,655	101,789	137,503

APPENDIX IV

Paleontology for vibracores 16-905, 18-1230, and 27-1520.

Table XII.—List of Samples Studied for Ostracode Assemblages in Centimeters from Top of Core for All Cores Studied.

Core	Seismic Unit	Sample Depths (cm from top of core)		
16-835	Q2/Q1	90-92		
		92-95		
		170-180		
16-842	Q2	312		
		395		
		530-540		
16-850	Q2	280-281		
		281-282		
		582-583		
		583-584		
		584-585		
16-905	Top of core is -16.77 m MSL Top of sediment is at -17.23 m MSL*			
		5-7		
	Q2	15-17	255-257	520-522
		25-27	265-267	525-527
		35-37	275-277	530-532
		45-47	285-287	535-537
		55-57	295-297	540-542
		65-67	314-316	545-547
		75-77	336-338	555-557
		85-87	365-367	565-567
		95-97	375-377	570-572
		105-107	385-387	575-577
		115-117	395-397	580-582
		125-127	405-407	
		135-137	415-417	
		144-145	425-427	
		155-157	435-437	
		165-167	455-457	
		175-177	465-467	
		185-187	475-477	
		195-197	485-487	
		215-217	495-497	
		225-227	505-507	
		235-237	510-512	
		245-247		

Note — to get actual depth of samples below MSL, add 46 cm to each. Sample at 5-7 cm is actually -17.73 m MSL, not -17.27.

*0.46 meters of the top of core 16-905 was lost during core recovery.

Core	Seismic Unit	Depths Analyzed
18-1230	Q2/Q1	59-61
		150-152
		280-282
		290-292
		300-320
		315-317
		320-322
		326-328
		330-335
		370-375
		405-410
		442-447
		540-545
		607-610
18-1248	Q2/Q1	300-302
		409-411
16-935	Q5/Q3	0-73 Holocene Marine
		270-275 barren
		425-430 barren
16-1005	Q4	88-91 barren
		424-429 barren
27-1425	Q2	250-255
		280-285
		302-306
		315-320
27-1440	Q2	110-115
		140-150
		162-167
		168-172
		210-215
		233-236
27-1520	Q2/Q1?	100-113
		239-241
		338-340
		353-355
		360-362
		370-372
		377-379
		380-390
		430-440
		490-500
		585-590
29-1750	Q2	300-305
		320-325
		335-340

Table XIII.—Ostracode Paleoclimatology Data.

Group 1: Cold temperate to subfrigid

1. *Baffinocythere emarginata*
2. *Cytheropteron nodosoalatum*
3. *Elofsonella concinna*
4. *Hemicythere villosa*
5. *Hemicytherura clathrata*
6. *Munseyella mananensis*
7. *Palmenella limicola*
8. *Sarsicytheridea bradii*
9. *Robertsonites tuberculata*

Group 2: Cold temperate to mild temperate

10. *Actinocythereis dawsoni*
11. *Bensonocythere americana*
12. *Bensonocythere arenicola*
13. *Bensonocythere* sp. B of Valentine (1971)
14. *Cytheridea* sp. A
15. *Eucythere declivis*
16. *Finmarchinella finmarchica*
17. *Hulingsina* sp. A
18. *Leptocythere angusta*
19. *Loxoconcha cf. L. impressa*
20. *Loxoconcha sperata*
21. *Loxoconcha williamsi*
22. *Muellerina canadensis*
23. *Muellerina ohmerti*
24. *Neolophocythere subquadrata*
25. *Pseudocytheretta edwardsi*
26. *Puriana rugipunctata*

Group 3: Mild Temperate to subtropical

27. *Cushmanidea seminuda*
28. *Hulingsina americana*
29. *Hulingsina* sp. C of Valentine (1971)
30. *Tetracytherura choctawhatchensis*
31. *Tetracytherura norfolkensis*
32. *Pontocythere*
33. *Bensonocythere valentinei*
34. *Campylocythere laeva*
35. *Cytherura forulata*
36. *Hulingsina* sp. B of Valentine (1971)
37. *Peratocytheridea bradyi*
38. *Proteoconcha gigantica* and *P. tuberculata*

Table XIV.—Number of Individuals for Each Ostracode Species Per Sample in Core.

CORE 16-905

Species #	Sample depth in core: cm 5-7	15-17	25-27	35-37	45-47	55-57	65-67	75-77	85-87	95-97	105-107	115-117	125-127	135-137	144-145	155-157	165-167	175-177	185-187	195-197	215-217	225-227	235-237	245-247	255-257	265-267	275-277	285-287	295-297	314-316	336-338
1	0	0	0	0	0	0	0	0	0	0	0	0	0	0	0	0	0	0	0	0	0	0	0	0	0	0	0	0	0	0	0
2	0	0	0	0	0	0	0	0	0	0	0	0	0	0	0	0	0	0	0	0	0	0	0	0	0	0	0	0	0	0	0
3	0	0	0	0	0	0	0	0	0	1	13	5	0	1	0	0	0	0	0	0	0	1	0	2	1	0	0	0	0	2	2
4	0	0	0	0	0	0	0	0	0	0	0	0	0	0	0	0	0	0	0	0	0	0	0	0	0	0	0	0	0	2	2
5	0	0	0	0	0	0	0	0	0	0	0	0	0	0	0	0	0	0	0	0	0	0	0	0	0	0	0	0	0	0	0
6	0	0	0	0	0	0	0	0	0	0	0	0	0	0	0	0	0	0	0	0	0	0	0	0	0	0	0	0	0	0	0
7	0	0	0	0	0	0	0	0	0	0	0	0	0	0	0	0	0	0	0	0	0	0	0	0	0	0	0	0	0	0	0
8	0	0	0	0	0	0	0	0	0	0	0	0	0	0	0	0	0	0	0	0	0	0	0	0	0	0	0	0	0	0	0
9	0	0	0	0	0	0	0	0	0	0	0	0	0	0	0	0	0	0	0	0	0	0	0	0	0	0	0	0	0	0	0
10	0	0	0	0	0	0	0	0	0	0	0	0	0	0	0	0	0	0	0	0	0	0	0	0	0	0	0	0	0	1	0
11	0	0	0	0	0	1	2	0	0	0	3	1	0	2	2	1	0	0	0	0	3	3	0	0	2	6	2	0	4	19	9
12	0	0	0	0	0	0	0	0	0	0	0	0	0	0	0	0	0	0	0	0	0	0	0	0	0	1	0	0	1	1	10
13	0	0	0	0	0	0	0	0	0	0	0	2	0	5	5	0	0	0	1	0	2	0	1	2	3	3	0	0	0	15	13
14	0	0	0	33	51	1	49	77	26	32	395	300	11	53	355	172	30	6	25	0	39	127	174	415	275	34	19	83	61	245	148
15	0	0	0	0	0	0	0	0	0	0	0	0	0	0	0	0	0	0	0	0	0	0	0	0	0	0	0	0	0	0	0
16	0	0	0	0	0	0	0	0	0	0	0	0	0	0	0	0	0	0	0	0	0	0	0	0	0	0	0	0	0	0	0
17	0	0	0	0	0	0	0	0	0	0	0	0	0	0	0	0	0	0	0	0	0	0	0	0	0	0	0	0	0	2	0
18	0	0	0	0	0	0	0	0	0	0	0	0	0	0	0	0	0	0	0	0	0	0	0	0	0	0	0	0	1	1	0
19	0	0	0	0	0	0	0	0	0	0	0	0	0	0	0	0	0	0	0	0	0	0	0	0	0	0	0	0	0	0	0
20	0	0	0	0	0	1	38	18	10	8	19	34	2	52	110	23	6	3	1	0	17	29	3	6	30	12	3	16	15	45	46
21	0	0	0	0	1	1	16	16	8	3	14	13	1	27	105	25	1	2	2	0	11	28	10	2	29	6	3	11	10	39	26
22	0	0	0	0	0	0	0	0	0	0	4	3	0	0	0	0	0	0	0	0	0	1	0	7	0	1	0	0	0	12	10
23	0	0	0	0	0	0	0	0	0	0	0	0	0	0	0	0	0	0	0	0	0	0	0	0	0	0	0	0	0	0	0
24	0	0	0	0	0	0	0	0	0	0	0	0	0	0	0	0	0	0	0	0	0	0	0	0	0	0	0	0	0	0	0
25	0	0	0	0	0	0	0	0	0	0	0	0	0	0	0	0	0	0	0	0	0	0	0	0	0	0	0	0	0	0	0
26	0	0	0	0	0	0	0	0	0	0	0	0	0	0	0	0	0	0	0	0	0	0	0	0	0	0	0	0	0	0	0
27	0	0	0	0	0	0	0	0	0	0	0	0	0	0	0	0	0	0	0	0	0	0	0	0	0	0	0	0	0	0	0
28	0	0	0	0	0	0	0	0	0	0	0	0	0	0	0	0	0	0	0	0	0	0	0	0	0	0	0	0	0	0	0
29	0	0	0	0	0	0	0	0	0	0	0	0	0	0	0	0	0	0	0	0	0	0	0	0	0	0	0	0	0	0	0
30	0	0	0	0	0	0	0	0	0	0	0	0	0	0	0	0	0	0	0	0	0	0	0	0	0	0	0	0	0	0	0
31	0	0	0	0	0	0	0	0	0	0	0	0	0	0	0	0	0	0	0	0	0	0	0	0	0	0	0	0	0	2	0
32	0	0	0	0	0	0	0	0	0	0	0	0	0	0	0	0	0	0	0	0	0	0	0	0	0	0	0	0	0	0	0
33	0	0	0	0	0	0	0	0	0	0	0	0	0	0	0	0	0	0	0	0	0	0	0	0	0	0	0	0	0	0	0
34	0	0	0	0	0	0	0	0	0	0	0	0	0	0	0	0	0	0	0	0	0	0	0	0	0	0	0	0	0	0	0
35	0	0	0	0	0	0	0	0	0	0	0	0	0	0	0	0	0	0	0	0	0	0	0	0	0	0	0	0	0	0	0
36	0	0	0	0	0	0	0	0	0	0	0	0	0	0	0	0	0	0	0	0	0	0	0	0	0	0	0	0	0	0	0
37	0	0	0	0	0	0	0	0	0	0	0	0	0	0	0	0	0	0	0	0	0	0	0	0	0	0	0	0	0	0	0
38	0	0	0	0	0	0	0	0	0	0	0	0	0	0	0	0	0	0	0	0	0	0	0	0	0	0	0	0	0	0	0
Total	0	0	0	33	52	4	106	112	44	44	448	359	14	140	577	221	37	11	29	0	72	190	188	434	340	63	27	111	93	387	267

Table XIV.—Number of Individuals for Each Ostracode Species Per Sample in Core, continued.

CORE 16-905

365-367	375-377	385-387	395-397	405-407	415-417	425-427	435-437	455-457	465-467	475-477	485-487	495-497	505-507	510-512	520-522	525-527	530-532	535-537	540-542	545-547	555-557	565-567	570-572	575-577	580-582			Totals
0	0	0	0	0	0	0	0	0	0	0	0	0	0	0	0	0	0	0	0	0	0	0	0	0	0	0	0	0
0	0	0	0	0	0	0	0	0	0	0	0	0	0	0	0	0	0	0	0	0	4	0	0	0	0	0	1	0
0	0	0	0	5	2	1	29	0	0	0	1	2	0	0	2	0	12	2	0	0	9	0	1	0	7	1	7	108
0	0	0	0	0	0	0	0	1	0	1	0	0	0	1	0	0	0	0	0	0	0	0	0	0	0	0	1	4
0	0	0	0	0	0	0	0	0	0	0	0	0	0	0	0	0	0	0	0	0	0	0	0	0	1	0	0	1
0	0	0	0	0	0	0	0	0	0	0	0	0	0	0	0	0	0	0	0	0	0	0	0	0	0	0	0	0
0	0	0	0	0	0	0	0	0	0	0	0	0	0	0	0	0	1	0	0	0	0	0	0	0	0	0	0	1
0	0	0	0	0	1	0	0	1	0	0	0	0	0	0	0	0	1	1	0	0	4	0	0	0	0	0	0	8
0	0	0	0	0	0	0	0	0	0	0	0	0	0	0	0	1	0	0	0	0	1	0	0	0	5	1	2	10
0	0	0	0	0	0	0	0	0	0	0	0	0	0	0	0	0	0	0	0	0	0	0	0	0	0	0	0	1
0	0	0	0	0	0	0	6	3	0	0	0	0	0	0	0	0	2	0	0	0	12	0	0	0	0	2	2	87
0	0	0	0	0	0	0	0	0	0	0	0	0	0	0	0	0	0	0	0	0	0	0	0	0	0	0	0	13
0	1	0	1	0	0	1	7	6	0	0	0	0	0	3	1	0	1	0	0	0	17	0	2	0	9	0	6	107
11	8	0	1	6	0	0	27	12	0	0	2	8	4	9	6	3	25	3	1	0	65	0	2	0	35	11	57	3532
0	0	0	0	0	0	0	0	0	0	0	0	0	0	0	0	0	0	0	0	0	1	0	0	0	0	0	0	1
0	1	0	0	0	0	0	0	0	0	0	0	0	0	0	0	0	0	0	0	0	0	0	0	0	1	0	0	2
0	0	0	1	2	0	0	4	3	0	0	0	0	0	4	0	0	5	0	0	0	8	0	0	0	0	0	1	31
0	0	0	0	0	0	0	0	0	0	0	0	0	0	0	1	0	0	0	0	0	4	0	0	0	0	0	2	9
0	0	0	0	0	0	0	0	0	0	0	0	0	0	1	1	0	0	0	0	0	3	0	0	0	0	0	8	13
2	1	0	0	0	0	0	0	0	0	0	0	0	0	0	0	0	0	0	0	0	2	0	0	0	1	0	6	559
1	2	0	0	1	0	0	2	0	0	0	0	0	0	0	0	0	0	0	0	0	0	0	0	0	0	0	0	416
2	0	0	0	0	0	0	0	0	0	0	0	0	0	1	0	0	4	0	0	0	0	0	0	0	3	0	0	48
0	0	0	0	0	0	1	0	0	0	0	0	0	0	2	0	0	1	0	0	0	9	0	0	0	0	2	0	15
0	0	0	0	0	0	0	0	0	0	0	0	0	0	0	0	0	0	0	0	0	0	0	0	0	0	0	0	0
0	0	0	2	0	2	0	6	2	0	1	0	0	0	3	0	0	2	0	0	0	5	0	0	0	2	0	0	25
0	0	0	0	0	0	0	0	0	0	0	0	0	0	0	0	0	2	0	0	0	0	0	0	0	0	0	0	2
0	0	0	0	0	0	0	0	0	0	0	0	0	0	0	0	0	0	0	0	0	7	0	0	0	0	0	0	7
0	0	0	0	0	0	0	0	0	0	0	0	0	0	0	0	0	0	0	0	0	0	0	0	0	0	0	0	0
0	0	0	0	0	0	0	0	0	0	0	0	0	0	0	0	0	0	0	0	0	1	0	0	0	1	0	0	3
0	0	0	0	0	0	0	0	0	0	0	0	0	0	0	0	0	0	0	0	0	0	0	0	0	0	0	0	0
0	0	0	0	0	0	0	0	0	0	0	0	0	0	0	0	0	0	0	0	0	0	0	0	0	0	0	0	2
0	0	0	0	0	1	0	3	2	0	0	0	0	0	7	0	0	0	0	0	0	0	0	1	0	1	0	0	15
0	0	0	0	0	0	0	0	0	0	0	0	0	0	0	0	0	0	0	0	0	0	0	0	0	0	0	0	0
0	0	0	0	0	0	0	0	0	0	0	0	0	0	0	0	0	0	0	0	0	0	0	0	0	0	0	0	0
0	0	0	0	0	0	0	0	0	0	0	0	0	0	0	0	0	0	0	0	0	0	0	0	0	0	0	0	0
0	0	0	0	0	0	0	0	0	0	0	0	0	0	0	0	0	0	0	0	0	0	0	0	0	0	0	0	0
0	0	0	0	0	0	0	0	0	0	0	0	0	0	0	0	0	0	0	0	0	0	0	0	0	0	0	0	0
0	0	0	0	0	0	0	0	0	0	0	0	0	0	0	0	0	0	0	0	0	0	0	0	0	0	0	0	0
16	13	0	5	14	6	3	83	30	0	2	3	10	4	31	11	4	57	6	1	0	153	0	6	0	66	17	96	5040

Table XIV.—Number of Individuals for Each Ostracode Species Per Sample in Core, continued.

	CORE 27-1520												CORE 18-1230														
Species #	100-113	239-241	338-340	353-355	360-362	370-372	377-379	380-390	430-440	490-500	585-590	Totals	59-61	150-152	280-282	290-292	300-302	315-317	320-322	326-328	330-335	370-375	405-410	442-447	540-545	607-610	Totals
1	0	0	0	0	0	0	0	0	0	0	0	0	0	0	0	0	0	0	0	2	0	0	0	0	0	0	2
2	2	0	0	0	0	0	0	0	0	1	0	0	2	0	0	0	0	0	0	0	0	0	0	0	0	0	0
3	1	5	0	1	0	1	0	0	0	0	0	8	0	6	0	3	0	0	0	2	0	0	0	0	0	0	11
4	0	0	0	0	0	0	0	0	0	0	0	0	0	0	0	0	0	0	0	0	0	0	0	0	0	0	0
5	0	0	0	0	0	0	0	0	0	0	0	0	0	0	0	0	0	0	0	0	0	0	0	0	0	0	0
6	0	0	1	0	0	0	0	1	0	2	0	4	0	0	0	0	0	0	0	0	0	0	0	0	0	0	0
7	0	0	0	0	0	0	0	0	0	0	0	0	0	0	0	0	0	0	0	0	0	0	0	0	0	0	0
8	0	0	0	0	0	0	0	0	0	0	0	0	0	0	0	0	0	0	0	0	0	0	0	0	0	0	0
9	0	0	0	0	0	0	0	0	0	0	0	0	0	0	0	0	0	0	0	0	0	0	0	0	0	0	0
10	1	0	0	0	0	0	0	0	0	4	0	3	1	1	0	0	0	0	0	3	2	2	0	1	0	1	11
11	0	0	2	0	0	0	2	0	1	0	0	3	0	0	0	2	0	0	1	7	2	4	1	1	0	0	18
12	0	0	0	0	0	0	0	1	0	1	1	3	0	5	0	0	2	0	0	9	1	0	7	0	0	0	24
13	19	0	2	1	0	0	0	0	0	5	0	27	6	4	0	0	0	0	2	11	0	6	2	3	0	0	34
14	11	42	118	38	170	107	46	136	35	304	26	1033	0	27	7	4	1	0	8	17	22	14	11	1	7	23	142
15	0	0	0	0	0	1	0	0	0	1	1	3	0	0	0	0	0	0	0	3	0	2	1	2	0	0	8
16	0	0	0	0	0	0	0	0	0	0	0	0	0	0	0	0	0	0	0	2	1	0	0	0	0	0	3
17	0	0	3	2	9	2	2	15	10	12	3	58	0	0	0	0	0	0	2	39	13	14	16	2	2	2	90
18	0	0	1	0	0	2	0	1	1	2	0	7	0	0	0	0	0	0	0	4	1	3	0	2	0	0	10
19	0	0	1	0	0	0	0	0	0	0	0	1	1	0	0	0	0	0	0	1	1	0	0	0	0	0	3
20	14	3	3	2	0	5	2	8	0	0	0	37	60	0	0	0	0	0	0	0	2	0	0	0	0	0	62
21	2	1	2	0	0	1	1	11	0	1	0	19	63	0	0	0	0	0	0	1	1	1	0	1	1	0	68
22	0	0	0	2	7	2	2	11	2	30	3	59	10	0	0	0	0	0	0	14	13	12	1	7	6	18	81
23	1	2	1	0	1	1	0	2	0	3	3	14	7	0	0	0	0	0	2	31	14	11	17	4	0	1	87
24	0	0	0	0	0	0	0	0	0	0	0	0	0	0	0	0	0	0	0	2	0	0	0	0	0	0	2
25	2	0	0	2	5	10	7	38	21	52	0	137	0	0	0	0	1	0	4	51	34	6	8	18	6	17	145
26	0	0	0	1	0	0	0	0	0	1	0	2	0	0	0	0	0	0	0	2	0	0	0	0	0	0	2
27	1	0	0	0	0	0	0	0	0	0	0	1	0	0	0	0	0	0	1	0	0	0	0	0	0	0	1
28	0	0	0	0	0	0	0	0	0	0	0	0	0	0	0	0	0	0	0	0	0	0	0	0	0	0	0
29	12	0	0	0	0	0	0	0	0	0	0	12	0	0	0	0	0	0	0	0	0	4	1	0	0	0	5
30	0	0	0	4	0	0	0	0	0	0	0	4	0	0	0	0	0	0	0	1	0	0	0	0	0	0	1
31	1	0	1	0	0	0	0	0	0	1	0	3	0	0	0	0	0	0	0	1	0	0	0	0	0	0	1
32	6	0	0	0	0	2	1	5	1	0	0	15	0	0	0	0	0	0	9	37	59	21	6	7	5	14	158
33	0	0	0	0	0	0	0	0	0	0	0	0	0	0	0	0	0	0	0	0	0	0	0	0	0	0	0
34	0	0	0	0	0	0	0	0	0	0	0	0	0	0	0	0	0	0	0	0	0	0	0	0	0	0	0
35	0	0	0	0	0	0	0	0	0	0	0	0	0	0	0	0	0	0	0	0	0	0	0	0	0	0	0
36	0	0	0	0	0	0	0	0	0	0	0	0	0	0	0	0	0	0	0	0	0	0	0	0	0	0	0
37	0	0	0	0	0	0	0	0	0	0	0	0	0	0	0	0	0	0	0	0	0	0	0	0	0	0	0
38	0	0	0	0	0	0	0	0	0	0	0	0	0	0	0	0	0	0	0	0	0	0	0	0	0	0	0
Totals	91	53	135	53	192	134	64	237	74	421	37	1491	151	43	7	10	4	0	33	272	169	1-6	72	50	27	76	1020

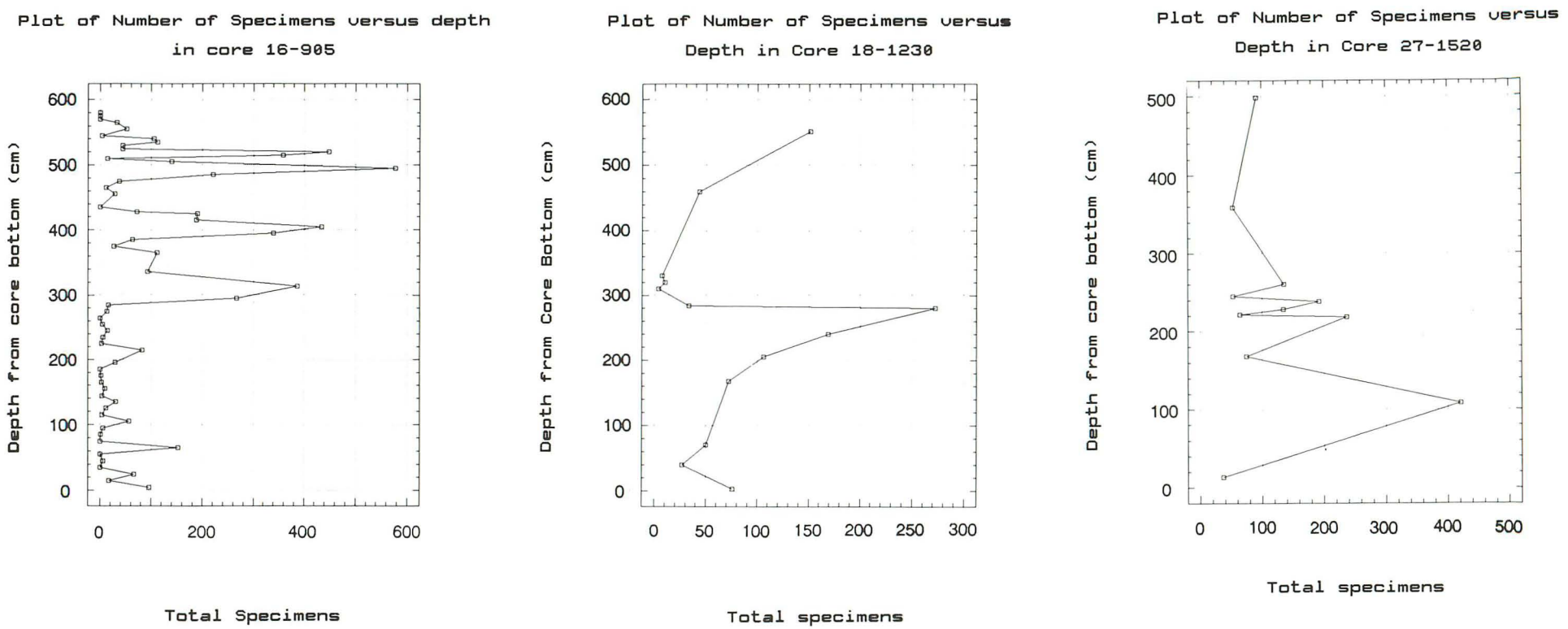

Figure 33.—Plot of number of ostracodes vs. depth in core from vibracores 16-905 (A), 18-1230 (B), and 27-1520 (C).

APPENDIX V

Lithologic logs for twenty-nine (29) vibracores collected off Assateague Island, Maryland. See Plate 2 for location of vibracores.

Summary of General Vibracore Information; July 1986

Core No.	Dist. from Shore (NM)	km	Latitude	Longitude	Water Depth (M)	Meas. Core Length (M)	Subbottom Structure
16-835	1.65	2.65	38°13′1.2″	75°6′1.1″	13.7	6.05	Parallel
16-842	2.2	3.54	38°12′58.1″	75°5′28.3″	11.9	6.10	Top of shoal; parallel
16-850	2.9	4.67	38°12′53.5″	75°4′24.4″	14.3	6.11	Top of shoal; parallel
16-905	4.1	6.59	38°12′43.9″	75°2′55.6″	16.77	6.26	Parallel; top is structureless
16-935	6.5	10.5	38°12′25.1″	75°00′1.8″	19.8	6.10	Channeled
16-945	7.2	11.6	38°12′20.1″	74°58′59.5″	19.5	6.11	Channeled
16-1002	8.7	14.0	38°12′9.9″	74°57′8.1″	21.0	5.17	Distinct channel
16-1005	8.9	14.3	38°12′8.3″	74°56′46.5″	20.4	5.59	Shallow channels
16-1029	10.9	17.5	38°11′53.5″	74°54′8.3″	21.0	5.9	Possible shallow channels
18-1135	9.4	15.1	38°10′17.2″	74°56′50.7″	18.0	6.13	Channel?
18-1142	8.8	14.2	38°10′27.0″	74°57′40.0″	18.9	4.92	Distinct channel
18-1215	5.6	9.0	38°10′52.7″	74°1′45.2″	14.6	5.12	Shoal axis
18-1230	4.2	6.75	38°11′1.7″	75°3′22.7″	19.5	6.10	Parallel
18-1248	2.45	3.9	38°11′14.2″	75°5′52.1″	16.5	5.88	Parallel
20-1340	2.7	4.3	38°9′30.2″	75°5′57.3″	15.24	5.47	Channel
20-1430	7.5	12.1	38°8′53.0″	74°59′57.0″	18.9	4.15	Trough; pinchout of shoal
20-1446	9.0	14.5	38°8′41.5″	75°58′2.7″	20.4	6.05	Parallel adj. to channeling
20-1500	10.27	16.5	38°8′34.1″	74°56′33.9″	20.1	6.10	Parallel
20-1518	12.15	19.5	38°8′17.6″	74°54′17.2″	21.6	5.53	Channel
20-1605	9.6	15.4	38°6′55.3″	74°57′56.4″	20.4	5.92	Parallel; not shoal
23-928	3.0	4.0	38°6′3.3″	75°6′37.2″	12.8	6.09	Wide, shallow channel
25-1215	8.6	13.8	38°3′37.1″	75°1′0.6″	18.9	5.5	Trough on west (landward) side of shoal
25-1308	3.6	5.8	38°4′19.6″	75°7′11.7″	13.7	5.8	Parallel underlain by deeper channel
27-1425	2.75	4.4	38°2′45.5″	75°9′25.2″	14.3	2.02	Parallel; trough between shoals
27-1425 (run 2)	2.75	4.4	38°2′45.5″	75°9′25.2″	15.8	3.32	
27-1440	4.0	6.4	38°2′34.5″	75°7′42.2″	14.9	3.91	Parallel; flat seabed
27-1520	7.6	12.2	38°2′5.6″	75°3′19.2″	16.9	5.98	Parallel
29-1640	10.2	16.4	38°0′7.6″	75°1′38.4″	16.2	5.8	East shoal flank
29-1730	5.3	8.5	38°0′45.6″	75°7′23.2″	8.8	4.59	Shoal axis; parallel
29-1750	3.3	5.3	38°1′1.4″	75°9′43.6″	11.3	3.54	Parallel; not on shoal

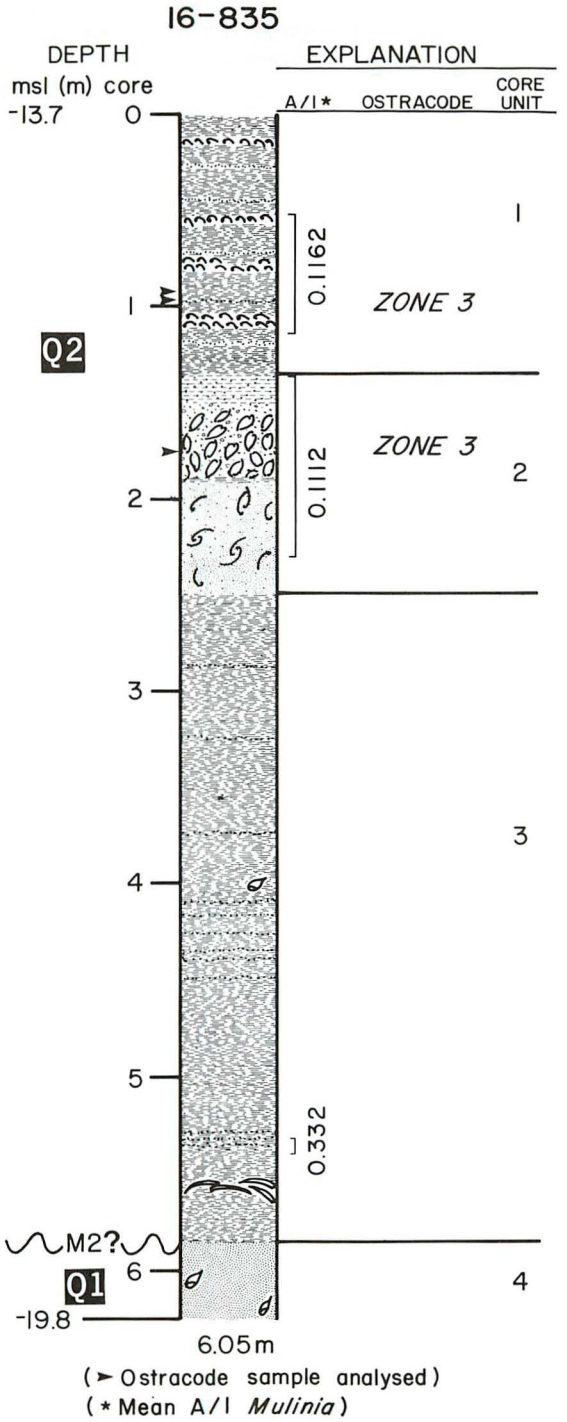

Core 16-835

Unit 1 0-134
MUD: dewatered, dark greenish-gray (5GY 4/1) silt-clay; massive with thin laminations of fine sand and silt; *Mulinia* layer.

Unit 2 134-247
SAND: light gray (N5-N6) fine sand (unit 2B) coarsening upward to olive gray (5Y 6/1) coarse sand with gravel (unit 2A); at 188, 8 cm dark gray (5GY 4/1) mud layers separates fine sand from coarse sand; medium sand and mud occur at top of unit (134-151 cm): abundant articulated *Mulinia* and several gastropods in Unit 2B.

Unit 3 247-584
MUD: dewatered, dark greenish gray (5GY 4/1) silt-clay; massive to wavy bedding with occasional fine sand-silt lamination; shells sparse.

Unit 4 584-605
SAND: olive gray (5Y 5/2) fine sand with some silt/clay, gastropods.

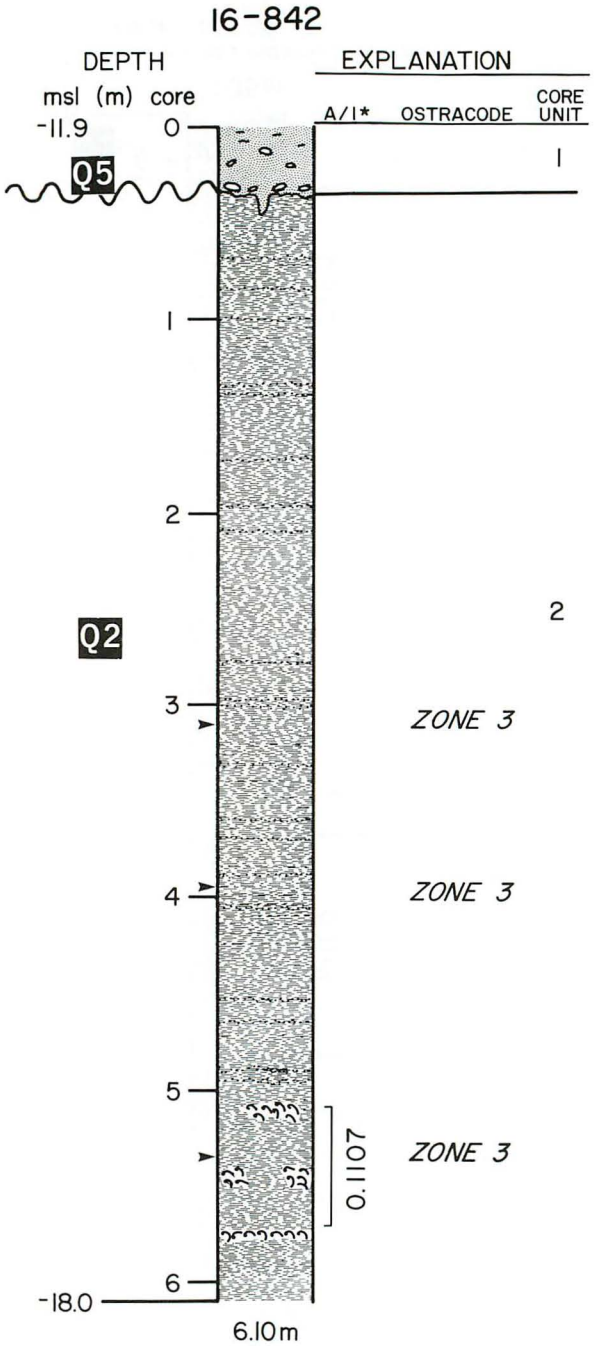

Core 16-842

Unit 1 0-31
SAND: light to dark gray (5GY 3/2) coarse to fine sand; fining upward, gravels up to 13 mm at lower contact; sand-filled burrows at lower contact into underlying unit.

Unit 2 31-610
MUD: dewatered, dark greenish gray (5GY 4/1) silt-clay with fine sand lenses; coarse sand and gravel layers at 222-233, 240-250, and 251-259 separated by dewatered silt-clay.

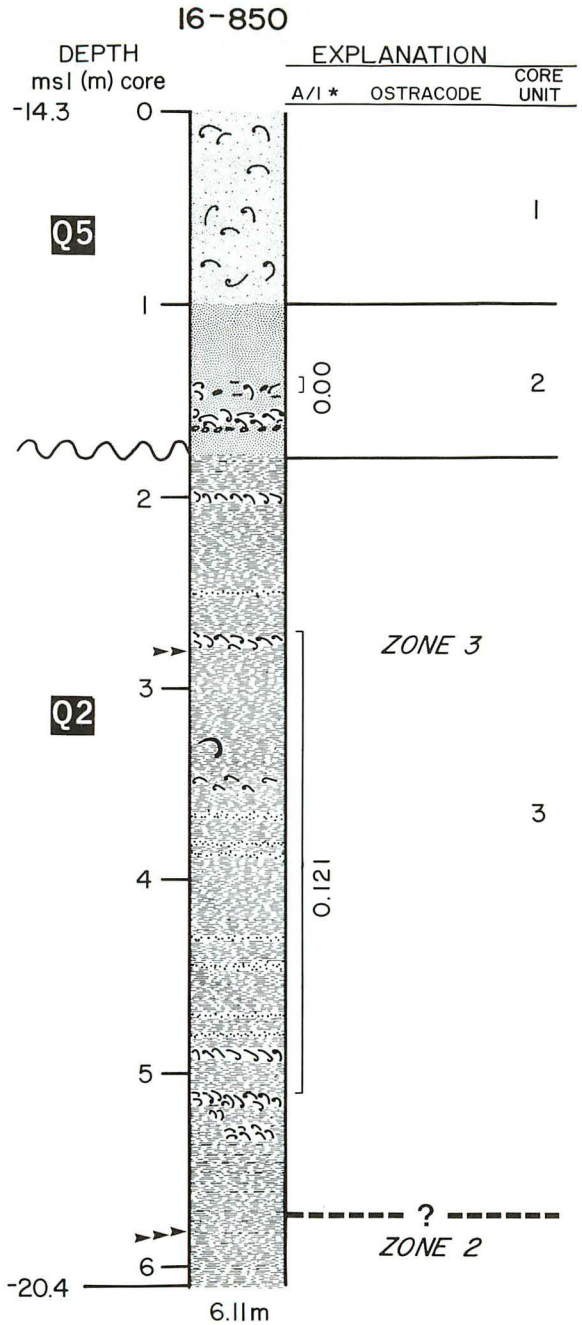

Core 16-850

Unit 1 0-11
SAND: yellowish gray (5Y 6/2) medium to fine; *Spisula* scattered throughout.

Unit 2 100-175
SAND: light olive gray (5Y 3/1) medium to fine sand; heavy mineral layers; at 155-167 coarse to medium sand with shells and pebbles.

Unit 3 175-611
MUD: dewatered, olive gray (5Y 3/2) silt-clay; *Mulinia* assemblages; at 541 to 611 cm, silt-clay darker in color and more organic rich; shells lacking.

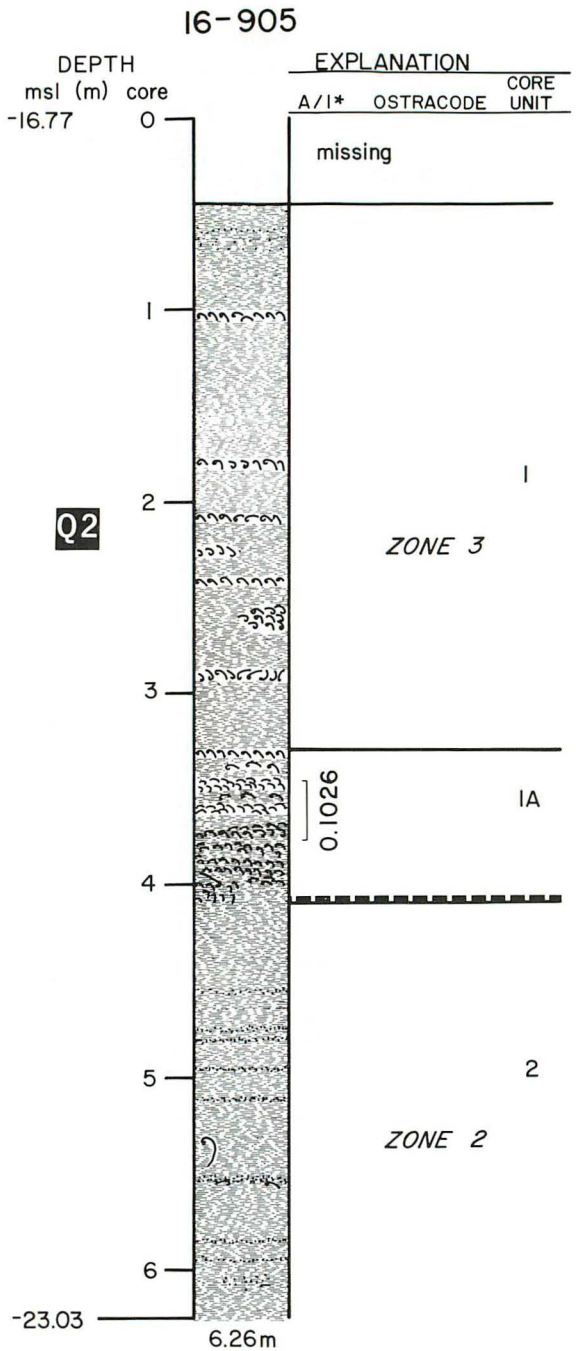

Core 16-905

Unit 1 0-411
MUD: dewatered, dark greenish gray (5GY 3/1) silt-clay; fine sand laminations; *Mulinia* layers; from 329 to 411 cm, unit more fossiliferous with *Mulinia, Ensis,* and *Nassarius.*

Unit 2 411-626
MUD: dewatered, dark olive gray (5GY 3/1) mottled silt-clay; fine sand laminations.

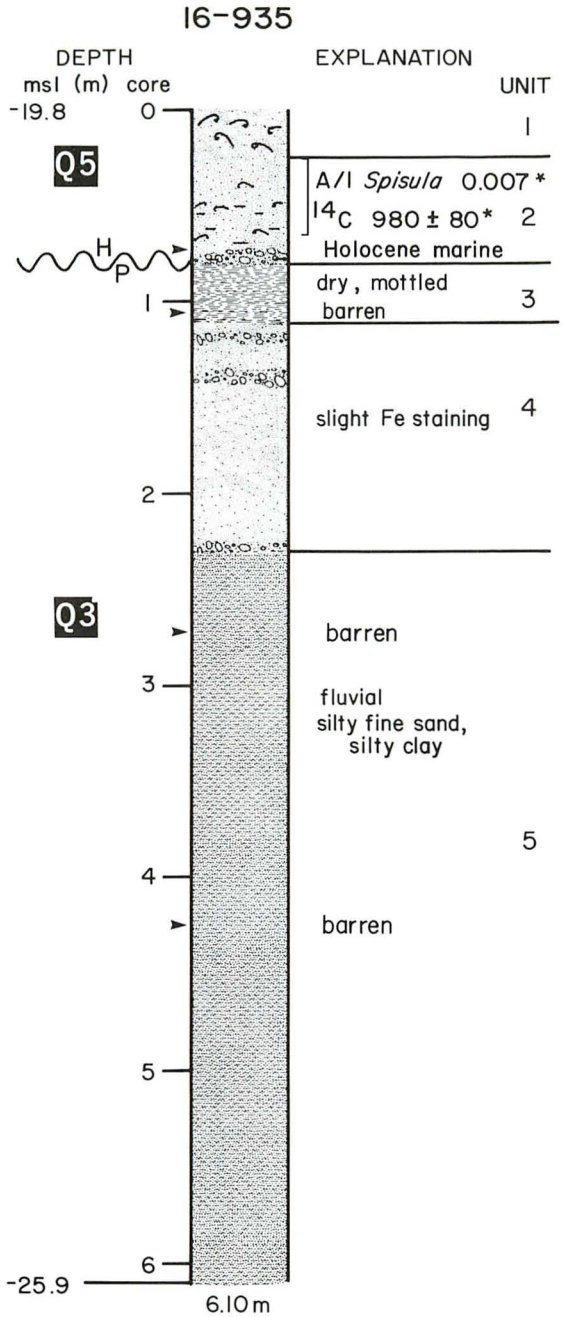

(➤ Sample for microfaunal analysis)
(* A/I, Radiocarbon on same valves)
(^{13}C adj., extended count)

Core 16-935

Unit 1 0-24
SAND: Light olive gray (5Y 6/2), medium to fine sand; *Spisula.*

Unit 2 24-81
SAND: olive gray (5Y 4/1) medium to fine sand; interbedded muddy sand/mud with medium to fine sand; pebbly at lower contact, sandy mud at upper contact; *Spisula.*

Unit 3 81-113
MUD: dewatered, grayish olive green (5GY 3/2) silt-clay.

Unit 4 113-232
SAND: medium olive gray (5Y 4/2) medium to fine sand; iron-stained gravelly sand at 140-154 and 225-232 cm.

Unit 5 232-610
SAND: fine sand to silty sand; color varies, olive brown to olive gray (5Y 5/6 to 5Y 4/2); thin silt-clay layers at 270-275 and 286-290 cm.

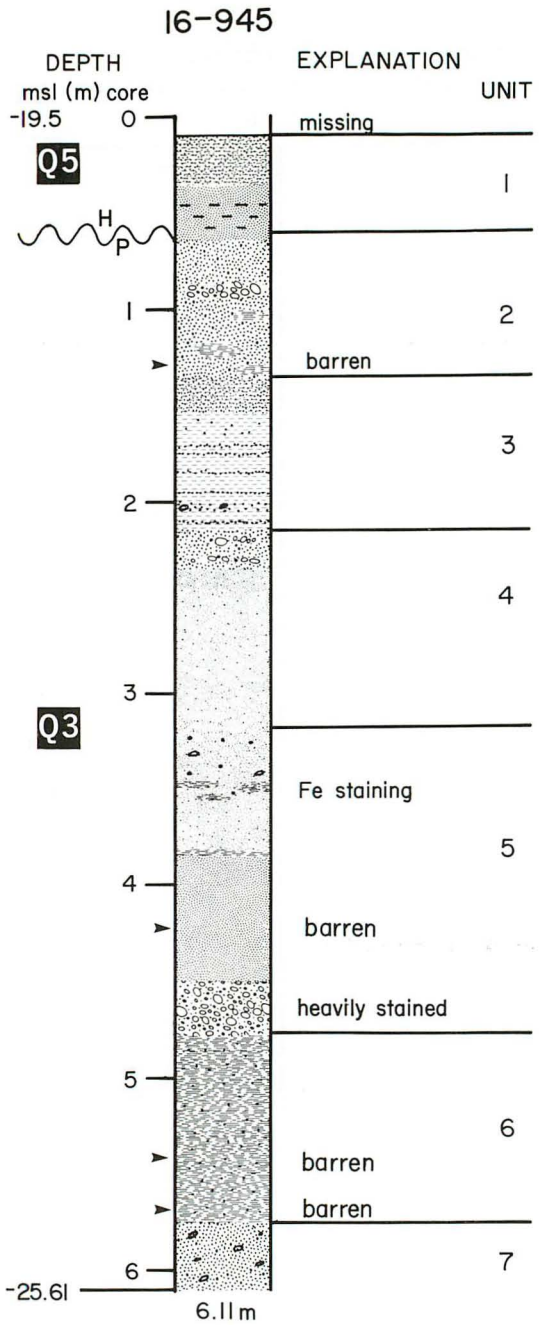

0-11
Missing

Unit 1 11-61
SAND: dark gray (N3) to light gray (N7) muddy to fine sand; pebbles at 22 cm; dark gray muddy sand from 11 to 34 cm; light gray fine sand from 34 to 61 cm.

Unit 2 61-135
SAND: light olive gray (5Y 6/1) medium to fine sand; coarsening upward to coarse to medium sand with gravel; mud lenses at 122 and 130 cm.

Unit 3 135-214
MUD: medium blue gray (5B 5/1) sandy mud interbedded with fine sand; olive brown (5Y 5/6) gravelly sand at 200 to 205 cm.

Unit 4 214-318
SAND: light olive gray (5Y 4/1) coarse to medium sand; gravelly sand at 214 to 232 cm.

Unit 5 318-477
SAND: yellowish brown (10 YR 5/4) medium to fine sand with gravel, iron-stained, interbedded with light brown (5Y 5/6) medium to fine sand; at 382 to 458 cm, grayish olive (10Y 4/2) to light brown (5Y 5/6) fine sand; mud and iron-stained sand stringers throughout. Iron-stained, very coarse, gravelly sand at lower contact.

Unit 6 477-566
MUD: grayish olive green (5GY 4/2) silt-clay with sandy silt-clay; increasing sand at lower contact; iron-stained at lower contact.

Unit 7 566-611
SAND: medium olive brown (5Y 4/4), coarse to medium sand; gravel and heavy minerals present.

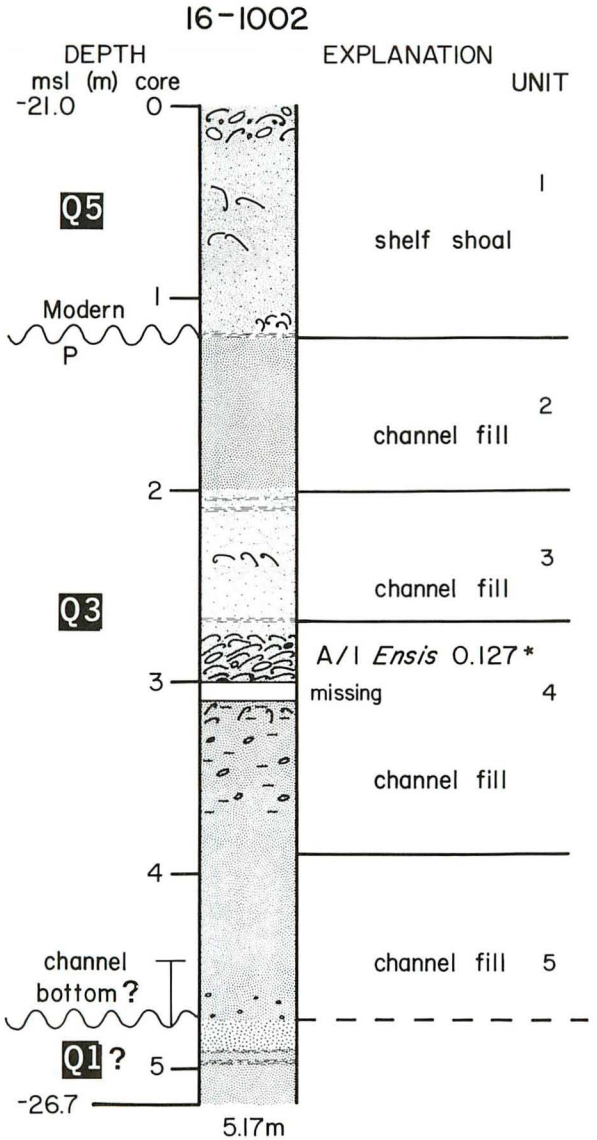

(* Est. Stage 5; reworked during channel aggradation)

Core 16-1002

Unit 1 0-120
SAND: light olive gray (5Y 6/1) medium to fine sand; coarse sand, gravel, shell in the top 20 cm; shell fragments present throughout; mud less at lower contact.

Unit 2 120-200
SAND: light olive gray (5Y 6/2), well sorted, fine to very fine sand.

Unit 3 200-268
SAND: light olive gray (5Y 6/2) well sorted fine to very fine sand; shell fragments and shell hash (at 237 cm); mud stringers at 205, 210, 202, and 268 cm.

Unit 4 268-390
SAND: olive gray (5Y 3/2) fine, muddy sand with shell and pebbles grading upward to dark olive gray (5GY 4/1) coarse to medium, gravelly sand with mud and shell at top. Shells are *Ensis, Spisula,* and *Mercenaria.*

Unit 5 390-517
SAND: olive gray (5Y 4/1) fine to very fine sand; at 439 to 450 cm, fine sand with increasing mud, at 450 to 460 cm, very fine sand; at 460 to 489 cm, fine sand with gravel grading downward to medium sand; at 490 to 500 cm, medium sand with mud stringers.

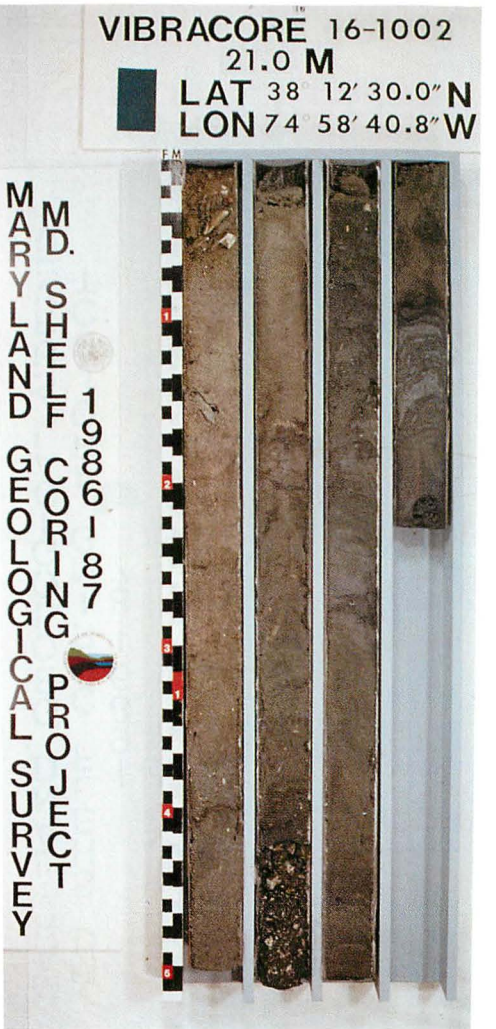

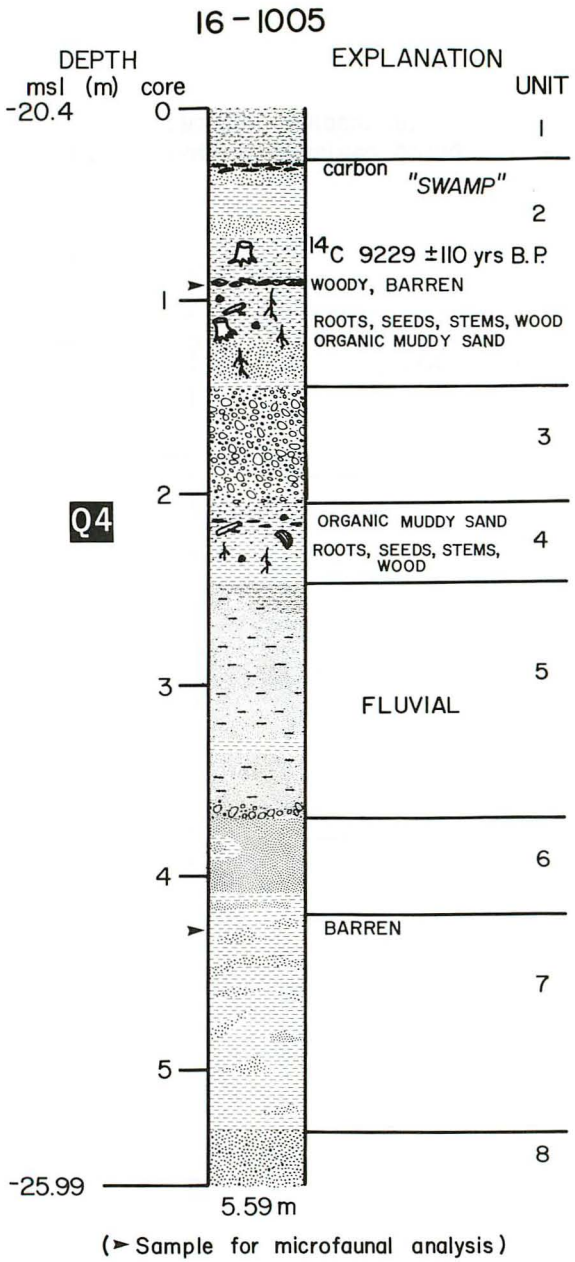

Core 16-1005

Unit 1 0-28
SAND: medium gray (N5) medium to fine sand with gravel; fining upward, gravel at bottom to increasing mud at top.

Unit 2 28-142
MUD: dark gray (N3) silt-clay with light olive gray (5Y 5/2) fine sand lenses; mud with woody material at 30 cm, 90 cm and 115 to 120 cm. Wood fragment *Fraxinus* at 71 to 79 cm dated at 9229 ± 110 BP.

Unit 3 142-202
SAND: light olive gray (5Y 5/2) coarse to fine sand with gravel; some iron-stained pebbles.

Unit 4 202-248
MUD: yellowish brown (10YR 2/2) to olive black (5Y 2/1) silt-clay; coarsening upward to olive black (5Y 2/1) muddy sand; at 212-220 cm, organic material.

Unit 5 248-370
SAND: medium gray (N5) medium to fine sand, with mud; mud lenses 331 to 335 cm; coarse sand and gravel at 350 to 370 cm; fining upward, upper contact gradational into Unit 4.

Unit 6 371-424
SAND: light to medium gray (N7-N6), fine sand; heavy minerals present; clay clasts at 380-385 cm, and at 410-415 cm.

Unit 7 424-532
MUD: medium greenish gray (5G 5/1) silt-clay, with interbedded fine sand.

Unit 8 532-558
SAND: olive gray (5Y 4/1) coarse to medium sand; heavy minerals.

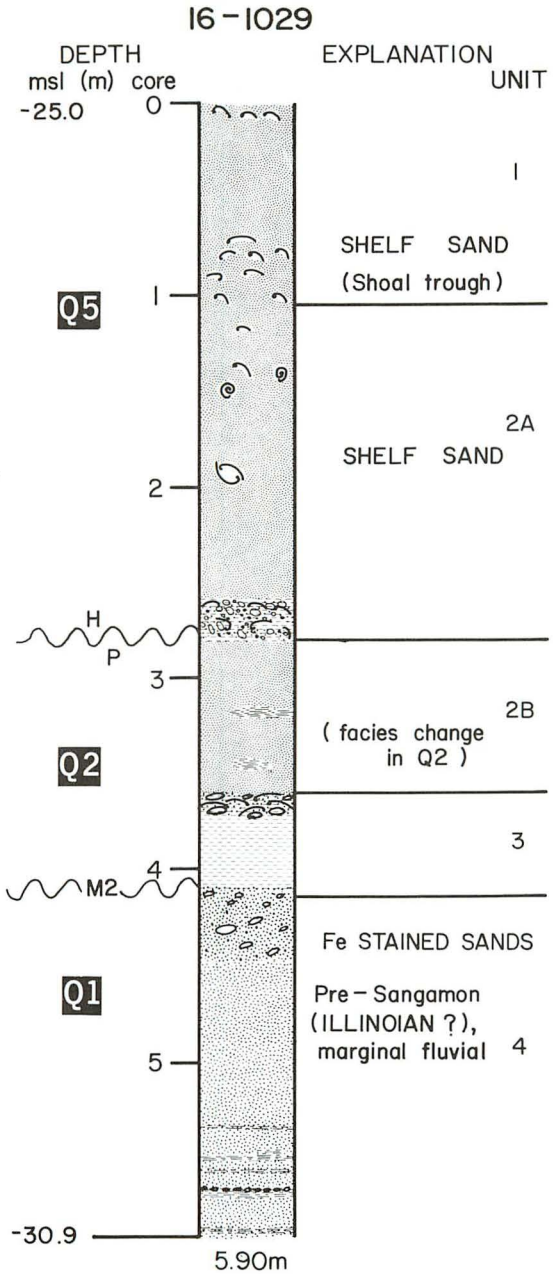

Core 16-1029

Unit 1 0-105
SAND: light olive gray (5Y 5/2) fine sand; large shell fragments and whole shells at lower contact.

Unit 2A 105-279
SAND: medium gray (5Y 5/1) fine sand; occasional whole shell. At 260-279 cm, muddy sand with shell and pebbles.

Unit 2B 279-365
SAND: medium gray (N5) to olive gray (5Y 4/1) fine sand; heavy minerals, clay clasts 345 and 360 cm.

Unit 3 365-412
MUD: olive gray (5Y 3/2) silt-clay, large shells *(Spisula)* at upper contact; sand increases at lower contact.

Unit 4 412-590
SAND: dark yellowish orange (10YR 6/6) medium to fine sand; iron-stained in upper part of unit. From 550 to 590 cm, interbedded sand with mud and coarse sand and gravel; some iron staining.

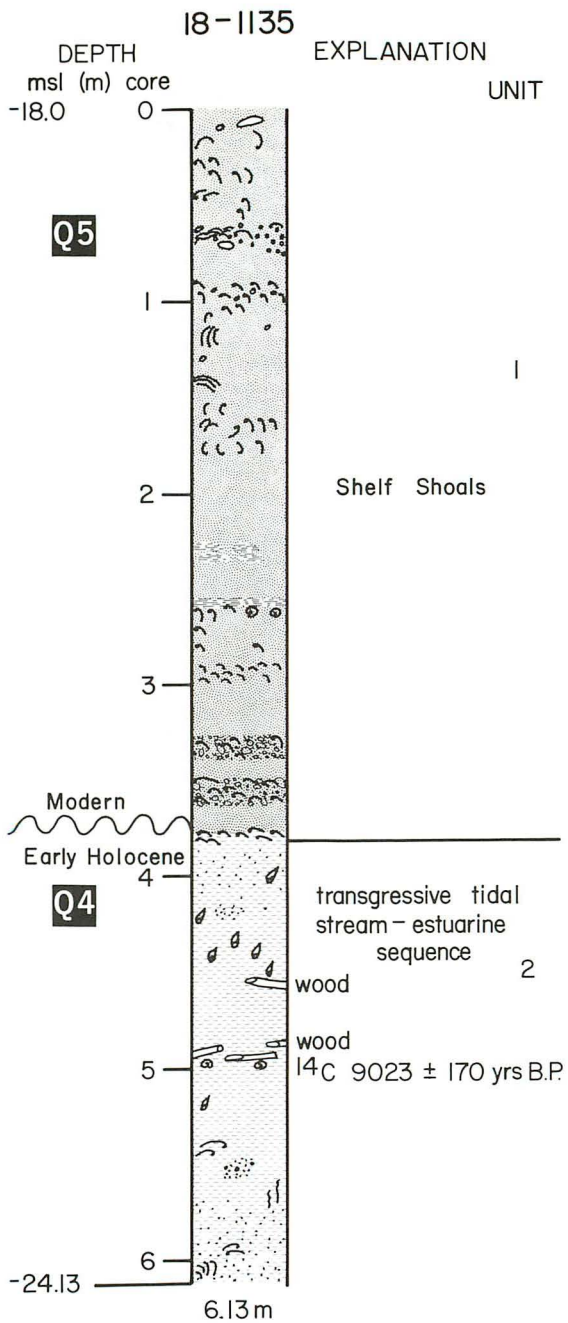

Core 18-1135

Unit 1 0-382
SAND: light olive gray (5Y 5/2) to olive gray (5Y 3/2) medium to fine sand; numerous shell fragments and shells; scattered pebbles; at 330-342 and 350-361 cm medium sand with gravel and shell fragments *(Spisula)*.

Unit 2 382-605
MUD: moist, dark olive gray (5Y 3/1) silt-clay with sand, shells, and plant debris; *Nassarius* and *Crassostrea*.

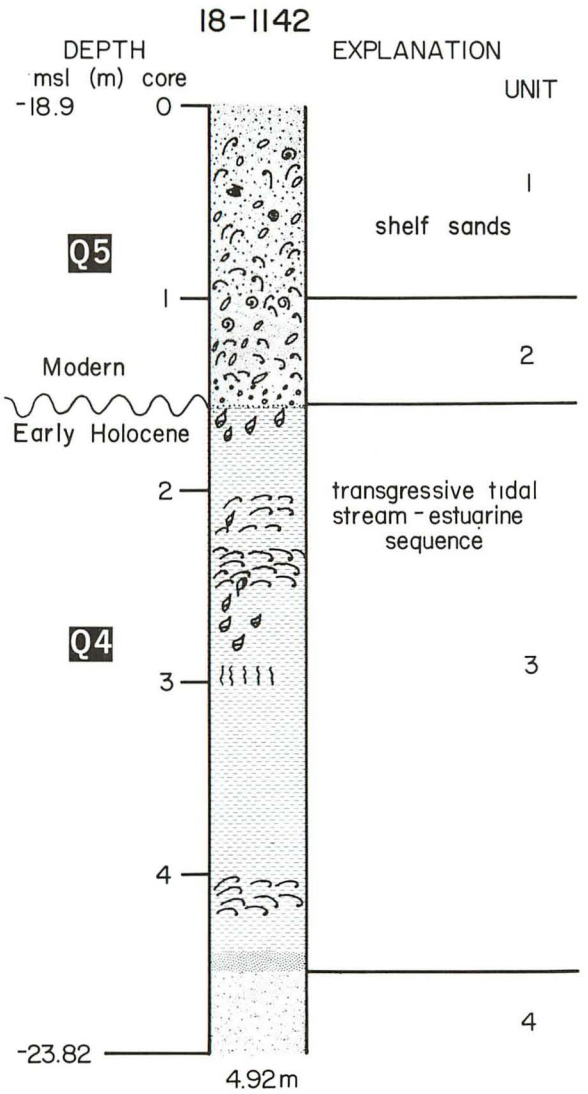

Core 18-1142

Unit 1 0-100
SAND: light olive gray (5Y 5/2), medium to fine sand with gravel, shells, and shell fragments.

Unit 2 100-155
SAND: light olive gray (5Y 5/2) fine sand with shell fragments and heavy minerals; at 145 to 155 cm, medium, gravelly sand.

Unit 3 155-452
MUD: dark gray (N3) mud; at 200 to 250 cm, and at 400 to 410 cm, *Crassostrea* and at 250 to 280 cm, *Nassarius*.

Unit 4 452-492
SAND: olive gray (5Y 3/2) to light olive gray (5Y 5/2) well sorted, medium to fine sand; some gravel, some organic material.

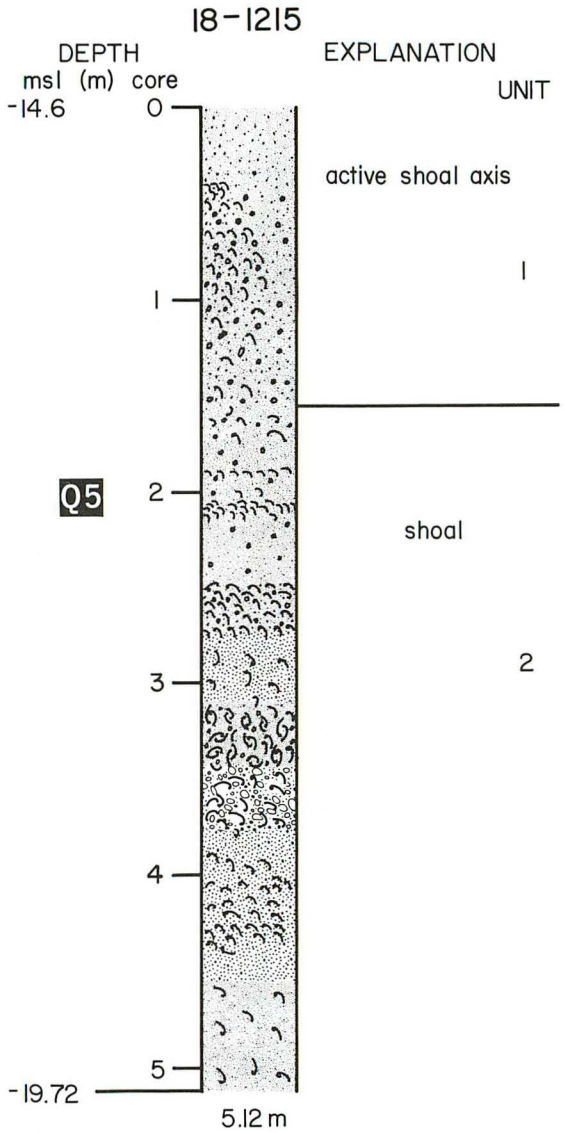

Core 18-1215

Unit 1 0-154
SAND: light olive brown (5Y 5/6) to olive black (5Y 2/1), poorly sorted medium to fine gravelly sand; whole shell *(Spisula, Mulinia)* and shell fragments throughout.

Unit 2 154-512
SAND: dusky yellow (5Y 6/4), interbedded, poorly sorted coarse gravelly sand with shell, coarse to medium sand with shells and medium to fine sand; shells – *Spisula* and *Mulinia.*

*Dark color in sediment at bottom of sections B, C, and D due to storage procedures.

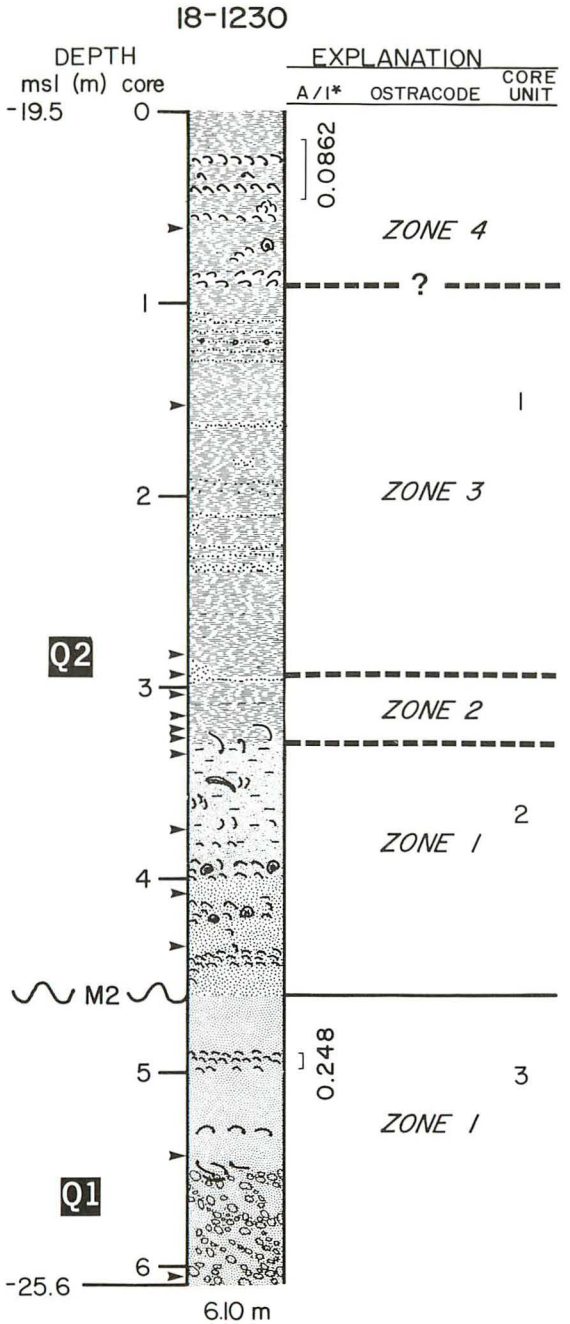

Core 18-1230

Unit 1 0-329
MUD: dewatered, olive gray (5Y 3/1) silt-clay with thin laminations of fine to very fine sand; shell fragments and shell hash in the upper 80 cm.

Unit 2 329-458
SAND: olive gray (5Y 3/2) medium to fine muddy sand; large *Spisula* fragments at 345 and 370 cm; from 400 to 458 cm, sand becomes coarser to medium sand with gravel: at 390 to 400, 410 to 420, and 437 to 445 cms, numerous shell fragments and whole shells.

Unit 3 461-610
SAND: light olive gray, fine sand with heavy minerals; at 488 to 505 cm, shell fragments and increase in mud content; at 530 to 610 cm, whole shells and shell fragments, rounded pebbles, color change to medium olive gray (5Y 3/1).

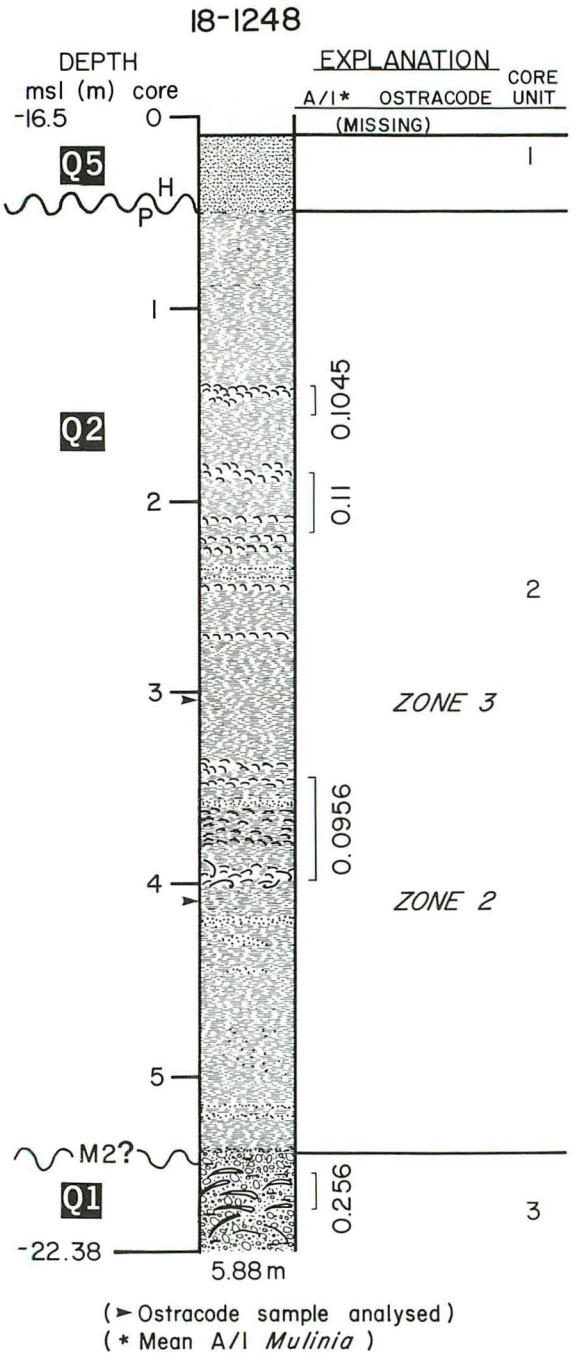

Core 18-1248

Unit 1 10-50
MUD: soft, black (N1) sandy silt/clay; few shell fragments.

Unit 2 50-540
MUD: dewatered, firm, olive gray (5Y 4/2) silt-clay; sand lenses (1-3 cm thick) throughout; shell layers *(Mulinia)* at 140-150, 180-210 and 335 to 400 cms.

Unit 3 540-588
SAND: light olive gray (5Y 5/2) coarse to fine muddy sand with gravel and shell fragment/whole shell *(Spisula)*.

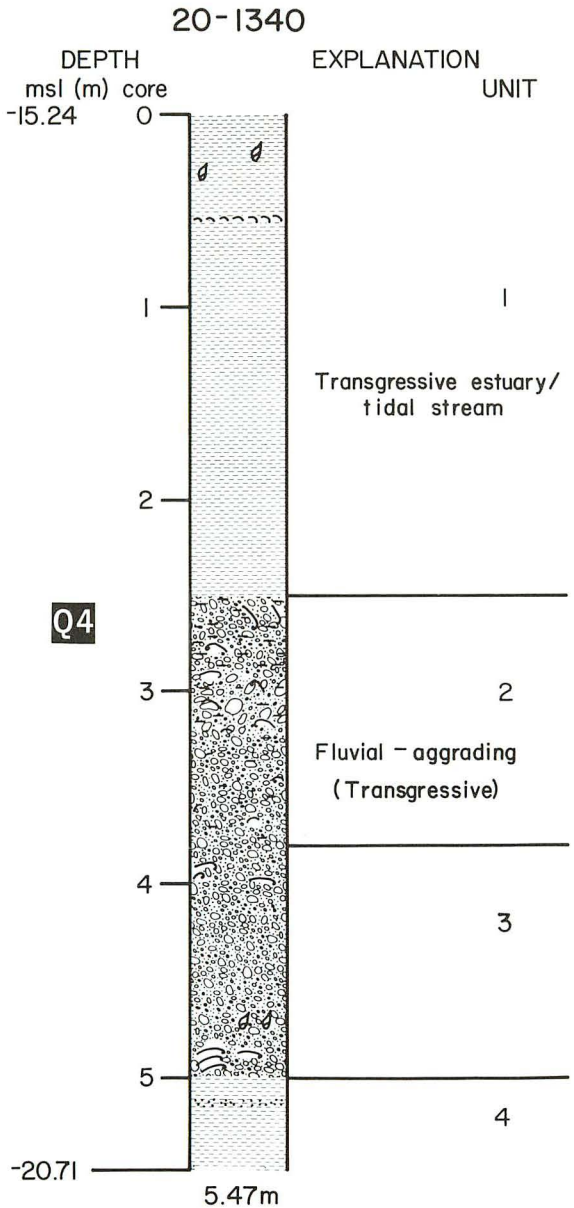

Core 20-1340

Unit 1 MUD:	0-260 moist, dark gray (N3) silt-clay with fine sand laminae; *Mulinia* at 52-53 cm.
Unit 2 MUD and SAND:	260-380 dark gray (N3), gravelly silt-clay and coarse to medium sand; shell fragments.
Unit 3 SAND:	380-500 light olive gray (5Y 6/1), coarse to medium, gravelly sand, shell fragment at 480 to 500 cm.
Unit 4 MUD:	500-547 medium dark gray (N4) silt-clay with shells; *Mulinia* at 540-545 cm.

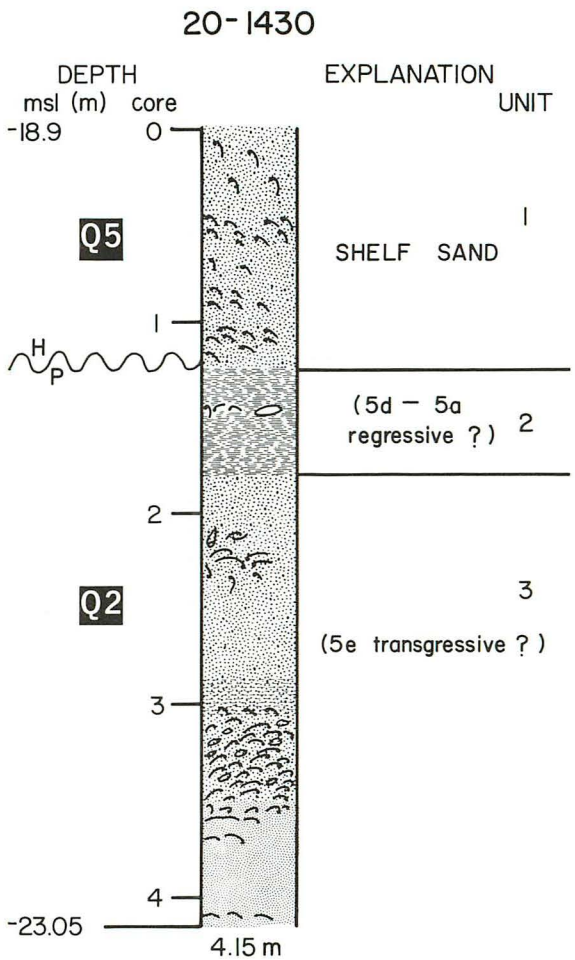

Core 20-1430

Unit 1 SAND: 0-137
light olive gray (5Y 5/2), medium to fine sand grading upward to coarse to medium sand; scattered shells *(Spisula)*; mud layer at 32 to 35 cm.

Unit 2 MUD: 137-177
dewatered, dark green gray (5G 3/1) silt-clay; some shell fragments and pebbles from 143 to 152 cm.

Unit 3 SAND: 177-415
olive gray (5Y 4/1), coarsening upward cycle of medium to fine sand, coarse to medium, gravelly sand; fine, muddy sand; shell fragments abundant in coarse to medium gravelly sand.

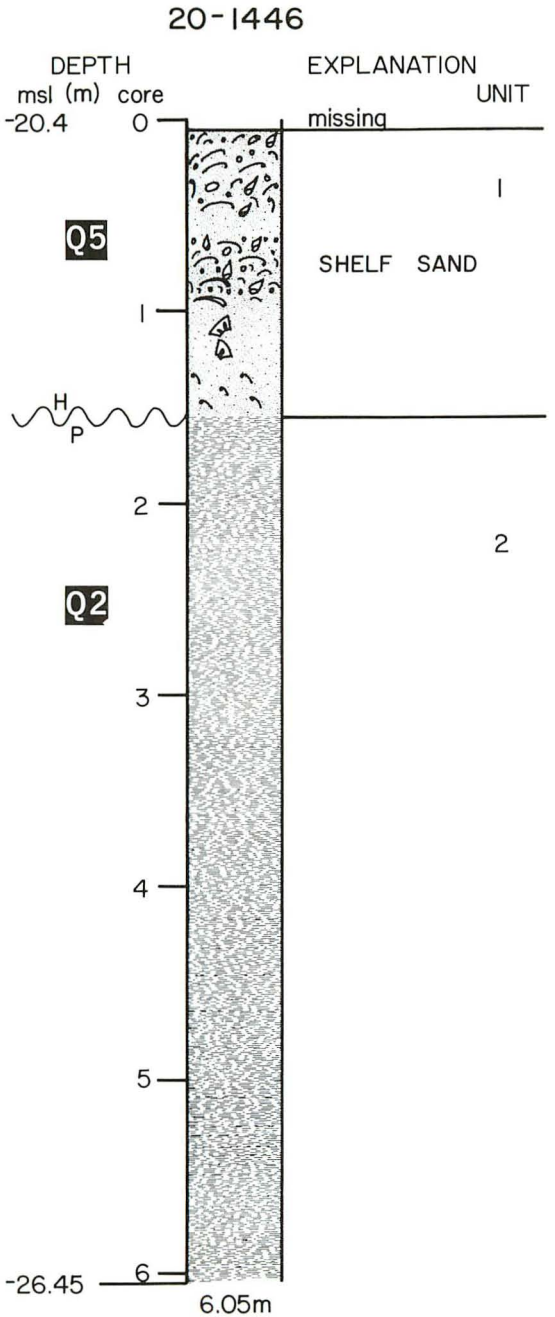

Core 20-1446

Unit 1 0-155
SAND: olive gray (5Y 3/2), medium to fine sand with shell fragments and pebbles; heavy minerals present.

Unit 2 155-605
MUD: dewatered, dark greenish gray (5GY 4/1) silt-clay, no shells.

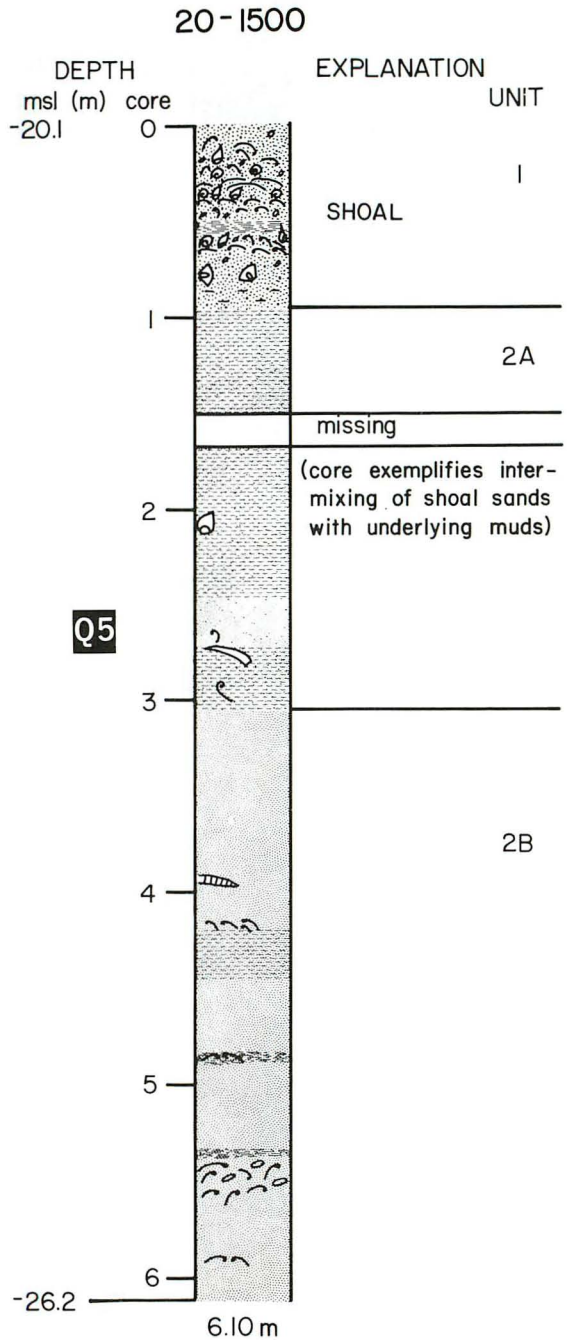

Core 20-1500

Unit 1 0-94
SAND: light olive gray (5Y 5/2), poorly sorted, coarse to fine sand with thin mud lenses; shell fragments abundant.

Unit 2A 94-245
SAND: olive gray (5Y 3/2), muddy, medium to fine sand; few scattered shell fragments.

Unit 2B 245-610
SAND: olive gray (5Y 3/2), medium to fine sand with mud; at 533 to 555 cm, gravel and shell fragments.

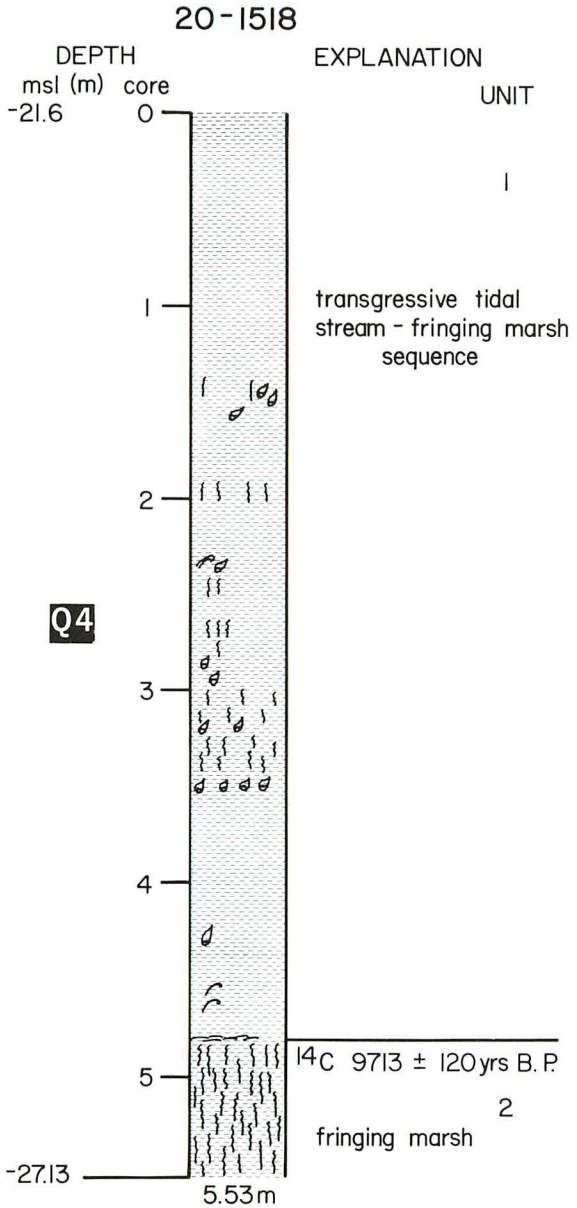

Core 20-1518

Unit 1 0-478
MUD: olive gray (5Y 3/2) silt-clay; scattered shell fragments.

Unit 2 478-553
MUD: olive gray (5Y 4/1) silt-clay with plant debris and shell fragments; C^{14} date at 490 to 510 cm.

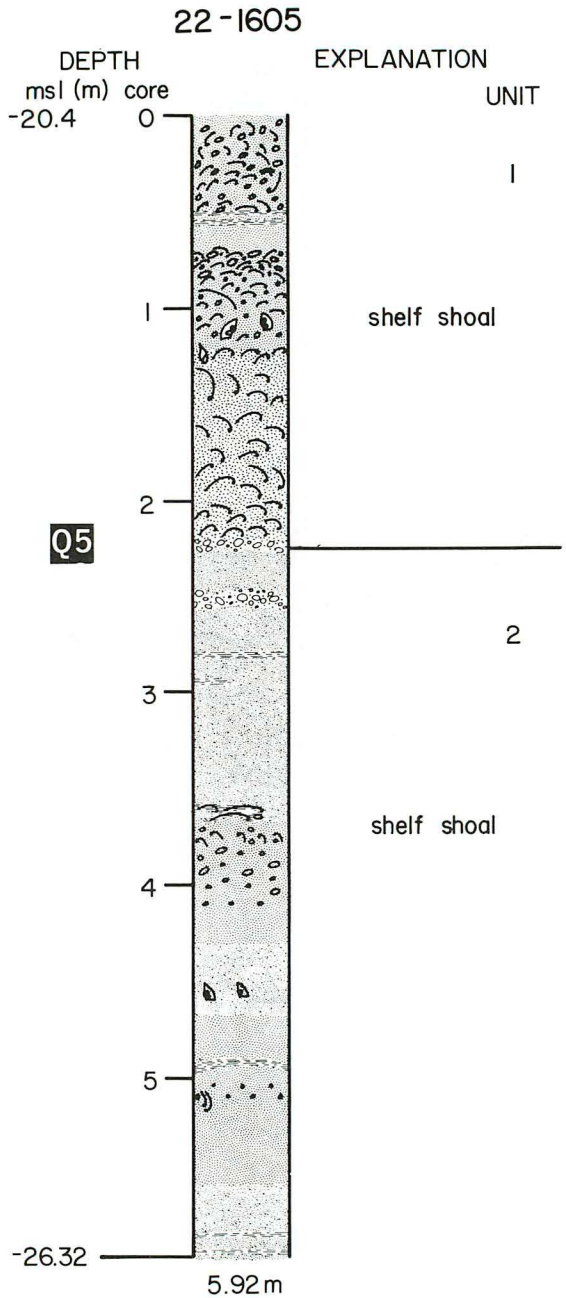

Core 22-1605

Unit 1 0-225
SAND: light olive brown (5Y 5/6) to light olive gray (5Y 6/1), fining upward of medium to fine sand to coarse to medium sand with gravel; shells abundant, *Ensis, Spisula, Astarte;* thin mud lense at 54 to 56 cm.

Unit 2 225-592
SAND: yellowish gray (5Y 7/2), medium to fine sand to light olive gray (5Y 6/1), medium to fine sand; thin occasional mud lense; shell layer and gravel; at 360 to 370 cm, *Crassostrea* in muddy sand.

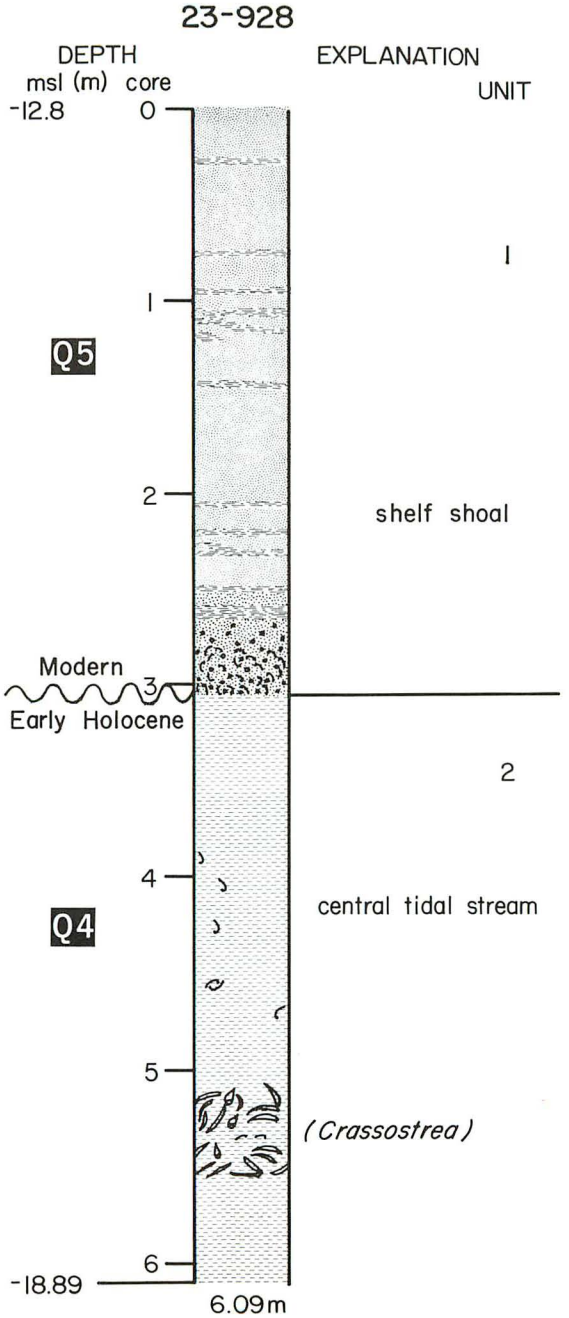

Core 23-928

Unit 1 0-305
SAND: light olive gray (5Y 6/2) fine sand with 4 to 5 cm thick mud lenses at random intervals; at 220 to 305 cm, coarse sand with gravel and shell fragments.

Unit 2 305-609
SAND: dry, olive gray (5Y 3/2) silt-clay. At 510 to 555 cm, numerous *Crassostrea* valves.

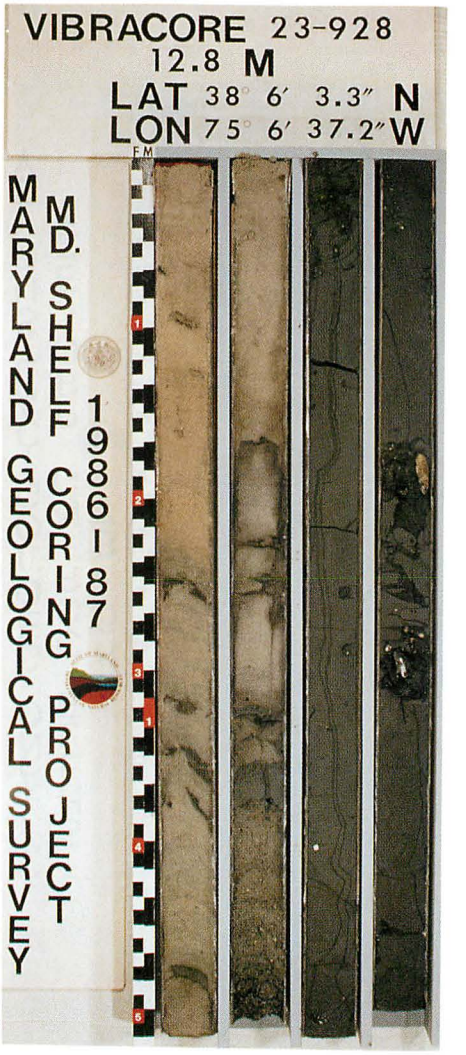

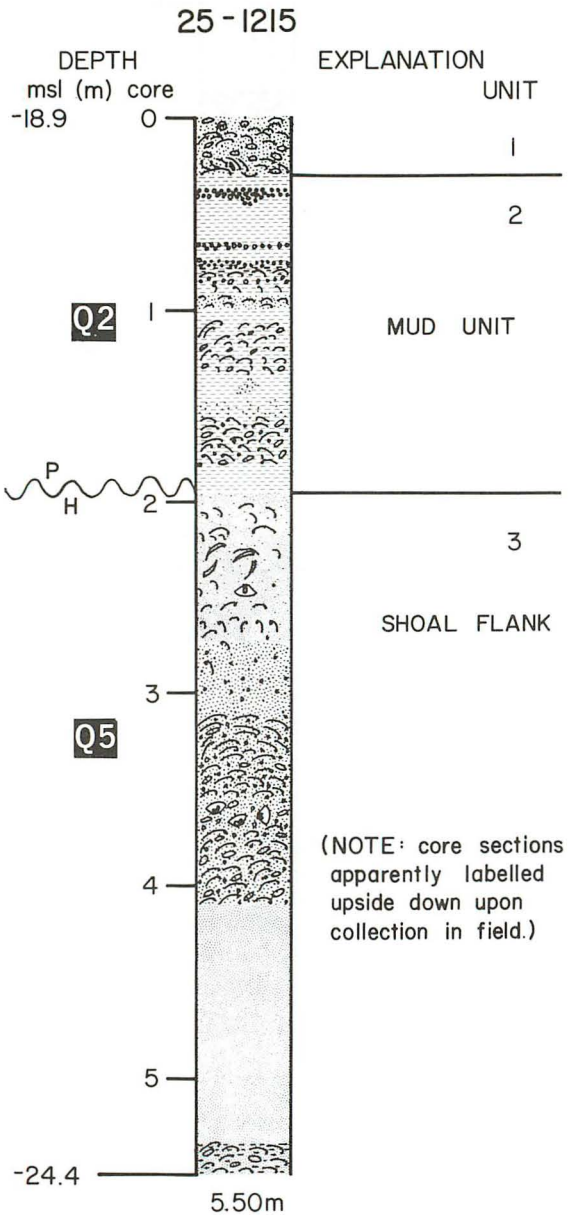

Core 25-1215

Unit 1 0-29
SAND: light olive gray, medium to fine, gravelly sand; shell fragments *(Spisula, Mercenaria, Ensis).*

Unit 2 29-143
MUD: olive gray (5Y 3/2), firm, silt-clay interlayered with 3 to 6 cm thick medium sand/medium sand with gravel layers; shell fragments with sand layers *(Mulinia, Spisula).*

Unit 3 143-550
SAND: light olive gray (5Y 5/2), medium to fine sand alternating with coarse to medium sand with numerous shell fragments.

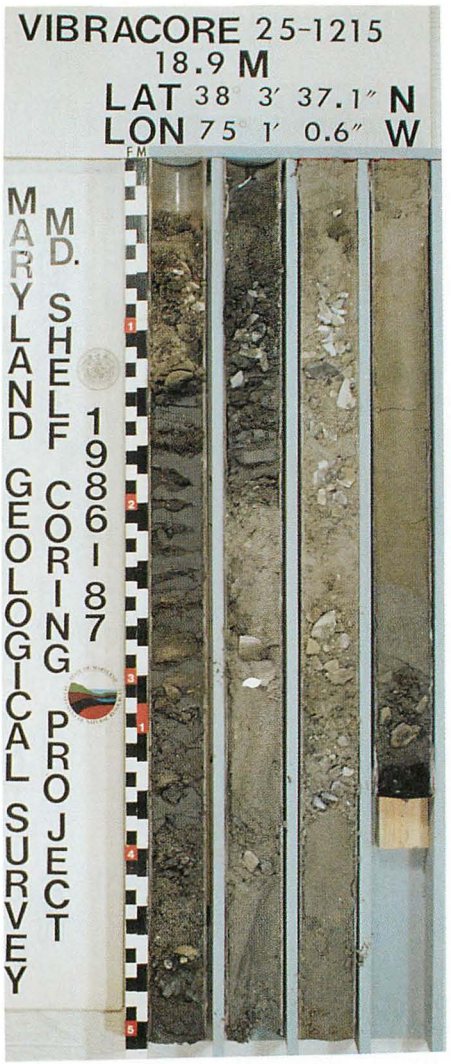

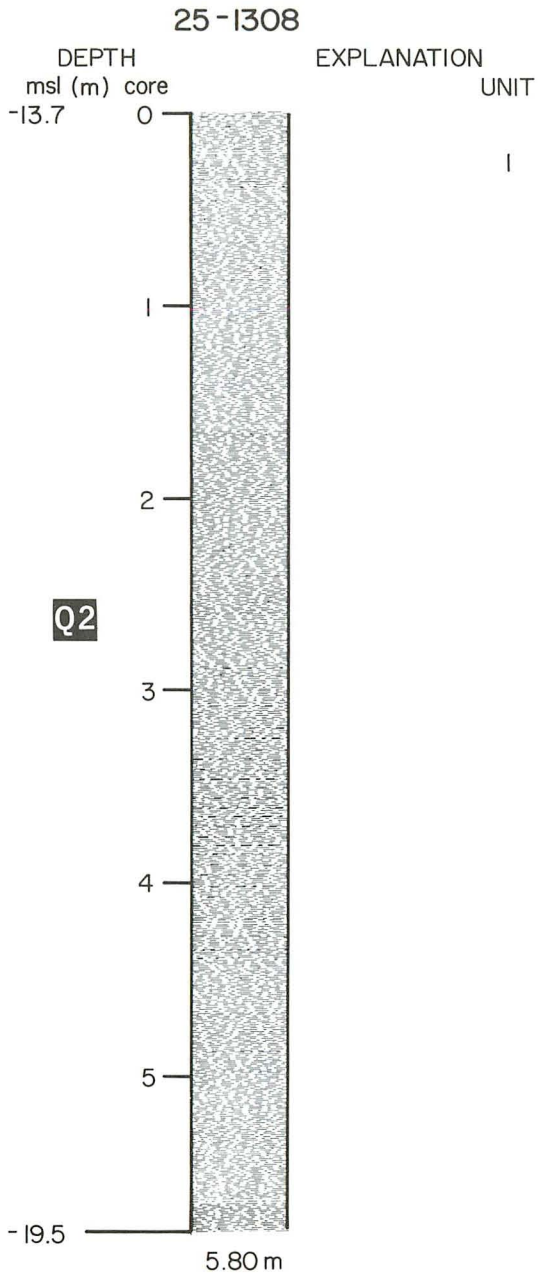

Core 25-1308

Unit 1 0-580

MUD: dewatered, olive gray (5Y 3/2) silt-clay; thin sand laminae scattered throughout.

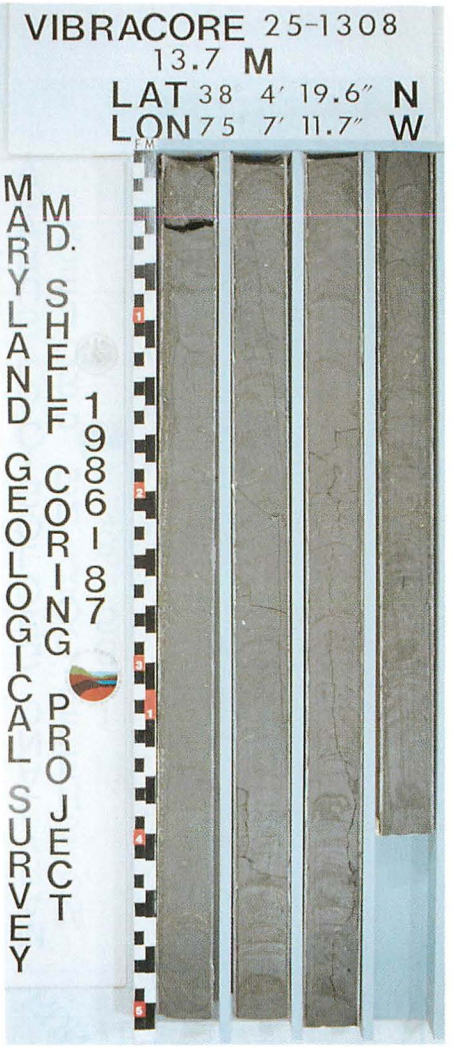

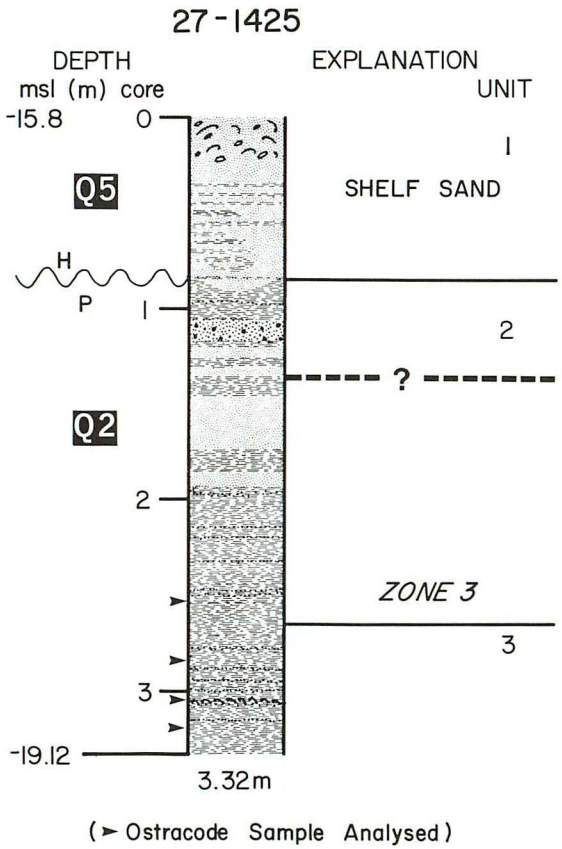

Core 27-1425

Unit 1 0-87
SAND: yellowish gray (5Y 7/2), medium to fine sand interlayered with thin (1-4 cm) olive gray (5Y 3/2) silt-clay.

Unit 2 87-266
MUD: olive gray (5Y 3/2) silt-clay alternating with yellowish gray (5Y 3/2), medium to fine sand to olive gray silt-clay with thin fine sand layers.

Unit 3 266-332
MUD: olive gray (5Y 3/2) silt-clay with thin fine sand layers.

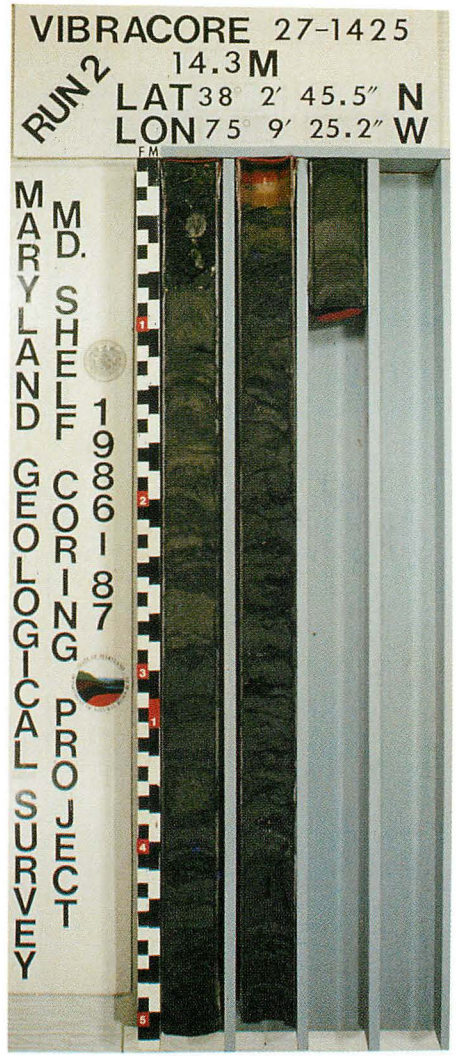

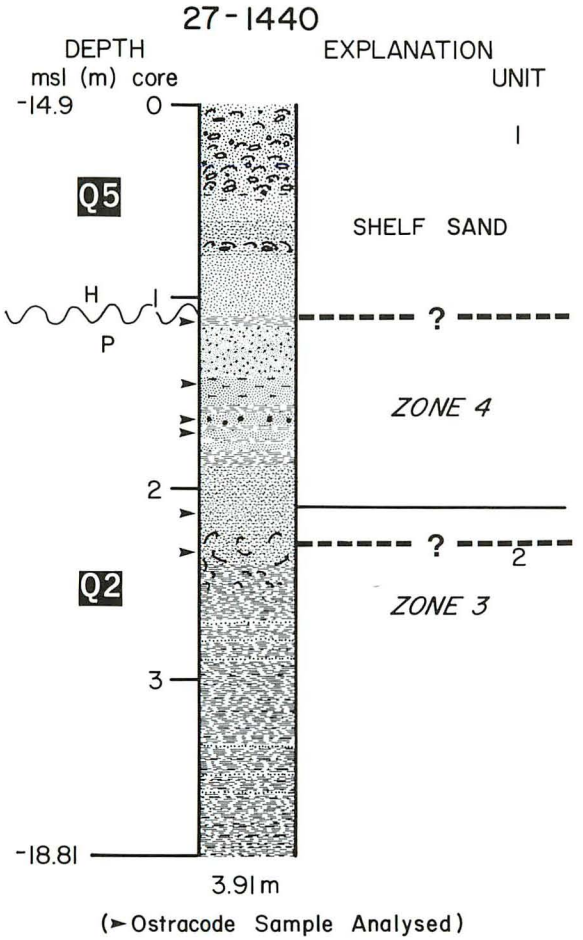

Core 27-1440

Unit 1 0-209
SAND: Light olive gray to olive gray, medium to fine sand interlayered with silt-clay with sand and shell; coarsening upward sequence with medium sand with gravel.

Unit 2 209-391
MUD: olive gray (5Y 3/2), firm, silt-clay with shell fragments and fine sand from 209-252 cm. Below 252 cm, very little shell fragments.

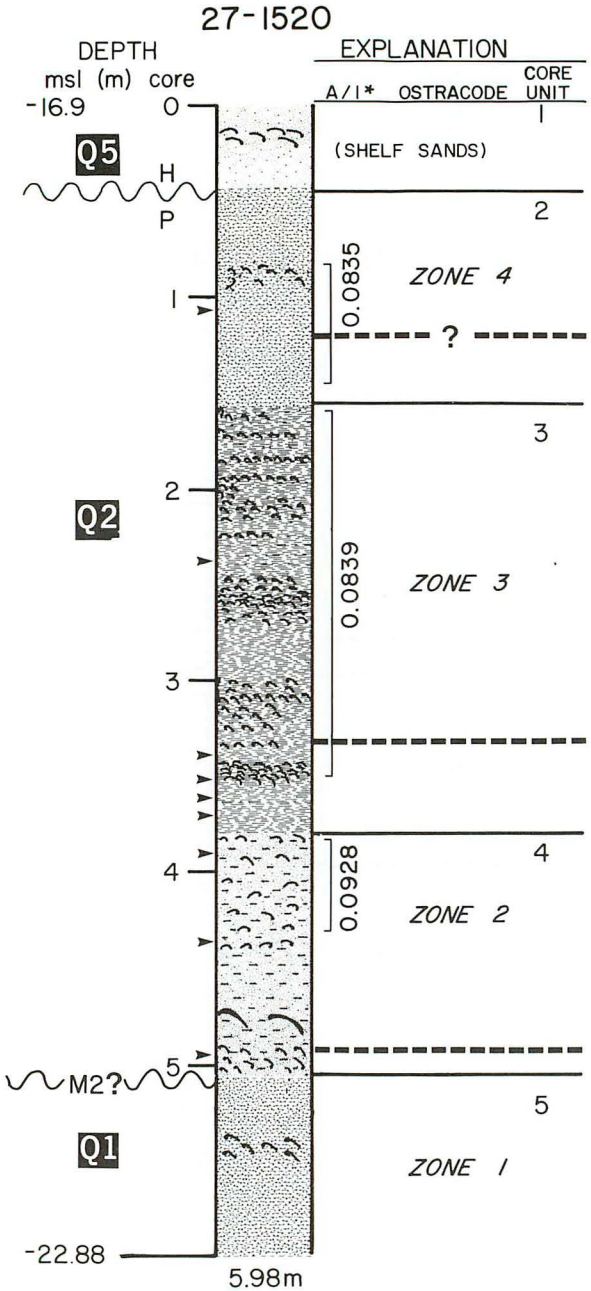

Core 27-1520

Unit 1 0-42
SAND: light olive gray (5Y 6/2), medium to fine sand with occasional pebbles and shell fragments *(Spisula)*.

Unit 2 42-156
MUD: olive gray (5Y 3/1), firm, silt-clay interlayered with fine sand/coarse silt; pebbles and shell fragment/shell hash from 70 to 100 cm.

Unit 3 156-379
MUD: dewatered, medium olive gray (5Y 4/2) silt-clay with distinct layers of shell *(Mulinia)*; at 340 to 355 cm, dense layer of articulated *Mulinia*.

Unit 4 379-505
SAND: light olive gray (5Y 5/2), medium to fine, muddy sand; *Spisula* and *Mulinia* shells scattered throughout.

Unit 5 505-598
MUD: olive gray (5Y 3/1), firm, silt-clay with fine sand and shell fragments.

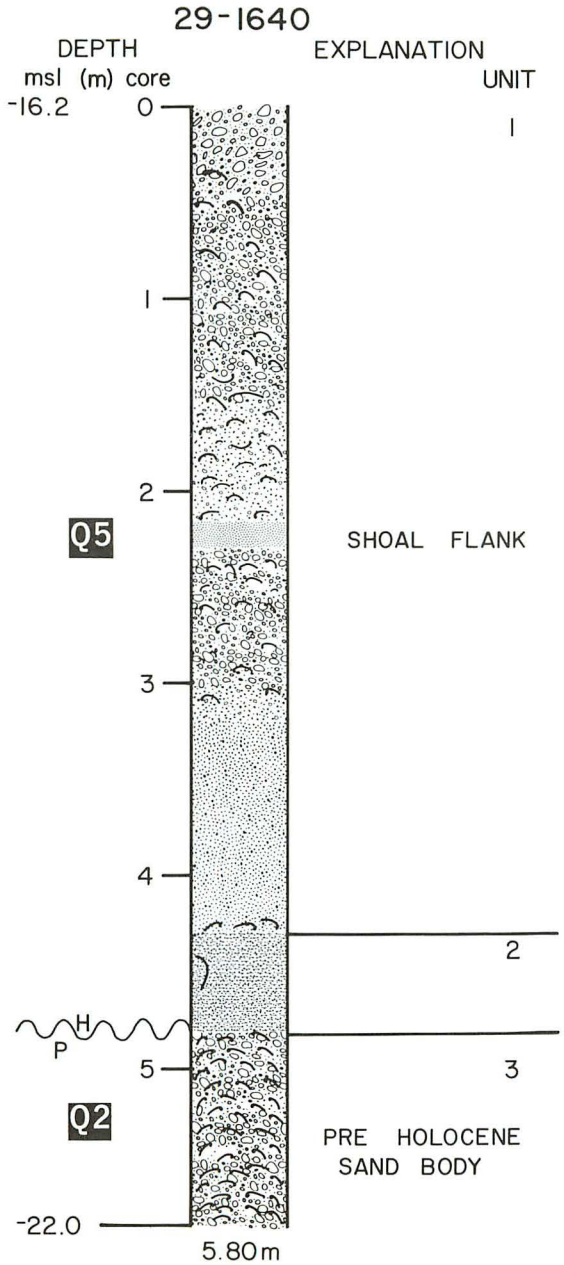

Core 29-1640

Unit 1 0-435
SAND: light olive brown (5Y 5/6) to yellowish orange (10YR 6/6), coarse to medium sand; coarsening upward sequence with pebbles and shell fragments increasing.

Unit 2 435-481
MUD: olive gray (5Y 3/2) firm, sandy, silt-clay.

Unit 3 481-580
SAND: light olive gray (5Y 5/2), coarse to medium sand with gravel and shell fragments.

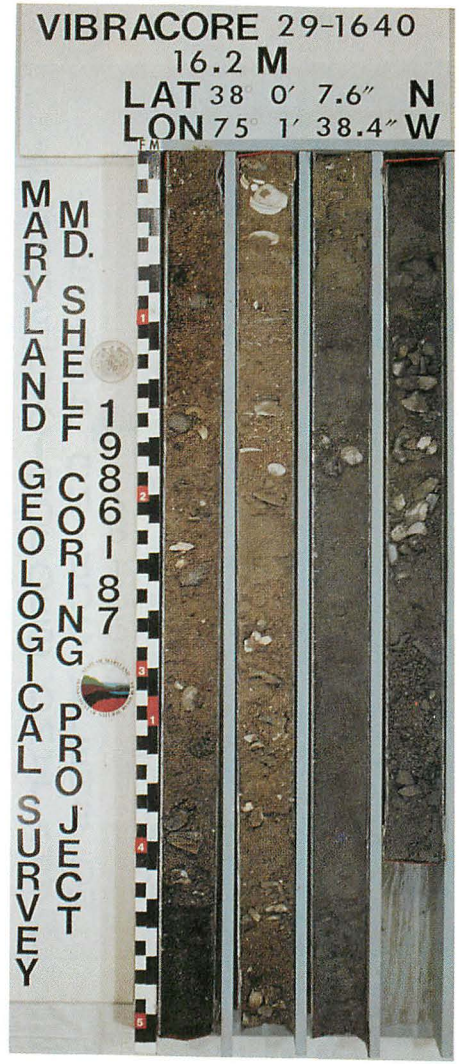

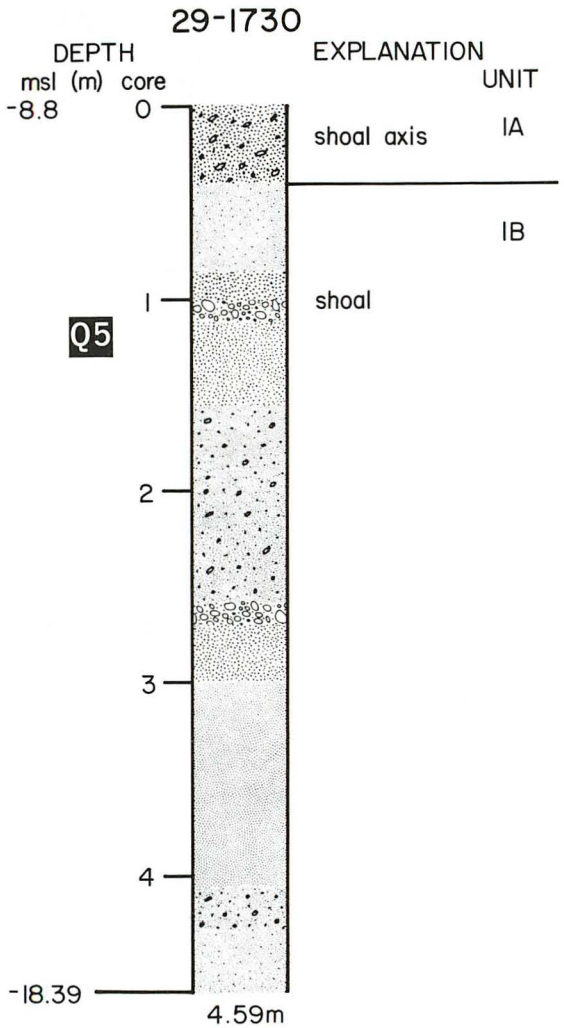

Core 29-1730

Unit 1A 0-40
SAND: dark yellowish-orange (10YR 6/6), coarse to medium gravelly sand with shell fragments.

Unit 1B 40-459
SAND: yellowish-light olive gray (5Y 6/2) medium to fine sand; coarsening upward to medium sand; thin gravel layers at 100-109 cm, 130-134 cm and 260-270 cm.

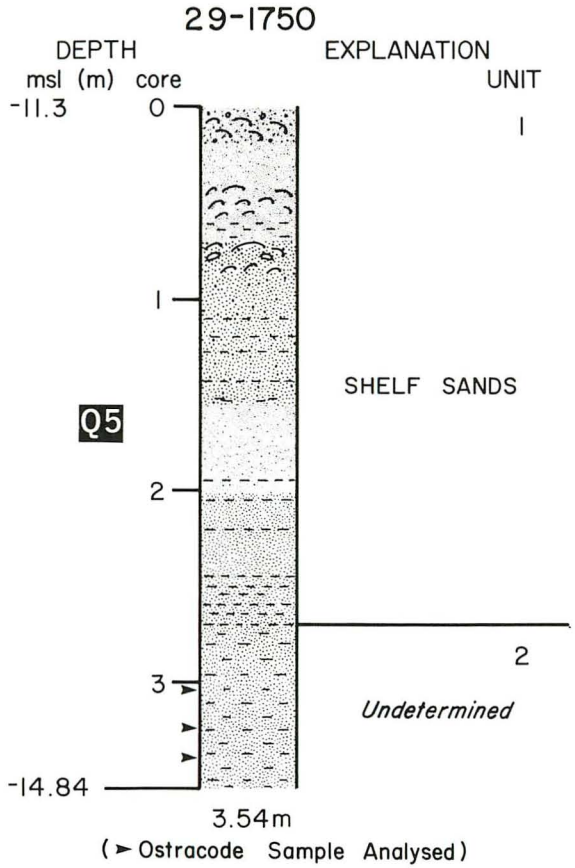

Core 29-1750

Unit 1 0-269
SAND: dark yellowish-orange to light olive gray, medium to fine muddy sand; coarsening upward; medium sand with gravel and shell; iron-staining at 90 to 103 cm.

Unit 2 269-354
MUD: olive gray (5Y 3/2), firm, silt-clay interlayered with muddy fine sand.

APPENDIX VI

PALEOCHANNEL DIMENSIONS

Table XV.—Paleochannel Dimensions Determined from the Geophysical Records Used in Construction of Figures 26, 27, and 28.

Channel #	Time fixes	width (km)	Depth(m) below MSL (m)	Seismic unit of fill	Remarks
Line 14					
1	1412-1420	0.65	22	Q3/Q4	
2	1529-1531	0.2	19	Q4	
3	1554-1556	0.4	24	Q4	
4	1609-1612	0.4	16	Q4	
5	1630-1633	0.6	20	Q4	
6	1634-1640	0.7	21	Q4	
Line 16					
9	0924-0951	3.9	35	Q3	
10	0956-1002	0.7	31	Q3	
10a	1005	?	shallow	Q4	
Line 18					
11	1132-1135	0.4	26	Q3/Q4	
12	1140-1144	0.3	32	Q3/Q4	
13	1145-1200	1.2	35	Q3/Q4	
14	1232-1234	0.2	26	Q4	
Line 20					
15	1339-1345	0.7	38	Q3/Q4	
16	1430-1449	3.3	33	Q3	
17	1515-1520	0.9	32	Q3/Q4	
Line 22					
18	1554-1625	2.8	28	Q3	
19	axed				
Line 23					
20	0911-0914	0.2	22	Q4	or part of M2 reflector
21	0927-0930	0.1	22	Q3/Q4	steep
22	0933-0937	0.25	25		
23	1018-1026	0.65	29		under M2
24	1036-1043	0.5	32		under, part of M2
Line 25					
25	1303-1310	1.3	23-27	Q2	M2
26	1324-1326	0.2	12	Q4	
Line 27					
27	1413-1414	0.2	26	Q1	M2
28	1422-1424	0.4	26	Q1	M2
29	1439-1446	1.1	22	Q3	
Line 29					
30	1741-1748	1.3	31	Q3	

Table XV.—Paleochannel Dimensions Determined from the Geophysical Records Used in Construction of Figures 26, 27, and 28, continued.

Channel #	Time fixes	width (km)	Depth(m) below MSL (m)	Seismic unit of fill	Remarks
Line 38					
31	1216-1222	0.8	34	Q3/Q4	deep
Line 36					
32	0837-0848	2	43	Q3	
Line 40					
33	1041-1048	1.2	26	Q1	M2, same spot as 25-1308
Line 44					
34	1036-1042	1.0	43	Q3/Q4	2 smaller separate channels accounted for
Line 62					
35	0736-0744	1.2	28	Q3/Q4	
36	0759-0809	1.0	32	Q3/Q4	
Line 42					
37	1249-1257	0.6	35	Q3/Q4	
Line 43					
38	1237-1253	1.3	46	Q3/Q4	
39	1359-1408	0.8	32	Q4	
Line 35					
40	1216-1219	0.4	33	Q3	
41	1257-1307	2.1	31	Q3	
Line 49					
42	1158-1201	0.25	32	Q1	M2
Line 51					
43	1331-1338	1.2	30	Q3	
44	1327-1330	0.4	28	Q3	
Line 50					
45	1259-1307	1.4	35	Q1	M2
46	1310-1316	0.5	27	Q3/Q4	
Line 52					
47	1409-1416	0.5	32	Q3?	
48	1419-1422	0.6	29	Q3/Q4	
Line 41					
49	1436-1438	0.35	26	Q3/Q4	

Table XV.—Paleochannel Dimensions Determined from the Geophysical Records Used in Construction of Figures 26, 27, and 28.

Line 39a				
50	0855-0915	2.8	31	Q3/Q4
51	0935-0938	0.4	25	Q3/Q4
52	0953-0956	0.4	32	Q3/Q4
53	1008-1021	1.5	25	Q3/Q4
Line 61				
54	1037-1039	0.6	30	Q4
55	1145-1154	1.4	42	Q3

Form 5/90 B20269

Plate 1

High-Resolution seismic reflection profiles

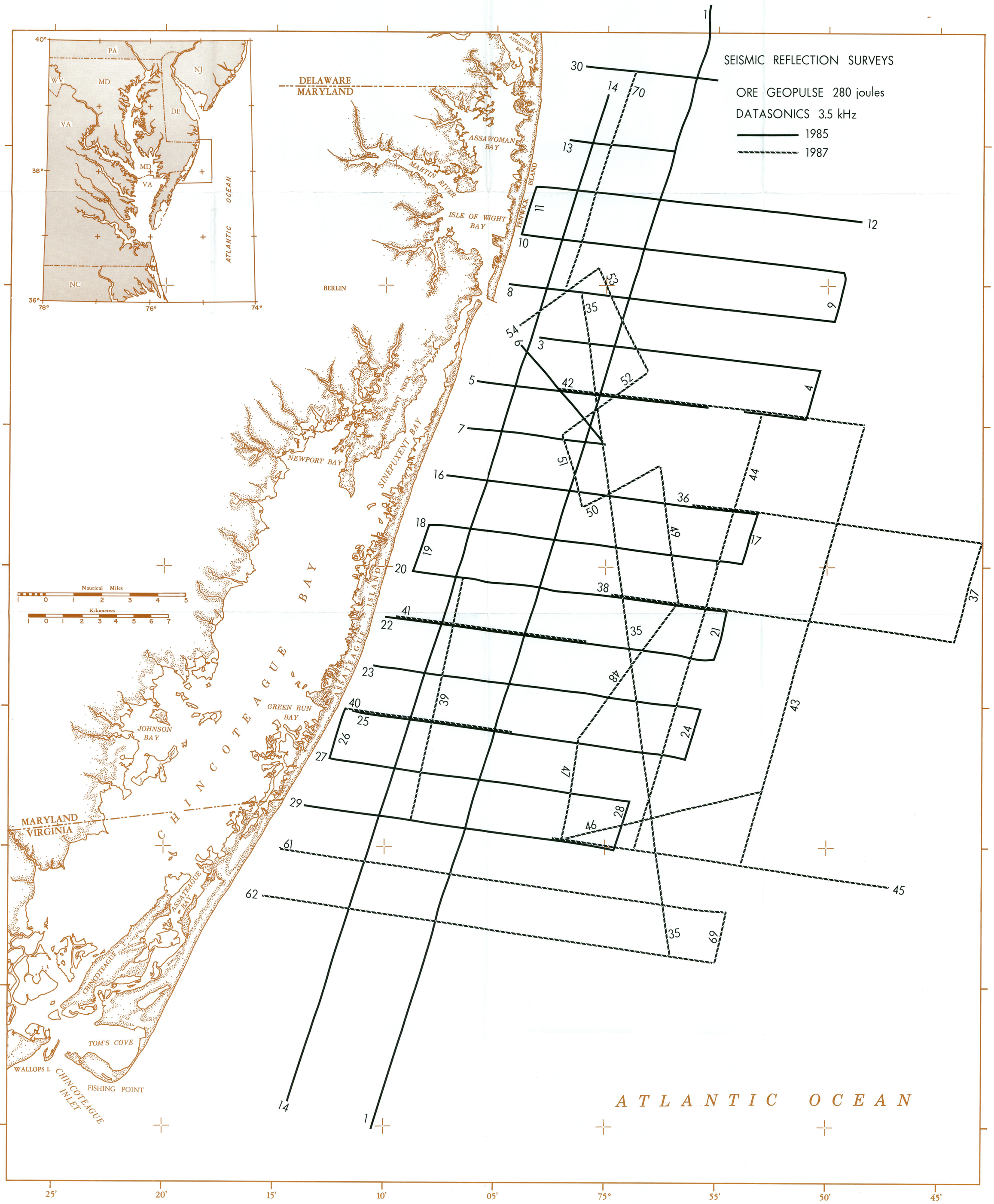

VIBRACORE LOCATIONS
By seismic line number and and time-fix
DELAWARE
MARYLAND
MARYLAND
VIRGINIA
ATLANTIC OCEAN
ASSAWOMAN BAY
ST. MARTIN RIVER
ISLE OF WIGHT BAY
FENWICK ISLAND
LITTLE ASSAWOMAN BAY
BERLIN
SINEPUXENT NECK
SINEPUXENT BAY
NEWPORT BAY
CHINCOTEAGUE BAY
ASSATEAGUE ISLAND
GREEN RUN BAY
JOHNSON BAY
CHINCOTEAGUE
ASSATEAGUE BAY
TOM'S COVE
WALLOPS I.
CHINCOTEAGUE INLET
FISHING POINT
Nautical Miles
Kilometers
16–835
16–842
16–850
16–905
16–935
16–945
16–1002
16–1005
16–1029
18–1248
18–1230
18–1215
18–1142
18–1135
20–1340
20–1430
20–1446
20–1500
20–1518
22–1605
23–928
25–1308
25–1215
27–1425
27–1440
27–1520
29–1750
29–1730
29–1640
ATLANTIC OCEAN

Plate 3

Structure contour on M1 reflector

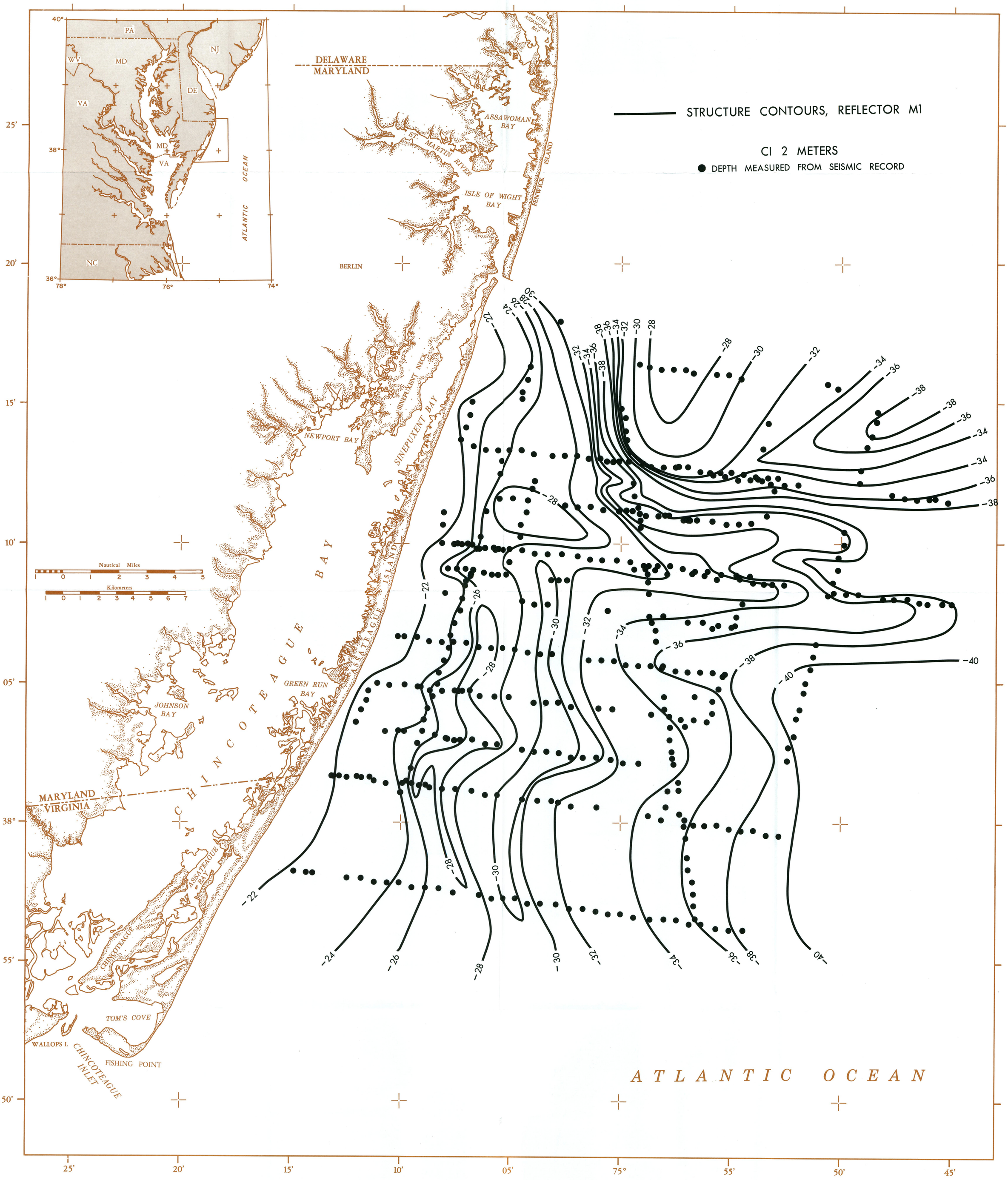

Plate 4

Interpretative geophysical records, Unit Q2

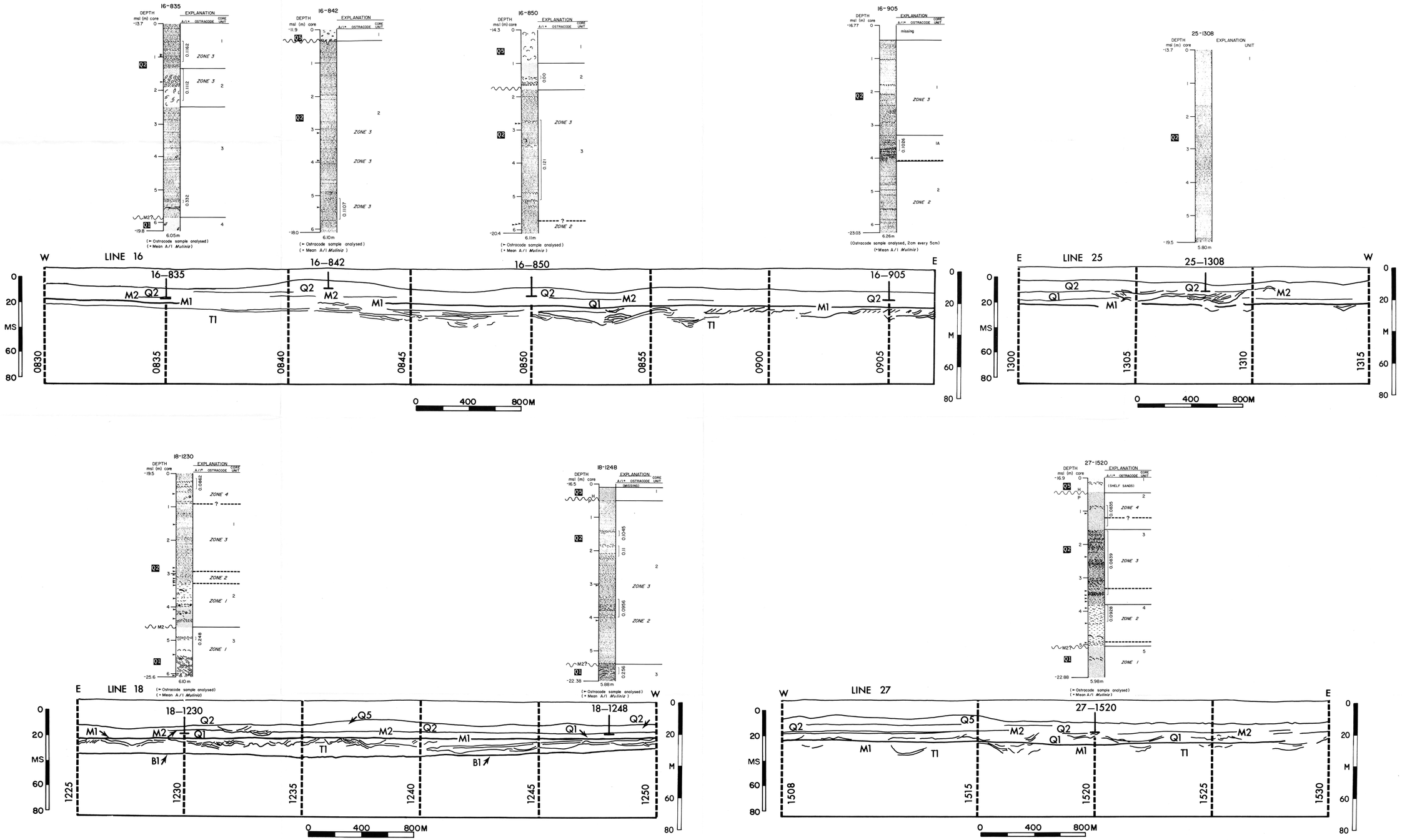

Plate 5
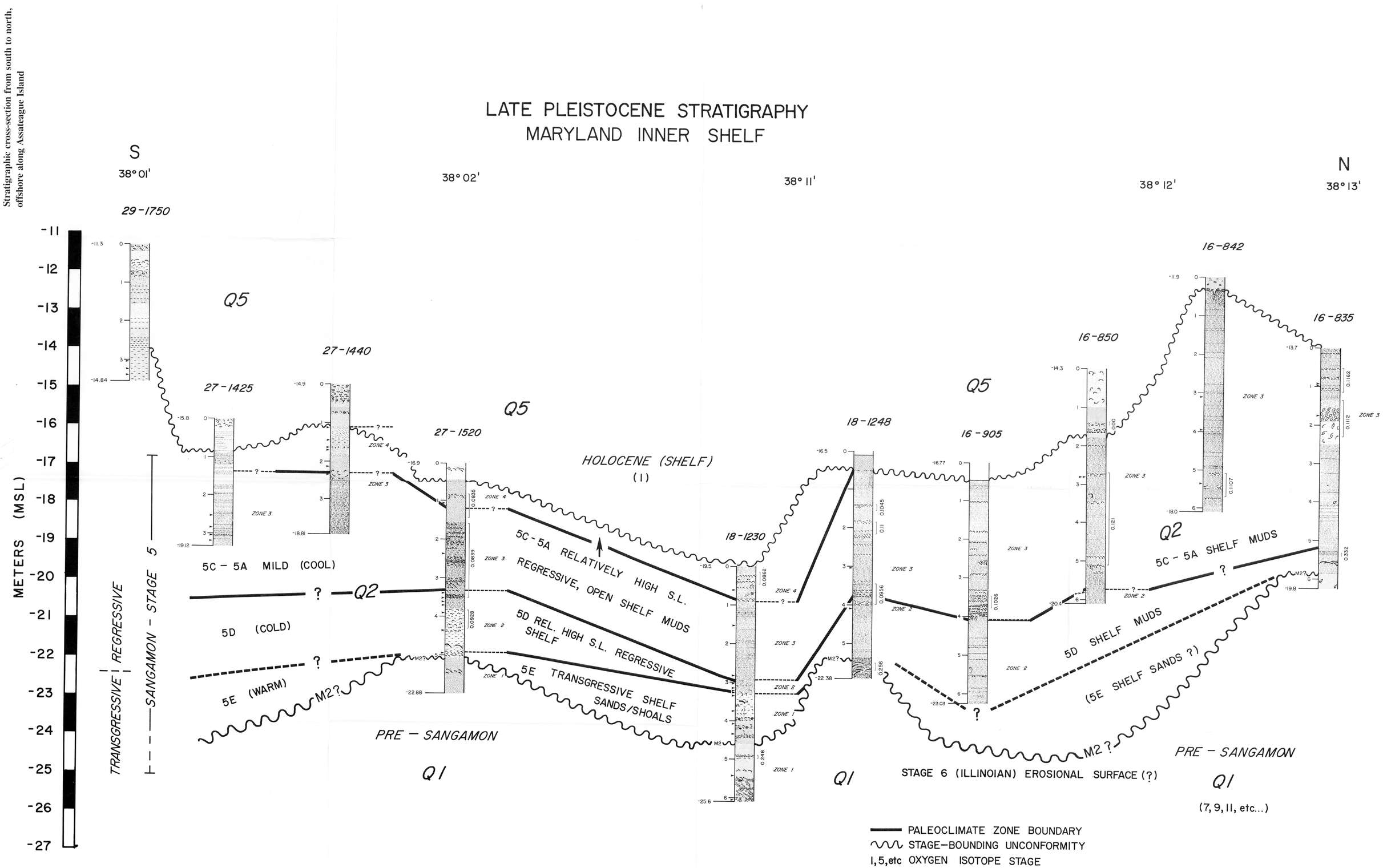
Stratigraphic cross-section from south to north, offshore along Assateague Island